Landing gear design in an automated design environment

N.C. Heerens

Master of Science Thesis

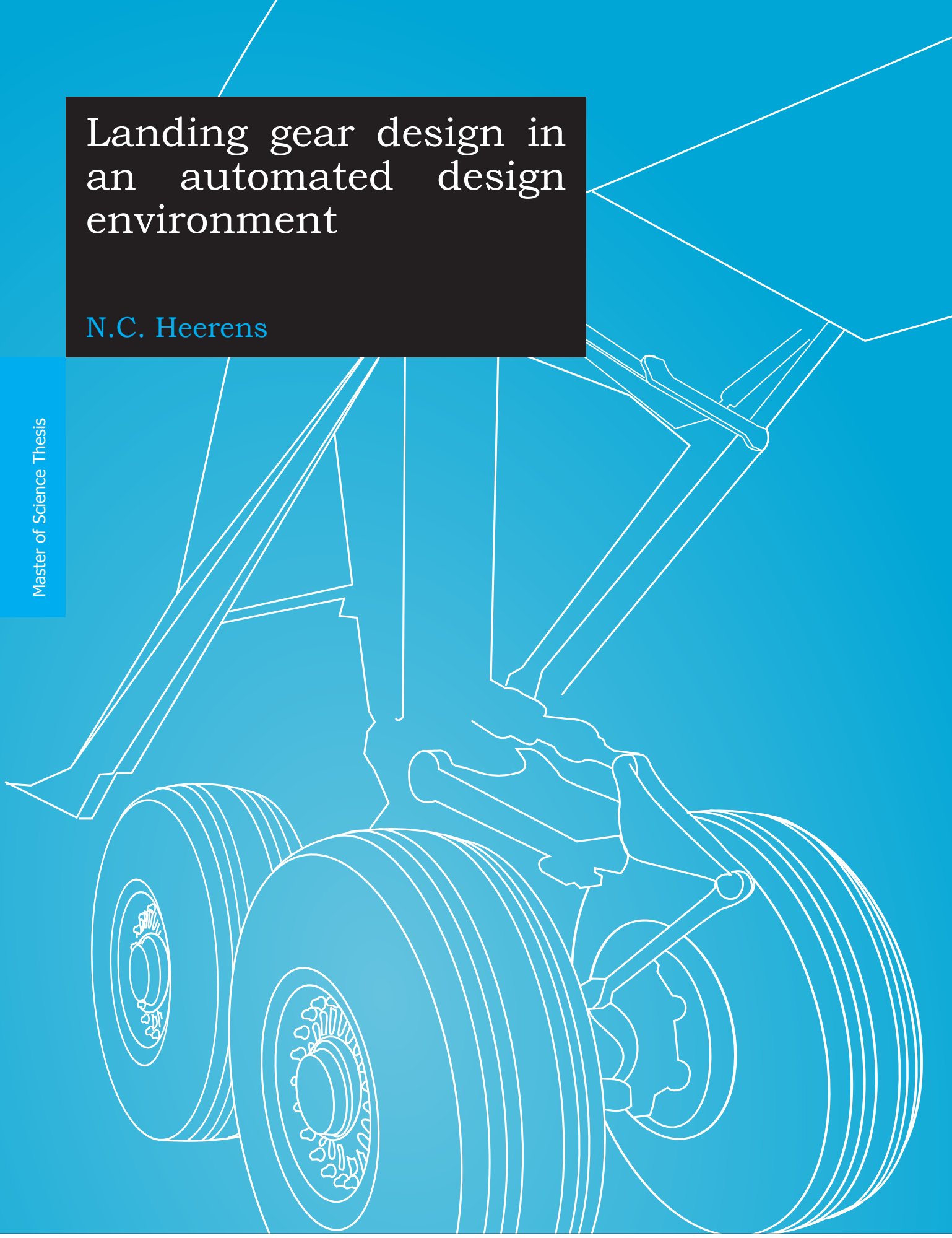

TU Delft Delft University of Technology

Challenge the future

Landing gear design in an automated design environment

Master of Science Thesis

by

N.C. Heerens

in partial fulfillment of the requirements for the degree of

Master of Science
in Aerospace Engineering

at the Delft University of Technology,
to be defended publicly on Friday March 7, 2014 at 13:00.

Faculty of Aerospace Engineering - Delft University of Technology

TU Delft Delft University of Technology

DELFT UNIVERSITY OF TECHNOLOGY

DEPARTMENT OF

FLIGHT PERFORMANCE AND PROPULSION

The undersigned hereby certify that they have read and recommend to the Faculty of Aerospace Engineering for acceptance a thesis entitled **"Landing gear design in an automated design environment"** by **N.C. Heerens** in partial fulfillment of the requirements for the degree of **Master of Science Aerospace Engineering**.

Dated: February 24, 2014

Head of department: _____

Prof.dr.ir. L.L.M. Veldhuis

Supervisor: _____

Dr.ir. M. Voskuijl

Supervisor: _____

Dr.ir. R. Vos

Reader: _____

Dr.ir. R. de Breuker

Abstract

The design of the landing gear is one of the prime aspects of aircraft design. Literature describes the design process thoroughly, however the integration of these design methods within an automated design framework has had little focus in literature.

Landing gear design includes different engineering disciplines including structures, weights, kinematics, economics and runway design. Interaction between these different disciplines makes the landing gear a complex system. Automating the design process has shown to have the advantage of increased productivity, better support for design decisions and can provide the capability of collaborative and distributed design. The automation tools improve performance of current designs and simplify the development of new aircraft configurations. In this thesis a systematic and automated landing gear design procedure is proposed.

Positioning the landing gear on the aircraft is limited by several requirements. Requirements include take-off stability, touchdown stability, wing-tip and engine clearance, ground handling and stability while taxiing. Evaluation of all these limits results in a feasible design space from which the shortest possible landing gear is found. From the resulting landing gear position, loads on the landing gear struts are calculated. Tyres and wheels are selected and brakes and shock absorbers are designed. The assembly of landing gear components can then be used to make an analytical weight estimation. This analytical weight estimation is based on maximum stresses occurring within the structure due to extreme load cases prescribed in certification specifications. Preventing yielding and buckling within the structure then results in required component thicknesses.

A multi-body model is then made, where structural parts are seen as rigid bodies. The multi-body model evaluates and visualises the system dynamics. The oleo-pneumatic shock absorber forces and motion are modelled using an analytical relation. An empirical tyre model models tyre motion and forces at the contact point. These two models can accurately describe forces within the tyres and shocks due to externally applied forces, which then allows for the evaluation of extreme landing load cases. This is done to verify empirically estimated dynamic landing loads used in the weight estimation. And this is done to identify loading peaks that could occur during a landing. In addition to the landing simulation a simulation of the landing gear retraction mechanism is done to check the kinematic feasibility and compliance to certification requirements.

Verification of results of the implemented landing gear with reference aircraft shows that landing gear positions closely match with actual landing gear positions. The analytical weight estimation of the landing gear assembly estimates the total gear weight with an error of 15 percent. This is comparable to the result of an empirical weight estimation that has an error of 17 percent.

Multi-body simulation results show that dynamic loads during an extreme landing are similar to empirically estimated dynamic loads. For landing gears with multiple rows of tyres it is especially important to look at landing loads, since a hard landing then creates peaks at high frequency in the shock loads. These peaks originate from the interaction between front and rear axle tyres hitting the ground at different times. A kinematic simulation of retraction and extension then verifies the kinematic feasibility. This simulation also shows that the retraction and locking mechanisms work and that it can be stowed within the available space. The resulting landing gear design and analysis tools complete the existing aircraft design tools, which then forms the basis for the future improvement of automated transport aircraft design.

Acknowledgements

I would like to thank my supervisors dr.ir. Mark Voskuijl and dr.ir. Roelof Vos for their advise and contributions while making this Master thesis. I would also like to thank the other members of my examination committee prof.dr.ir. Leo Veldhuis and dr.ir. Roeland de Breuker for taking the time to asses my thesis work. Thanks also to TNO, who provided me with the MF-Tyre tyre model and the aircraft tyre model data. Appreciation is also due to Arne, Kristian and Reno for their valuable input and cooperation while trying to solve similar programming and thesis problems.

I am grateful for all students and people at the department of Flight Performance and Propulsion who have made time spend on the faculty very pleasant. Finally many thanks go to my parents and sister, who always supported me in my efforts.

Niels Heerens
Delft, February 2014

List of symbols

symbol	unit	description
A	(-) / (m^2)	aspect ratio / area
b	(m)	wing span / wheelbase
C	(N s / m)	damping coefficient
C_d	(-)	discharge coefficient
C_L	(-)	lift coefficient
$C_{L\alpha}$	(-)	lift slope gradient
c	(-)	load distribution factor
DIA	(m)	diameter
E	(Pa)	Young's modulus
e_s	(m)	static tyre and shock deflection
F	(N)	force
g	(m/s^2)	gravitational acceleration
h	(m)	height
I	(m^4)	moment of inertia / pitch and roll moment of inertia
J	(m^4)	polar moment of inertia
K	(N / m)	spring stiffness
KE	(J)	kinetic energy
L	(N)	lift
l	(m)	length
M	(kg) / (Nm)	mass / moment
N	(-)	landing load factor
n	(-)	polytropic efficiency
P	(Pa)	pressure
p	(-)	scaling coefficient
Q	(m^3)	first moment of area
r	(m)	radius
S	(m) / (m) / (N)	distance to edge taxiway / shock absorber stroke / shear force
S_t	(m)	tyre deflection
T	(Nm)	torque / forward component of inertia
t	(s) / (m)	time / track / thickness
tt	(m)	bogie track
V	(m/s) / (m^3)	velocity / volume
W	(N)	weight

w	(m)	width
wb	(m)	bogie wheelbase
X	(m)	distance
$\dot{X}$	(m/s)	velocity
x	(m)	longitudinal position
y	(m)	lateral position / distance
z	(m)	vertical distance
α	(rad)	angle of attack
β	(rad)	nose gear steering angle
Γ	(rad)	dihedral
γ	(rad)	inclination or camber angle
Δ	(rad)	angle needed for minimum wheelbase
δ	(rad)	angle needed for turnover angle
η_s	(-)	shock efficiency
η_t	(-)	tyre efficiency
θ	(rad)	pitch angle / rotation angle
κ	(rad)	longitudinal slip angle
$\Lambda_{0.25}$	(rad)	quarter chord sweep
μ	(-)	friction coefficient
ρ	(kg / m)	density
σ	(Pa)	normal stress
σ_1	(Pa)	principal stress in 1 direction
σ_2	(Pa)	principal stress in 2 direction
τ	(Pa)	shear stress
Φ	(rad)	roll angle
Φ_t	(rad)	turn slip angle
Ψ	(rad)	yaw angle / sideways turnover angle
Ω	(rad/s)	radial velocity

List of subscripts

subscript	definition
0.25	quarter chord
1	at static condition
2	at extended condition
3	at compressed condition
180 deg turn	180 degree turn
c	circle
centreline	taxiway centre line
cg	centre of gravity
drag	drag strut
f	friction
fillet	taxiway fillet
fwd	forward
g	ground
h	hydraulic
i	inner
l	length between nose gear and forward cg
LOF	lift-off
M	main gear
max	maximum
min	minimum
N	nose gear
o	outer
p	pneumatic
side	side strut
TD	touchdown
Y	yield

Glossary

AAC	Airplane Approach Categories
ADG	Airplane Design Groups
AIP	Aeronautical Information Publications
AC	Advisory Circular
ACN	Aircraft Classification Number
CBR	California Bearing Ratio
cg	centre of gravity
EASA	European Aviation Safety Agency
FAA	Federal Aviation Administration
ICAO	International Civil Aviation Organization
LOF	lift-off
MAC	mean aerodynamic chord
MTOM	maximum take-off mass
PCN	Pavement Classification Number
RTO	rejected take-off
TD	touchdown

List of Figures

List of Tables

Contents

1

Introduction

The design of an aircraft landing gear is one of the fundamental aspects of aircraft design. Landing gear design has become highly sophisticated, because it includes many different engineering disciplines: structures, weights, economics and runway design. The process of the design of a landing gear is extensively documented in the books of Conway, Currey, Roskam and Torenbeek. Integration of the design methodology that can be used in an automated design environment however has had little attention in literature.

In complex engineering systems (such as an aircraft) many different disciplines interact together. An automation framework of the design has as aim to get a better design by using these different interactions (Cumnuantip et al., 2005, p. 2). Automation of the design process has shown to have the advantage of increased productivity, provide better support for design decisions and has the possibility of distributed and collaborative design. These new tools will improve the performance of current designs and ease the development of completely new aircraft configurations (La Rocca et al., 2012, p. 1).

The group of FPP is currently developing and extending an automated aircraft design framework. It supports multidisciplinary design, analysis and optimisation of aircraft. It consists of a number of interconnected multidisciplinary design and analysis tools, preventing that engineers need to do non-creative and repetitive design work. Within this framework the design of the landing gear has not been taken into account. However as the framework is continuously extended and becoming more detailed, the need for including the design of the landing gear has become apparent.

The aim of the master thesis is to expand and enhance the existing design tool by creating and integrating an automated landing gear design.

In this chapter first the landing gear design literature available is identified. Then the overall landing gear design process is explained, followed by an overview of the existing aircraft design framework. Then the current state-of-the-art in the field automated landing gear design and analysis is described. The last part of this chapter includes the overall structure of the master thesis research.

1.1. Preliminary landing gear design

During preliminary landing gear design there are a number of decisions that are made. It for example needs to be known what type will be used and if it needs to be retractable. There are a number of textbooks available that provide different methods for finding a good solution.

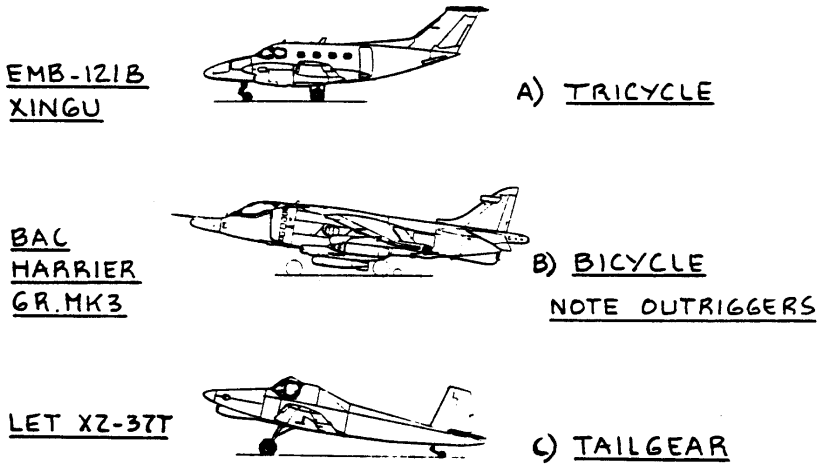

Figure 1.1: The tricycle, bicycle and tailwheel landing gear layouts (Roskam, 1989a, p. 9)

1.1.1. Textbooks

The book of Conway, 'Landing gear design' is the first book that has been written on landing gear design (Currey, 1988, p. ix). It was published in 1958 and therefore lacks some information needed for the design of a new landing gear today. The book of Currey, 'Aircraft landing gear design: principles and practices' is more recent and is one of the most valuable books that are available for landing gear design (Niu, 1999, p. 431). It includes all aspects of preliminary landing gear design.

The book of Roskam, 'Airplane design part 4: Layout design of landing gear and systems' just as the book of Torenbeek, 'Synthesis of subsonic airplane design' includes landing gear design procedures for initial design, without going into details of the structural design.

1.1.2. Landing gear types

All current high speed transport aircraft use the tricycle layout, but there are different general wheel arrangements possible. The tailwheel and the bicycle layout are other design solutions that could be considered (figure 1.1). For the tricycle layout, the main landing gear is behind the centre of gravity and there is a landing gear positioned at the nose. This tricycle layout is superior to other layouts due to its improved stability, braking and steering ability, good over-nose visibility, horizontal cabin floor attitude and good take-off rotation angle. Only specialised aircraft designs might require a different landing gear layout (Torenbeek, 1982). An example is the British Aerospace Harrier II with a bicycle landing gear. It has a vertical engine in the middle of the aircraft to provide lift and thus not enough room for a main landing gear in the middle.

Then there is also the choice if the landing gear is going to be fixed or retractable. The advantage of fixed gears compared to retractable gears is the low weight, low complexity and low cost. The main disadvantage is the high aerodynamic drag. Generally when cruise speeds go beyond 150 knots the drag penalty becomes too large and retractable landing gears are more beneficial (Roskam, 1989a).

1.1.3. General landing gear design process

Figure 1.2 shows in general the aspects that need to be considered during the preliminary design phase. Here flotation is the capability of the ground surface to support the aircraft. Preliminary design starts with a statement of the requirements and a concept formulation phase. During the concept formulation phase there are a number of completely different aircraft concepts formulated and analysed briefly. At this point, the minimum that needs to be known is the weight of the aircraft and the cg range. The number and the size of the

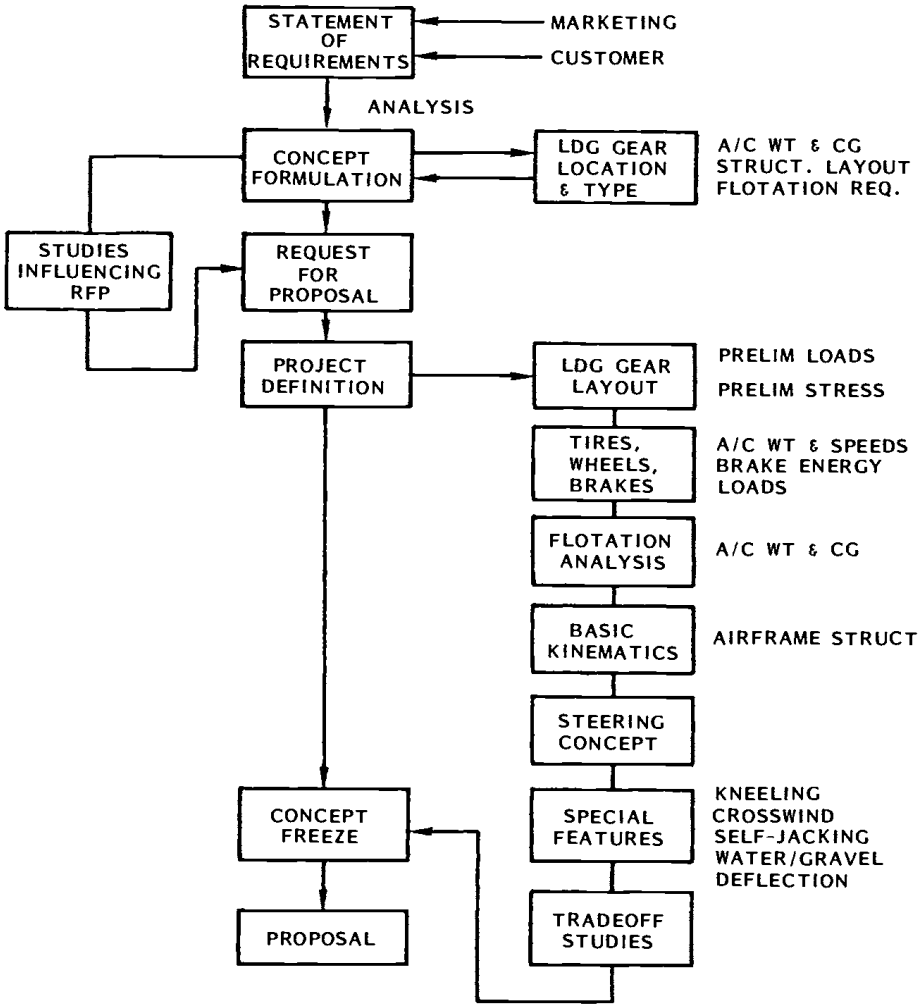

Figure 1.2: Activities during landing gear preliminary design (Currey, 1988)

wheels can then be determined and a review of runway flotation, compatibility with the airframe structure, cost, weight, availability and overall complexity can be done (Currey, 1988). The most cost effective solution will be determined from this review and will be presented in the commercial equivalent of the military Request for Proposal (RFP).

Following the concept formulation and the concept proposal is the more detailed project definition phase. In this phase aircraft weight and cg range estimates are improved. As a consequence loads on the landing gear can be better determined and the landing gear position can be further optimised. Then the stroke of the gear during landing, the gear dimensions, clearances, brake sizing, materials, weight and cost are evaluated. This is followed by a reiteration of runway pavement requirements, kinematics evaluation, steering concept selection and the design of special features (as a kneeling mechanism, a self-jacking capability or a capability to land on extremely rough surfaces).

In the project definition phase different trade-off studies are applicable and several trade-offs can be made:

- size and number of tyres against cost, weight and flotation;
- gear location against cost, weight and performance;
- different brake heat-sink materials;

- electric against hydraulic actuation systems.

The project definition phase is ended by a freeze of the landing gear design (Currey, 1988).

1.2. Aircraft design initiator

Computer aided aircraft design is becoming increasingly important, especially for multidisciplinary design optimisation for nonconventional aircraft concepts. The automated design tools consist of a number of multidisciplinary design and analysis tools and prevent that engineers need to do non-creative and repetitive design work.

Since 2002, the TU Delft department of Flight Performance and Propulsion has started with a Design and Engineering Engine (DEE) (La Rocca et al., 2012). This DEE supports multidisciplinary aircraft design, analysis and optimisation. Recently the DEE has been transformed into a new modular framework called the Initiator with new capabilities. It now has the capability to make initial aircraft designs for both conventional and nonconventional concepts as a blended wing body, a box-wing aircraft (Prandtl plane), canard or a three surface aircraft.

The Initiator is composed of a set of initial sizing tools. It uses a limited set of top level requirements, such as payload size, range, cruise speed, take-off field length and landing field length, to make a baseline aircraft design.

The Initiator has been build up out of several independent modules. Based on the need of the user only the required modules are executed. This is beneficial for reducing computation time and complexity. Different Initiator modules include aircraft component sizing, weight estimation and aerodynamic analysis modules. Classical synthesis methods from Raymer and Torenbeek are also implemented.

Another added capability of the Initiator is the possibility to manually introduce specific aircraft masses (such as the maximum ramp mass and landing mass) as input. When this is done initial design weight estimates are bypassed and only the input reference weight values are used. This makes verification of module results with reference data better, since inaccuracies of the initial sizing are factored out. A good information source for aircraft reference data are airport operations manuals published by aircraft manufactures.

1.3. Available research on automated landing gear design

In the field of automated landing gear design within a multidisciplinary design optimisation (MDO) environment not much research has been done. Most research in the field of MDO focus on other aspects such as wing geometry optimisation. The MDO environment described by Chai and Mason is one of the few that includes a detailed (similarly detailed as the thesis work) analysis of the landing gear design (Chai and Mason, 1996).

1.3.1. Landing gear design in an MDO procedure

Chai and Mason have integrated the landing gear design in an MDO procedure for the conceptual design of large transport aircraft. An automated model of the landing gear concept has been developed that can assess typical EASA requirements automatically. Airfield compatibility issues were automated and the results could be used in a complete MDO design program.

The main purpose of this implementation was to study the effects of variations of the landing gear design parameters on the configuration, system integration, airfield compatibility and weight. The work of Chai and Mason also includes methods for estimating cg range travel, analytical gear weight estimation, selection of tyres, wheels and brakes, shock absorber sizing and feasibility of retraction/extension. Kraus also describes an analytical method of weight estimation (Kraus, 1970) that could possibly be used in an automated analysis. This procedure however lacks essential information on load calculations and structural design criteria,

making implementation of the method very difficult. Other methods of Currey, Roskam and Torenbeek are all based on statistics.

1.3.2. Landing gear dynamics analysis and simulation

To analyse a landing gear design for the previously mentioned load cases the equations of motion need to be derived. These were normally determined in the past by hand and converted for use in a computer program. These programs were mainly developed in-house and written in FORTRAN code.

Now there is the option to use programs like Matlab/Simulink as developing platform that are more flexible than in-house created programs. Tools for eigenvalue analysis, plotting and much more can be easily used in the analysis (Besselink, 2000, p. 161).

Finite element analysis on landing gears is generally done for analysis of stresses and stiffness. Finite element packages as NASTRAN and ABAQUS do not efficiently address problems with mechanisms as the retraction system of the gear. This is because for each position of the shock absorber, actuator and other parts a separate analysis will need to be performed.

Multi-body analysis software is the preferred tool for dynamical analysis of mechanisms and ground-based vehicles. This type of software has shown to perform the analysis very efficiently (Spieck, 2004, p. 9). The advantage of using multi-body analysis software is that the equations of motion are automatically derived. With this software it is thus possible to focus on the engineering aspects instead on focussing on the derivation of the equations. Multi-body simulation packages provide important information and allow for the virtual testing of new designs and concepts.

Multi-body analysis software can be used for different aspects of ground dynamics in different phases of the aircraft design process, such as (Spieck, 2004, p. 25):

- landing loads, high speed roll;
- airframe and landing gear ground loads;
- aircraft ground manoeuvres, such as push-back, sharp taxi turns;
- behaviour on rough pavements;
- shimmy analysis;
- certification;
- unconventional configuration analysis, or analysis that are difficult or dangerous to perform physically.

Different modes of analysis exist for the analysis using multi-body tools. The analysis can be:

- static, when no motion occurs;
- kinematic, for closed loop systems such as the extension or retraction of the gear;
- linear, the equations of motion are linearized to represent dynamical behaviour;
- nonlinear, numerical solutions are used to determine the full non-linear behaviour on events such as touchdown.

Commercial multi-body simulation tools are nowadays being used by almost all major aircraft and landing gear manufacturers for the analysis of ground dynamics (Spieck, 2004, p. 17). Literature in the field of landing gear dynamics and simulation that makes use of multi-body dynamics tools is also numerous. This illustrates the importance that these tools have gained over the years.

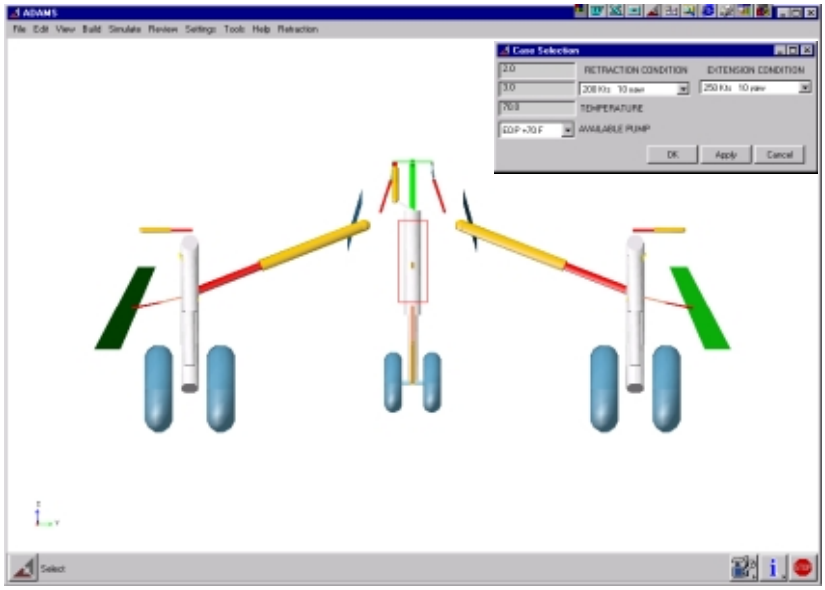

Figure 1.3: The landing gear model created in ADAMS for the simulation of retraction and extension kinematics (Zhang et al., 2000, p. 2)

ADAMS is a multi-body dynamics analysis tool also used by Airbus for the dynamical analysis of the landing gear (Coetzee et al., 2006). Messier-Dowty, the world's largest manufacturer of aircraft landing gears, uses ADAMS in the simulation of retraction and extension of the gear. The model consists of the gear structure and door mechanisms, including a hydraulic system as shown in figure 1.3. The simulation has shown to have a very good correlation with test results originating from test rigs and flight tests (Zhang et al., 2000). The simulation can be used for the sizing of the actuator and the hydraulic system.

Boschetto et al. has used ADAMS for the analysis of landing gear dynamics on the ground of a trainer aircraft. First the behaviour of the gear during drop-tests was simulated, by implementing different tyre models and a shock absorber model. Then the gear model was built into a complete aircraft rigid body to simulate ground manoeuvring load cases. The results of the simulation can be used for the analysis of load path into the fuselage structure during the design phase. The use of ADAMS in the preliminary design phase can be complex and thus less suitable (Boschetto et al., 2000, p. 8). For later stages of the design it can however prove to be very valuable.

Cessna for example uses the multi-body simulation package LMS Virtual.Lab to model the components of the landing gear of a new type of aircraft, including tyres, struts and trunnions. A separate model for the flexible tyres is thus also included. A parametric analysis can be performed with this software by running the simulations several times automatically for different aircraft cg positions. The simulation is used to verify compliance with FAA requirements for static and dynamic flight conditions, such as taxiing, take-off, retraction and landing (LMS International, 2008).

Then there is LMS Imagine.Lab that is capable of doing analysis for different disciplines, such as electrics and hydraulics simultaneously. Analysis can be done for landing, retraction, braking and steering systems. All ground loads can be analysed, since the software includes multi-body dynamics, structural dynamics and optimisation. Also validation of anti-skid systems or steering systems can be done within LMS Imagine.Lab.

Spieck uses the multi-body simulation package SIMPACK to accurately model the ground dynamics of the landing gear. Aeroelastic and aerodynamic influences have been included in the analysis, which is normally left out of the analysis. The aerodynamic and aeroelastic effects have shown to be of large importance on the total dynamic behaviour of the aircraft on the ground (Spieck, 2004, p. 110).

Multi-body dynamics packages allow the use of models for flexible bodies, such as tyres. But if vibrational

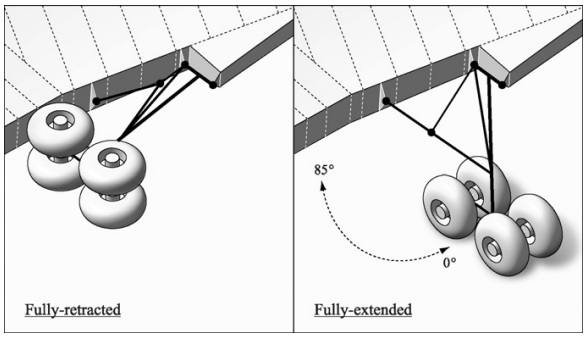

Figure 1.4: The modelling of landing gear kinematics within a CATIA MDO procedure (Hürlimann et al., 2011, p. 328)

analysis, such as shimmy analysis, needs to be performed, the flexibility characteristics cannot be changed much in these packages. SAMSEF MECANO would be a better option for this type of analysis (Besselink, 2000, p. 161).

Coetzee et al. used Matlab SimMechanics for the analysis of dynamical loads during ground handling. The advantage of using SimMechanics is that it is a very efficient toolset that can even be used for real-time applications (Coetzee et al., 2006, p. 3). The Initiator is largely made in Matlab and since Matlab and SimMechanics can be used seamlessly together this makes SimMechanics an excellent choice for performing kinematic and possibly other analysis.

1.3.3. Gear dynamics analysis and simulation in combination with MDO

In general multi-body dynamics software is used for separate case studies for a specific type of landing gear. When looking in literature for the combination of MDO procedures with more detailed landing gear design other than the work of Chai and Mason described in section 1.3.1, very little can be found. Hürlimann et al. shows a MDO implementation where landing gear kinematics are included for the estimation of the mass of a wing box structure. This implementation is made within CATIA and includes only a simplified model of the gear structure where the structure is represented by one-dimensional bar elements (figure 1.4). The landing gear model is used for assessing the position and clearances of the landing gear. When looking at the computational performance of CATIA within a MDO framework, it has proven to be insufficient for multidisciplinary optimisation (Hürlimann et al., 2011). The creation of a MDO framework within CATIA is therefore questionable.

Then Cumnuantip et al. shows a multi-body simulation integrated into a MDO process. The multi-body simulation is used for the selection of a landing gear layout for a Blended Wing Body aircraft. Cumnuantip et al. also states that this problem has had little attention in literature, confirming the low number of search results found on this topic.

The multi-body simulation program SIMPACK is used by Cumnuantip et al. for evaluating different landing gear layout concepts. First the gears overall dimensions, the shock strut length and oleo properties required are determined. The gear mass is then calculated analytically based on different load cases from regulations. These details are transferred to SIMPACK and simulated for the 3-point level, the one-wheel and the tail down landing load case. Then the maximum load on the gear support structure and the total mass of the aircraft concept is then calculated and used in the optimisation loop as the objective. Results of the optimisation were found satisfactory (Cumnuantip et al., 2005).

1.4. Thesis objective, aims and questions

The previous sections described that the focus of current research on automated multidisciplinary aircraft design is not on landing gear design. As a result a research void on a primary aircraft design aspect has been left to be investigated.

This thesis research will fill a part of the research void and add new understanding into this subject. The research objective of the master thesis is *to expand the knowledge base of the existing automated design environment by creating and integrating an automated landing gear design tool.* The automated landing gear design encompasses disciplinary analysis of structures, kinematics, runway pavement design and weight. The knowledge that is needed to achieve this research objective is formulated in the form of research questions.

The main research questions are formulated as follows:

- Which subjects are relevant for the development of an initial design sizing and selection tool, a parametric landing gear model and an analysis environment for landing gear kinematics and dynamic loads?
- How do we combine the sizing and selection tool, the parametric model and the analysis environment into a single landing gear design tool?
- How to integrate the landing gear design tool into the existing automated design environments?

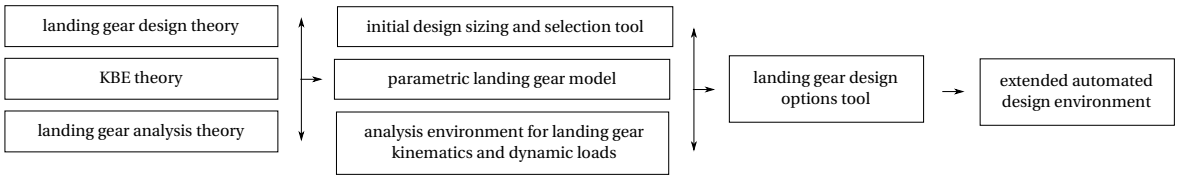

Figure 1.5: Research model

The research questions can be divided into several research subquestions:

- Which parts of landing gear design theory need to be included into an initial design?
- Based on which criteria can a initial landing gear design be sized and selected?
- Which parameters are required for a parametric landing gear model?
- Which landing gear analysis tests need to be performed in order to meet requirements?
- Based on which criteria are landing gear design options compared and selected?
- How to structure and combine landing gear design with the existing automated design environment?

The answers to these research subquestions together are needed for the main research questions. The main research questions provide a framework to achieve the research objective. The final result is a complete landing gear design tool that is integrated into the existing automated design framework.

Figure 1.6 considers the overall picture of the thesis work. New landing gear design capabilities are added to the Initiator and a new landing gear analysis tool is added. The overall structure is shown as a design optimisation loop, which is the final goal of the greater aircraft design framework. Design optimisation is however not the aim of the this thesis. It will be added in a future research project.

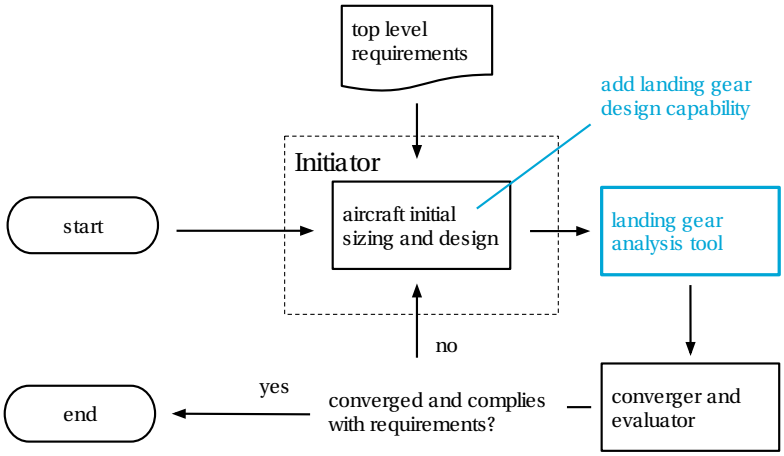

Figure 1.6: Overall structure of the thesis work. In blue the added capabilities are shown.

1.5. Thesis contents

The thesis is setup parallel to the research questions. In chapter 2 all landing gear design aspects and theory required to make an automated landing gear design are discussed. Then in chapter 3 the implementation of the landing gear design tool, how to use it and different use cases are explained. Results and a verification of the results is done in chapter 4. Finally a conclusion is drawn in chapter 5 and recommendations are made in chapter 6 based on the previous chapters.

2

Theory: landing gear design aspects

The landing gear provides several essential functions. The gear absorbs landing and taxiing loads and transmits these loads to the rest of the airframe. Manoeuvring and braking of the aircraft on the ground during taxiing, take-off roll and landing roll is done by the landing gear. The landing gear also provides the ability of aircraft towing and protection of damage to aircraft and ground surfaces.

2.1. Landing gear components

A typical main landing gear is built up out of several components, which fulfil different functions (figure 2.1). The shock absorber and tyres take up most of the shocks during landing and taxiing over rough surfaces. While the side and drag strut take up side loads on the gear due to engine thrust, braking or a sideways landing.

Requirements such as minimum weight, component maximum strength, maximum reliability, low cost, airfield compatibility and others can be conflicting (Currey, 1988, p.5). To prevent that a single requirements such as minimum cost, gets too much emphasis, aviation authorities prescribe safety requirements. Requirements for large aircraft powered by turbine engines have to follow the certification specifications from European Aviation Safety Agency (CS25) and have to follow the Federal Aviation Regulations from the Federal Aviation Administration (FAR25).

The regulations that will be looked at include:

- take-off and landing clearance;
- touchdown/take-off stability (CS 25.231);
- proper clearance between aircraft parts;
- taxi stability (CS 25.231 and CS 25.233);
- compatibility with runway pavement;
- landing load cases (CS 25.723 and CS 25.473);
- ground handling load cases (CS 25.235);
- landing gear emergency systems (CS 25.729 and CS 25.499);

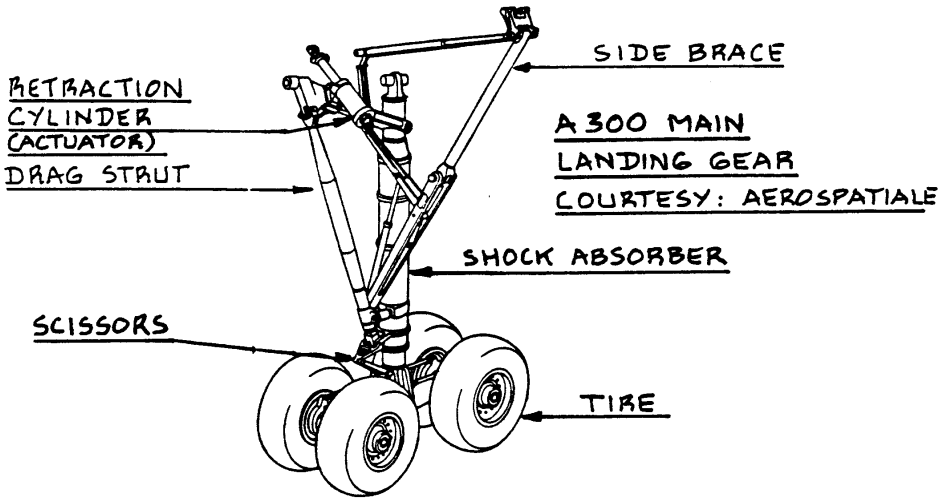

Figure 2.1: Typical main gear structure (Roskam, 1989a, p. 6)

The Acceptable Means of Compliance, AMC 25.723, AMC 25.729, AMC 25.735 and AMC 25.745 give information about shock absorption tests, the retraction system, the braking systems certification and nose wheel steering. The AMCs provide guidance that can be used as a means for showing compliance to the requirements. The relevant requirements and complementary documents are also listed in the AMCs (European Aviation Safety Agency, 2012).

2.1.1. Runway and taxiway surface compatibility

Airfield compatibility is an important issue. Landing gears of new aircraft need to be compatible with existing runways due to the high cost of runway modifications. The runway pavement bearing strength determines the arrangement and the number of tyres needed to comply with flotation requirements. Runway and taxiway geometry also constrain the location of the gears.

Loads on each landing gear strut and also the load on each tyre may not cause (European Aviation Safety Agency, 2012):

- structural damage to the landing gear or to the airplane;
- damage to the tyres;
- damage to runway or large ground surface deformations.

Different kind of runway surfaces could be considered in the design. For large commercial aircraft 2 types of pavements are considered: a flexible runway surface pavement with an asphalt top surface and a rigid pavement with a concrete top surface. About two-third of the major airports have flexible pavement runways.

To make a landing gear design compatible with all airport runways it is intended to operate on, one can compare aircraft loads with pavement ratings of runways. The pavement ratings are derived from engineering tests and traffic history or from aircraft currently using the airport. The standard rating is established by ICAO and uses the Aircraft Classification Number (ACN) and Pavement Classification Number (PCN). The ACN represents the relative load intensity of the main landing gear of the aircraft. Different methods are used to calculate the ACN for rigid and flexible pavements (Christy, 2009). ACN values are calculated by aircraft manufacturers and are published in so called aircraft characteristics for airport planning documents and in ICAO Annex 14.

The PCN describes the actual load carrying capability of the runway, taxiway or ramp of an airport. All major airports in the world have been assigned a PCN. PCN values are published in Aeronautical Information

Publications (AIP) and in the Jeppesen Airport Directory. When the ACN is lower than or equal to the PCN this means that the maximum take off weight is unrestricted.

The ACN value for a new aircraft cannot be calculated easily. The procedure is described in Annex 14 of the ICAO airport pavement design manual and requires a computer program. The computer program listed in Annex 14 is implemented in COMFAA, a computer program made by the FAA. COMFAA is able to calculate the ACN for different pavement sub-grade categories and it can calculate PCN values and pavement thicknesses. As input is required the aircraft gross weight, the percentage of GW on the main gear, the number of gear struts, the number of wheels per main gear and the tyre pressure (Federal Aviation Administration, 2011).

The COMFAA program is a stand-alone program and thus cannot be directly used in an automatic landing gear design procedure. The FAA though provides the source code of the COMFAA program and also provides a detailed documentation of how the ACN calculation procedures are implemented. It is thus possible to alter the source code into a new program that can be used in the flotation analysis of the aircraft design.

The COMFAA program has more capabilities than necessary for the calculation of ACN values. Therefore only parts of the COMFAA program are used for implementation in the flotation analysis.

2.1.2. General positioning requirements

In the following sections the basic design issues are discussed that need to be taken into account when positioning the landing gear. The issues include the take off/landing requirements, ground handling, ground clearance and stability requirements.

It is important to choose a landing gear position that does not need to be modified with respect to strut length and position under the wing when considering future aircraft growth options. An increase in fuselage length should be taken into account, because this reduces the maximum take-off rotation angle (Chai and Mason, 1997, p. 22). This is assuming the aircraft horizontal floor attitude is kept the same. Changing the floor attitude will make the aircraft less convenient for aircraft operations.

The result of positioning the landing gear is a minimum main gear length. From the main gear length and the desired attitude of the fuselage the nose gear length is found.

Take-off stability

On the ground, during landing and during take-off the aircraft should be able to safely pitch up or down without hitting the ground or having a tendency to turn on its side. To check whether or not this could occur the coupling of the gear position with the take-off/landing performance and the aircraft centre of gravity range needs to be considered.

The required pitch angle for taking off (when the landing gear is fully extended) is estimated using the equation (Torenbeek, 1982, p.350):

$$\theta_{\mathrm{LOF}} = \alpha_{\mathrm{LOF}} + \frac{d\theta}{dt}\left(\frac{2l_1}{V_{\mathrm{LOF}}} + \sqrt{\frac{l_2 C_{\mathrm{L\,LOF}}}{g C_{\mathrm{L}\alpha}}}\right) \tag{2.1}$$

This equation is based on the result of Pinsker (Pinsker, 1969) that takes into account the dynamics of the aircraft motion at take-off. When more accurate information is not available (typical in an initial design stage) the lift curve slope is estimated for high aspect ratio wings with (Torenbeek, 1982, p.351):

$$C_{\mathrm{L}\alpha} = \frac{dC_{\mathrm{L}}}{d\alpha} = \frac{2\pi\cos\Lambda_{0.25}}{1+2/A} \tag{2.2}$$

and the angle at lift-off:

$$\alpha_{\mathrm{LOF}} = \frac{1}{2\pi}\left[(1+\frac{2}{A})\left(\frac{(C_{\mathrm{L\,max}})_{\delta_{\mathrm{f}=0}}}{\cos\Lambda_{0.25}} - p\frac{(C_{\mathrm{L\,max}})_{\mathrm{to}}}{\cos\Lambda_{0.25}} - \frac{C_{\mathrm{L\,cr}}}{\cos\Lambda_{0.25}}\right) - \frac{1}{A}\right]\frac{180}{\pi} \tag{2.3}$$

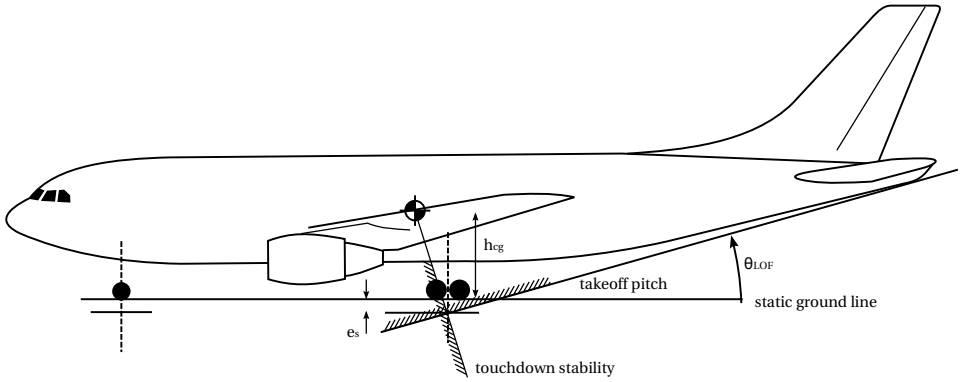

Figure 2.2: Side view showing limits used in the positioning of the gears

Here p is within the range of 0.15-0.20, dependent on aerodynamics. Equation 2.3 takes into account the ground effect, but tailplane trim is left out, flap deflection at take-off is assumed to have little effect on the critical lift coefficient and it is assumed that the fuselage is horizontal during cruise. If the lift coefficient with zero flap deflection is unknown it may be estimated as $(C_{\mathrm{L\,max}})_{\delta_{\mathrm{f=0}}} = 2.10 \cdot \cos \Lambda_{0.25}$ when slats are present on the aircraft.

Landing stability

The previous equations are applicable to the take-off rotation. For landing the maximum pitch angle that will be achieved is lower than for take-off. This is due to the flap deflection angle, which is higher at landing. Therefore and because there is limited information available the pitch angle at touchdown, θ_{TD} can assumed to be equal to the pitch angle at take-off, θ_{LOF} (Torenbeek, 1982, p.351).

During landing touchdown the aircraft should have a pitch down tendency. This sets a limit on the minimum longitudinal position for the main gear. The worst-case landing is a landing with the cg aft and the cg at the highest position. When there are no other loads influencing the pitch down tendency the main gear should be minimally behind the aft cg by a distance of (Torenbeek, 1982, p.352):

$$l_{\mathrm{m}} \geq (h_{\mathrm{cg}} + e_{\mathrm{s}}) \tan \theta_{\mathrm{TD}} \tag{2.4}$$

where e_s is the static deflection of the shock and tyre at the static condition and h_{cg} is the height from the ground of the cg while taxiing.

Sideways turnover and ground stability limits

A crosswind landing or a turn during taxiing at high speed can cause the aircraft to tip on its side. The sideways turnover angle Ψ, which should be lower than 63° (Currey, 1988, p.352), is equal to:

$$\tan \Psi = \frac{h_{\mathrm{cg}}}{l_{\mathrm{n}} \sin \delta} \tag{2.5}$$

where δ is equal to:

$$\tan \delta = \frac{t}{2(l_{\mathrm{m}} + l_{\mathrm{n}})} \tag{2.6}$$

Here the nose wheel track is assumed to be of minimal importance. Using equations 2.5 and 2.6 the minimum required track (t) can be determined to prevent turnover.

To ensure that the aircraft remains stable during taxiing and touchdown another limit should be taken into account. When assuming that the nose wheel location is fixed, a circle is drawn with a radius of $0.54 h_{\mathrm{cg}}$ placed at the forward cg position as in figure 2.4. This radius is based on the recommendations described

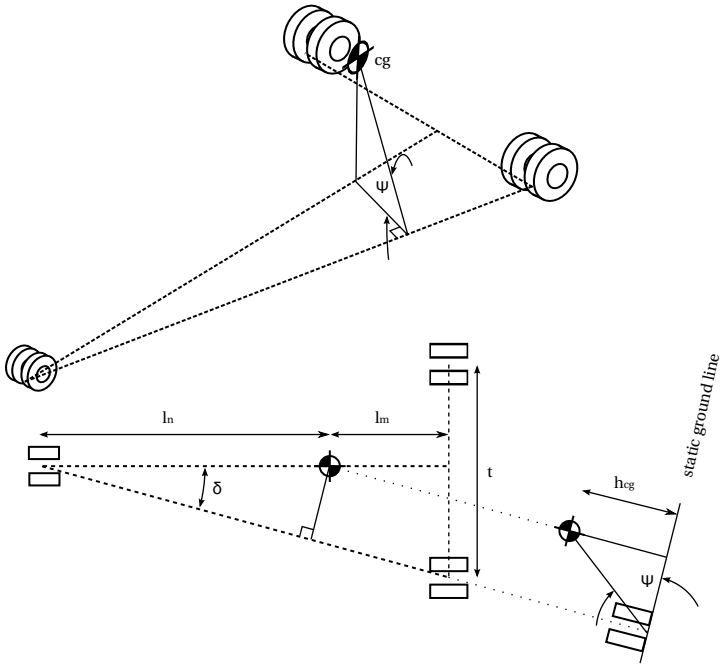

Figure 2.3: Dimensions used for the sideways turnover requirement

by Torenbeek (Torenbeek, 1982, p.354). Then the line drawn from the nose wheel position to the tangent of the circle determines the minimum lateral position of the main gear. This can also be calculated analytically using:

$$y_{\text{mlg min stability}} = \tan\left(\sin^{-1}\left(\frac{0.54h_{\text{cg}}}{l_{\text{n}}}\right)\right)(l_{\text{n}} + l_{\text{m}}) \tag{2.7}$$

When assuming the main gear location is fixed, a limit on the nose gear position can be found by drawing a line from the fixed main gear position to the tangent of a circle with radius $0.54h_{\text{cg}}$. This is also shown in figure 2.4 and this results in:

$$\Delta = \tan^{-1}\left(\frac{l_{\text{m}}}{t/2}\right) \tag{2.8}$$

$$l_{n\,min} = \tan\left(\sin^{-1}\left(\frac{0.54h_{\text{cg}}}{l_{\text{m}}\sin(\Delta)}\right) + \Delta\right)t/2 - l_{\text{m}} \tag{2.9}$$

Wing and engine clearances

During a crosswind landing the aircraft could roll on its side. This rolling should be possible to a certain degree, without aircraft parts hitting the ground. For the engine nacelles a roll angle of 5 degrees with an additional 6 inch clearance is given by Raymer (Raymer, 1999, p.62). This requirement is also visible in figure 2.5.

For transport aircraft the wings are usually swept aft. When the aircraft nose pitches up there is a risk that the wing touches the ground. This can be taken into account by calculating the limit roll angle when the wing tips just touch the ground (Torenbeek, 1982, p.350):

$$\tan\Phi = \tan\Gamma + \frac{2h_g}{b-t} - \tan\theta\tan\Lambda \tag{2.10}$$

Here Γ and Λ are the angles defined in figure 2.4 and 2.5, b is the wing span. In this equation the wings are assumed to stay in its rigid position.

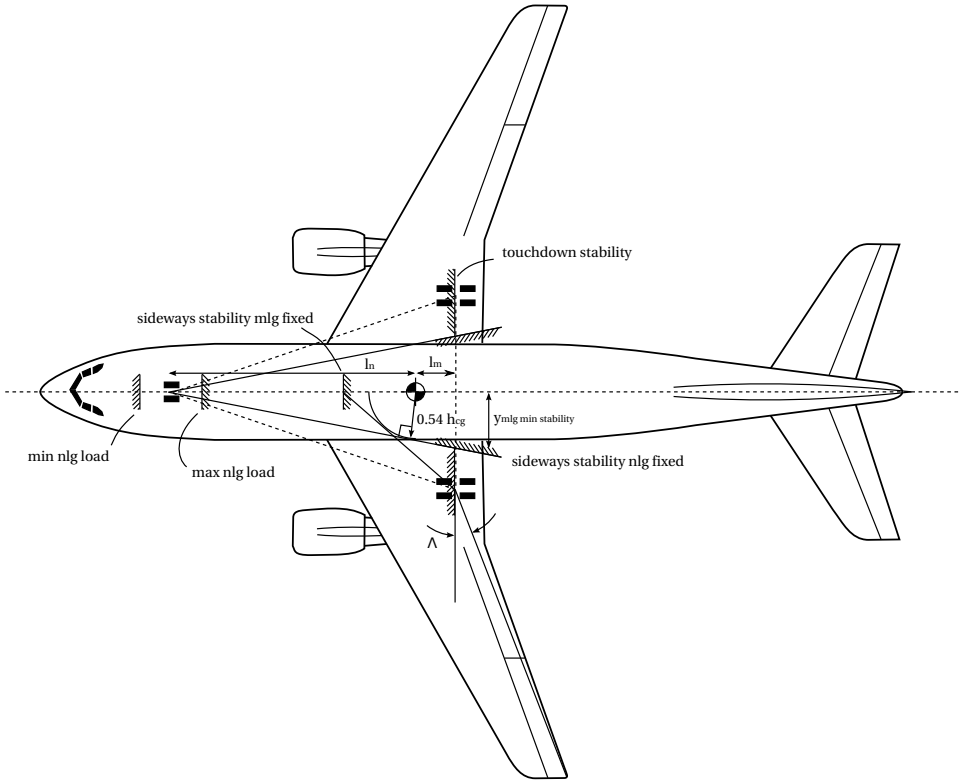

Figure 2.4: Top view showing stability limits used in the positioning of the gears

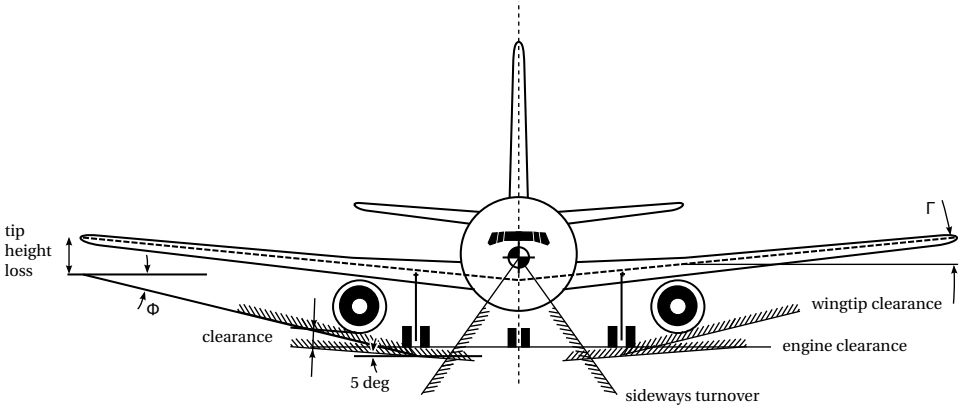

Figure 2.5: Front view showing limits used in the positioning of the gears

Centre of gravity and gear position

The aircraft's cg location is one of the most critical in the design and positioning of the landing gear. An improper cg position could result in tip back, turn over or tipping on the side of the aircraft. Also during the landing rollout the weight on the main gears should be high enough to make sure that the brakes can provide enough braking power.

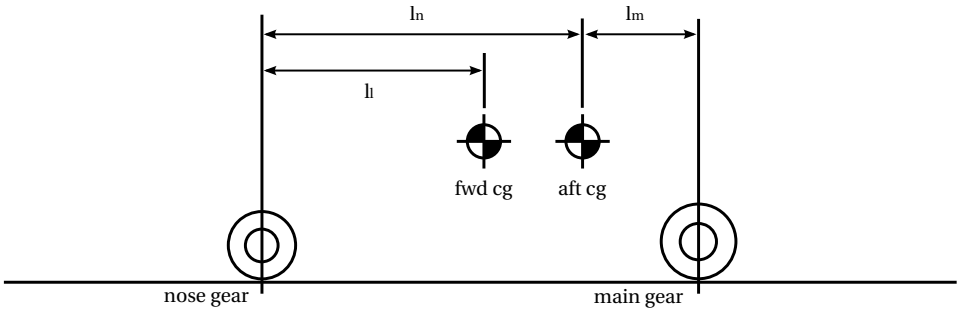

Figure 2.6: Definition of dimensions used in calculating landing gear loads

The load on the nose and main landing gear can be calculated using figure 2.6. The maximum main gear load for all main gear struts is subsequently equal to (Currey, 1988):

$$F_{\mathrm{m\,max}} = \frac{l_{\mathrm{n}}}{l_{\mathrm{m}} + l_{\mathrm{n}}} W \tag{2.11}$$

The maximum nose gear load is:

$$F_{\mathrm{n\,max}} = \frac{l_{\mathrm{m}} + l_{\mathrm{n}} - l_{\mathrm{l}}}{l_{\mathrm{m}} + l_{\mathrm{n}}} W \tag{2.12}$$

and the minimum nose gear load:

$$F_{\mathrm{n\,min}} = \frac{l_{\mathrm{m}}}{l_{\mathrm{m}} + l_{\mathrm{n}}} W \tag{2.13}$$

Here W is the maximum ramp weight. The maximum and minimum nose load is a design parameter that has a large influence on the gear positioning. If a first estimate has to be made, Currey advises a maximum and minimum nose load of 15 and 8 per cent of the maximum ramp weight.

Solving for l_{n} in equation 2.13, results in a maximum nose gear limit that is a function of the main gear longitudinal position. This limit is the maximum nose gear load limit in figure 2.7. Similarly solving for l_l in equation 2.12 gives the minimum nose gear limit, which is also shown in figure 2.7.

The longitudinal position of the main gear and nose gear is also limited by stowage constraints and by wing spar constraints. These constraints together leave open a small design space for feasible nose and main gear longitudinal positions.

Ground operations requirements

Airport taxiways are constructed based on standards defined by the FAA. The Federal Aviation Administration provides standards and requirements for the design of airports (Federal Aviation Administration, 2012b). In order to operate on most airports it is advisable to comply with these requirements. The Advisory Circular gives requirements on the turning radius and centreline guidance taxiing.

The FAA categorises aircraft in different Airplane Design Groups (ADG) and Airplane Approach Categories (AAC). In table 2.1 and 2.2 the different categories are listed. The aircraft is placed in the highest group based on its tail height or wingspan. From the AAC category and ADG group a required runway width can be obtained from table 2.3.

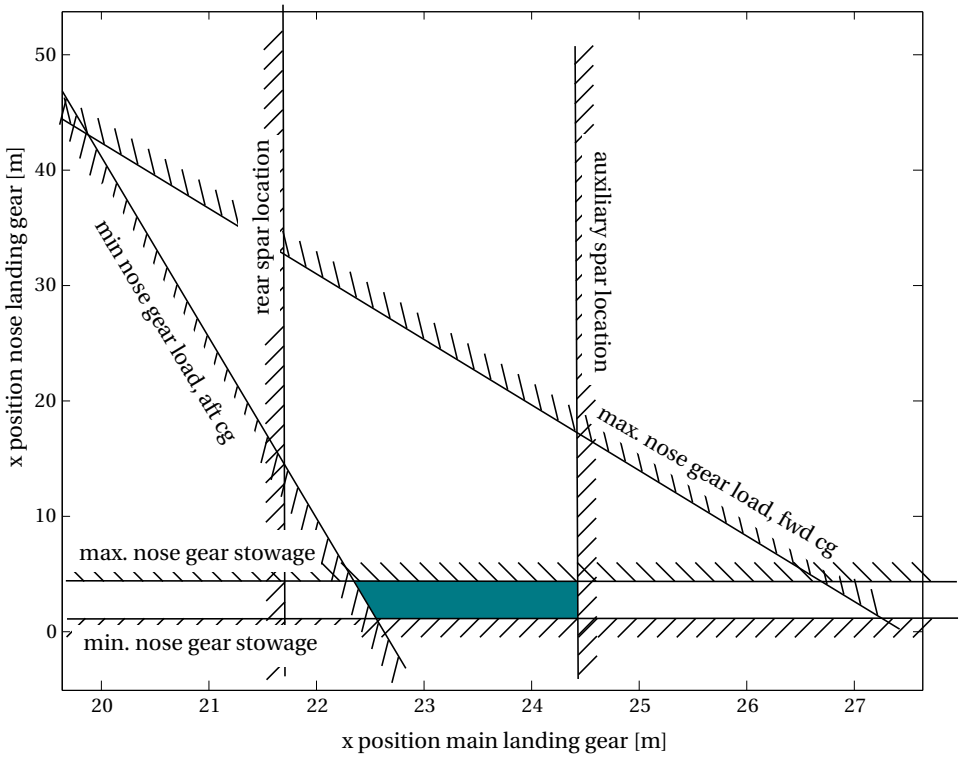

Figure 2.7: Nose and main gear longitudinal positions limited by nose gear loading limits and stowage limits. Green indicates feasible gear longitudinal locations.

The aircraft should be able to make a turn within this runway width. The turn radius of the aircraft is a function of the nose gear steering angle, β, assuming the aircraft only turns by pivoting the nose gear. A maximum steering angle for transport aircraft is about ± 60 degrees (Currey, 1988, p.198). Then the turning radius can be obtained graphically in figure 2.8 or by making use of the maximum steering angle and the following equation:

$$r_{180\text{ deg turn}} = b\tan(90-\beta) + \frac{t}{2} \tag{2.14}$$

If the turning radius poses a problem due to a too high gear track or wheelbase the turn radius can be decreased by installing a main gear steering system. This is for example done for the Boeing 747, Boeing 777 (Chai and Mason, 1997, p.24) and the Airbus A380 main gear bogies (Hebborn, 2008).

Chai and Mason provide a way to determine if the aircraft can turn on airport taxiways. This poses limits on the aircraft wheelbase and gear track. The angle between the tangent of the taxi turn centreline (with radius, $R_{\text{centreline}}$) and the aircraft centre line is called the castor angle, α_{castor}. This angle is equal to:

$$\sin\alpha_{\text{castor}} = \frac{b}{R_{\text{centreline}}} \tag{2.15}$$

The castor angle should be smaller than the maximum turn angle of the nose gear. This thus puts a constraint on the aircraft wheelbase b.

To avoid that the main gear goes off the taxiway while turning, the main gear should be kept a distance S away from the taxiway edge (see figure 2.8). Using taxiway dimensions and a safety margin in table 2.4 the maximum aircraft gear track can be found with:

$$R_{\text{fillet}} = \sqrt{R^2_{\text{centreline}} + b^2 - 2R_{\text{centreline}}\, b\sin\alpha_{\text{castor}}} - t/2 - S \tag{2.16}$$

ADG	Tail height (m)	Wingspan (m)
I	< 6	< 15
II	6 - < 9	15 - < 24
III	9 - < 13.5	24 - < 36
IV	13.5 - < 18.5	36 - < 52
V	18.5 - < 20	52 - < 65
VI	20 - < 24.5	65 - < 80

Table 2.1: Airplane Design Group (ADG) classification (Federal Aviation Administration, 2012b, p.13)

AAC	Approach speed (kts)
A	< 91
B	91 - < 121
C	121 - < 141
D	141 - < 166
E	> 166

Table 2.2: Airplane Approach Category (AAC) classification (Federal Aviation Administration, 2012b, p.13)

AAC \ ADG	I	II	III	IV	V	VI
A	60	75	100	150	-	-
B	60	75	100	150	-	-
C	100	100	150	150	150	200
D	100	100	150	150	150	200
E	100	100	150	150	150	200

Table 2.3: Required runway width (ft) for a given Airport Approach Category and Airplane Design Group (Federal Aviation Administration, 2012b, p.263)

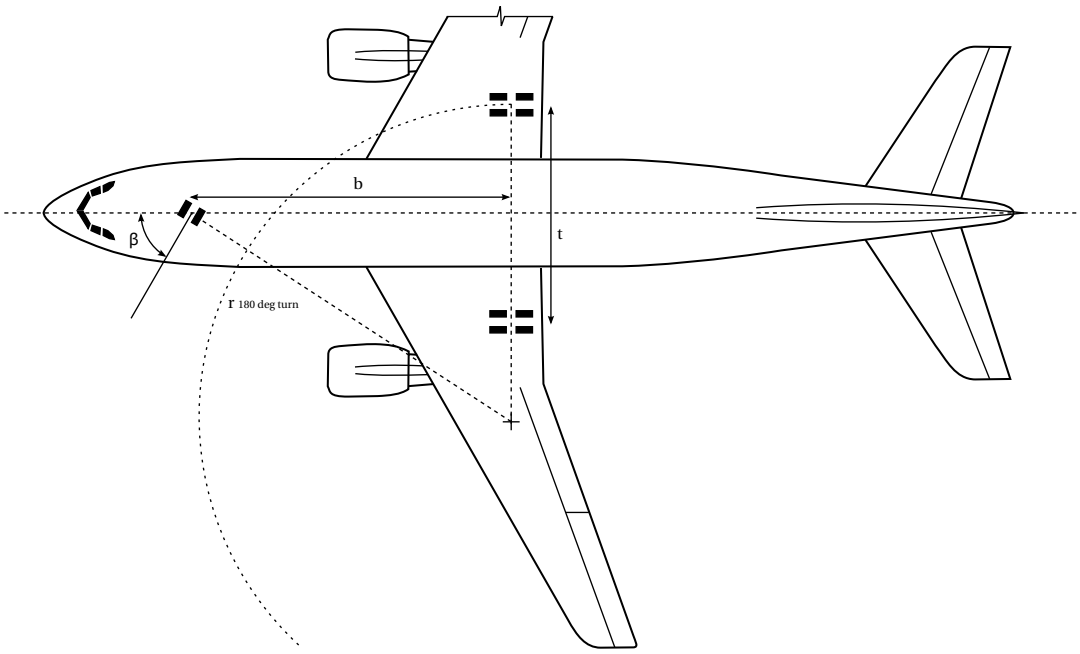

Figure 2.8: Dimensions for determining the radius of a 180 degree turn

	ADG III	ADG IV	ADG V	ADG VI
$R_{\text{centreline}}$	100	150	150	170
R_{fillet}	55	80	85	85
S	10	15	15	20

Table 2.4: Taxiway turn dimensions (Federal Aviation Administration, 2012b) (Chai and Mason, 1997, p.26)

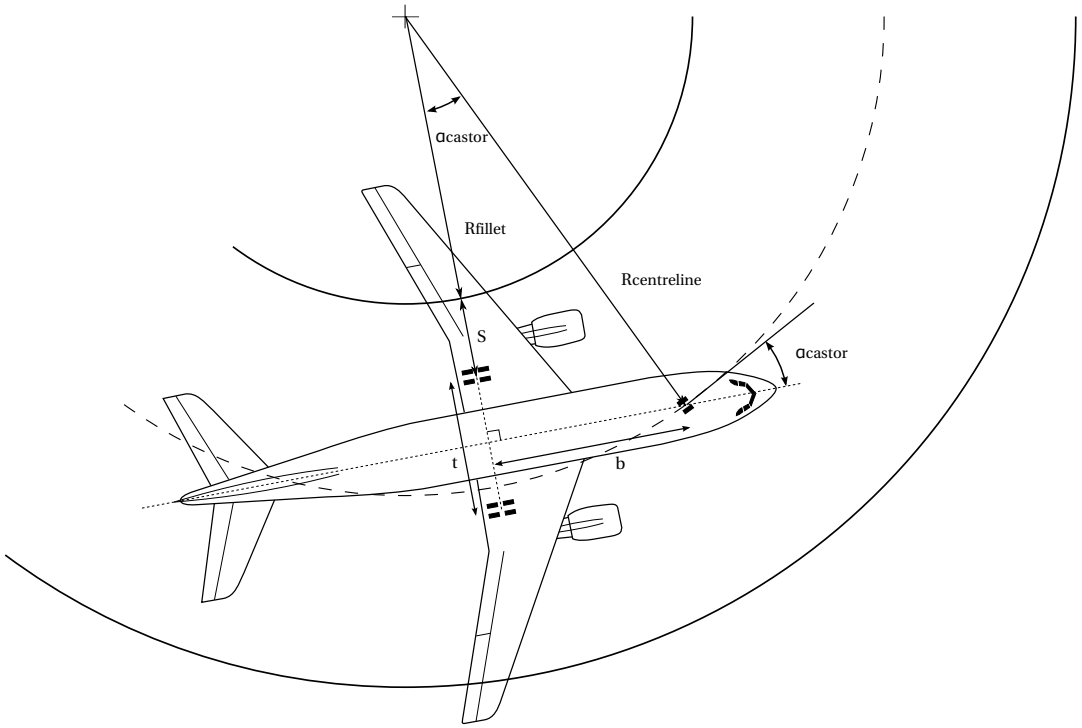

Figure 2.9: Centreline taxiing dimensions

2.1.3. Tyres

Tyres are exposed to quite severe dynamic and static loads during landing, take-off roll and taxiing. During touchdown the tyres provide a significant amount of the shock absorption capability of the landing gear. Tyres are designed around a maximum allowable static load. For any centre of gravity position in combination with the highest weight pressing on the landing gear this allowable load may not be exceeded.

When selecting tyres one can choose for a conventional bias-ply tyres or radial tyres. Radial tyres are more recently developed and have as advantage a lower weight and a longer lifespan. Wearing of the tread is reduced with 40 to 60 per cent (Currey, 1988). Radial tyres are therefore preferred for new aircraft types. Radial tyres are up to 20 per cent lighter due to their construction, which minimises the shear stresses in the rubber and efficiently distributes the loads. Radial tyres are constructed with additional steel belts that run in the radial direction and have an additional advantage that the footprint area is larger (about 10 per cent). A larger footprint area improves flotation characteristics and reduces hydroplaning. Radial tyres can withstand higher overload bearing stresses and can withstand under-inflation better. When the tyres do fail they do this less sudden than bias ply tyres and indications of damaged tyres can be more easily spotted.

For a conventional bias-ply tyre the belts run in varying angles, usually between 30 to 40 degrees. Bias-ply tyres are however still widely used on current commercial aircraft (Goodyear, 2002). Both bias-ply and radial tyres can be ordered with different options. An example option are tyres with so called chines. A chine is a circumferential bulge shaped to deflect water sideways from the engines. Tyres with chines were initially developed for aircraft with rear-mounted engines.

Aircraft tyre manufactures include Bridgestone, Goodyear, Dunlop and Michelin. All these tyre manufactures provide tyre rated loads, pressures and dimensions of all currently available aircraft tyres. From the available data the radius of the tyres at static load can be determined for both nose and main gear. This determines the vertical position of the aircraft with respect to the ground. This position is needed for determining the position of the shock strut at compressed and extended position and for determining the maximum rotation angle of the aircraft during take-off.

2.1.4. Wheels

Wheels will have to be dimensioned such that there is enough room to house the brakes. Also the selected tyre needs to fit on it. This should be done while keeping in mind that the weight should be minimal and the life should be maximal.

Two types of designs for the wheel are available at the moment, namely the A-frame type and the bowl-type wheels. The A-frame type can be made lighter, but has as disadvantage that there is less space available to accommodate the brakes (figure 2.11). Thus if braking requirements are too high, bowl type wheels are the only option.

Wheels are mainly constructed with forged aluminium. Trends to other materials such as magnesium are not seen due to serious problems with corrosion. Steel has the problem of increased weight and forged titanium the high cost.

2.1.5. Brakes

Brakes are used for stopping, turning, speed control and keeping the aircraft in parked position. Recently new materials are introduced that have a lower weight and better material properties. One of these relatively new brake materials is carbon.

Carbon has a high thermal conductivity and high specific heat giving a better more uniform distribution of the heat. At high temperatures carbon keeps most of its specific strength contrary to steel. Additional advantages are low maintenance, long service life (up to 5-6 times more landings than steel) and low weight.

Disadvantage is mainly the larger required volume to achieve the same amount of energy absorption. Minor problems that have largely been resolved are the sudden loss of strength due to oxidation of the carbon, temporarily loss of braking due to moisture and high initial cost. The economic advantages of carbon brakes have been the reason why they have been used on the most recent large transport aircraft (Chai and Mason, 1997).

To approximate the brake size and get a weight of the brakes, the following conditions are being considered (Currey, 1988, p.140). 250 stops at design landing weight (with 10 ft/s^2 deceleration), 5 stops at maximum landing weight (with 19 ft/s^2 deceleration) and a single rejected take-off stop (with 6 ft/s^2 deceleration) at the maximum take-off weight. To determine the total kinetic energy and the associated weight at landing the power-off stall speed is needed. This power-off stall speed is 1.2 times the stall speed, which depends on the reference wing area, the weight and maximum wing lift coefficient.

The kinetic energy is equal to:

$$KE = \frac{MV^2}{2} \tag{2.17}$$

To find the kinetic energy in lbf $\cdot$ ft the mass on each tyre M is in lbf and the velocity before applying the brakes V is in ft/s. Currey provides a figure (Currey, 1988, p.142) from which a relation is contracted that estimates the brake assembly weight (lbs) for a given kinetic energy at RTO:

$$W_{\text{brake RTO}} = -9.90e-3KE_{\text{to}}^2 + 5.41KE_{\text{to}} + 9.97e-1 \tag{2.18}$$

for 5 stops at maximum landing weight:

$$W_{\text{brake 5 stops}} = -2.99e-2KE_{\text{max landing}}^2 + 8.46KE_{\text{max landing}} - 2.10 \tag{2.19}$$

and for 250 stops at design landing weight:

$$W_{\text{brake 250 stops}} = -1.12e-1KE_{\text{landing}}^2 + 16.7KE_{\text{landing}} + 13.7 \tag{2.20}$$

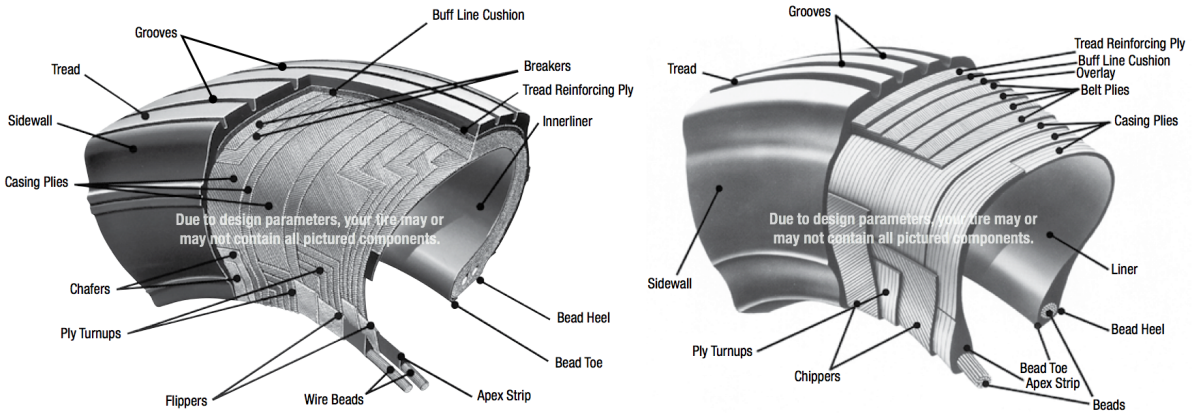

Figure 2.10: A schematic representation of the structure of a bias ply tyre on the left and of a radial tyre on the right (Goodyear, 2002)

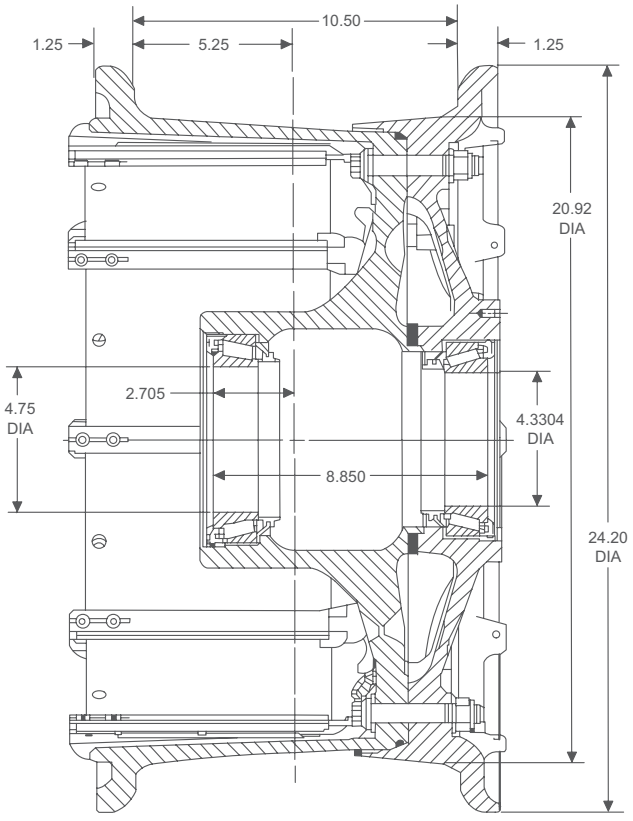

Figure 2.11: An A-frame type wheel cross-section. This wheel can be installed on the Boeing 737. (Honeywell, 2008)

Rim diameter (in)	Outer diameter (in)	Inner diameter (in)	Volume per in width (in^3)
8	7.25	4.75	23.8
9	8	5.1	29.25
10	8.625	5.501	34.7
11	9.375	5.9	40
12	10	6.25	47.9
13	11	6.8	59
14	12	7.376	70.4
15	13	8.126	80.9
16	13.75	8.75	88.4
17	14.75	9.5	100.0
18	15.75	10.126	114.3
19	16.5	10.75	123.1
20	17.5	11.5	136.7
21	18.5	12.25	150.9
22	19.5	12.876	168.5
23	20.375	13.751	176.3
24	21.375	14.375	195.2
25	22.375	15.125	212.1

Table 2.5: Heatsink dimensions (Currey, 1988, p.143)

By averaging these weights the brake weight is found and the brake volume is then estimated with (Currey, 1988, p.142):

$$V = 3.3 W_{\text{brake}} - 84.2 \tag{2.21}$$

Dimensions of the heatsink can then be found by finding the closest match to the selected rim diameter within table 2.5:

Carbon brakes sizing can be derived from steel sizing procedures using scaling factors of 1.28 and 0.40 for the volume and weight respectively (Chai and Mason, 1997).

2.1.6. Brake actuation

Brake actuation systems are currently are mainly hydraulic brake systems. A recent development on the brake actuation system is the development of electric brake systems. Currently electrically actuated brakes are already in service on the Boeing 787 aircraft (see figure 2.12. Advantages of electric brakes includes (Goodrich, 2012):

- reduced maintenance cost and brake system can be easily replaced;
- higher reliability due to redundancy with multiple independent actuators installed on a single wheel;
- system health and brake wear reported automatically.

The hydraulic or electric brake system is however not analysed by the landing gear analysis tool, since it is part of a more detailed design and only the preliminary design is considered.

2.1.7. Kinematics

The design and analysis of landing gear parts relating to the retraction and extension of the gears is called kinematics. Stowage of the landing gear has to be possible within the available space while the increased

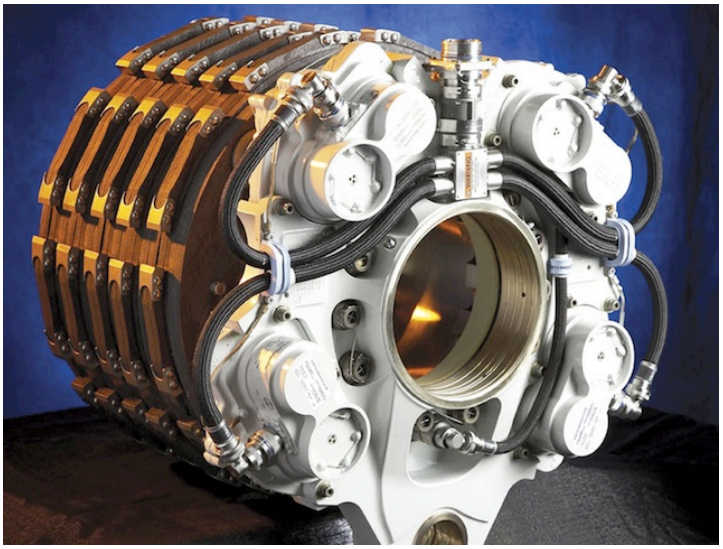

Figure 2.12: The electrically actuated carbon brakes developed by Goodrich and currently in operation on the Boeing 787 (Goodrich, 2012)

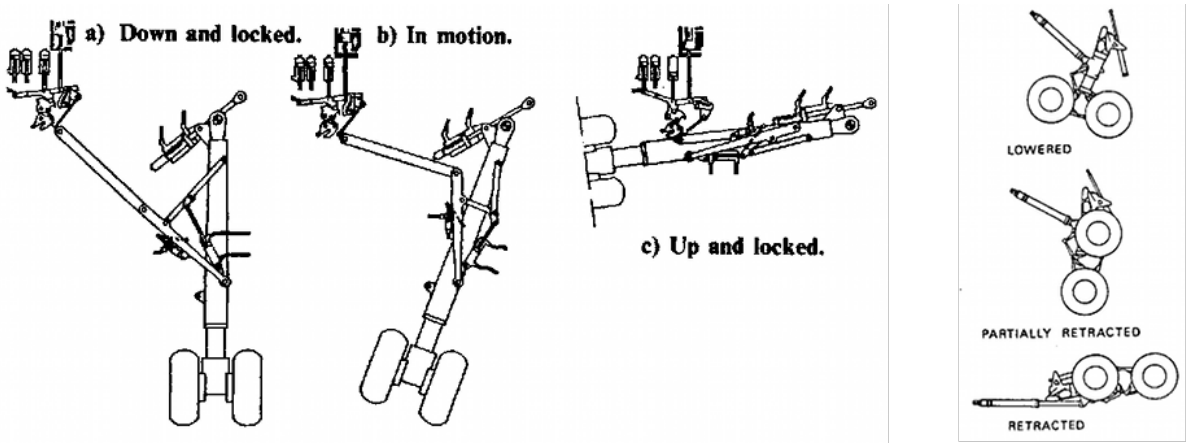

Figure 2.13: A typical retraction scheme of a wing mounted main landing gear on the left (Currey, 1988) and a fuselage mounted main gear on the right (Torenbeek, 1982)

weight due to structural reinforcements is minimal. Goal is to make the retraction scheme as simple as possible (based on economic considerations) (Currey, 1988, p.175). The reduced number of parts and the maintenance cost will increase the total cost more than the increase in weight when more complexity is considered (Chai and Mason, 1997). A requirement that may increase complexity and cost is the requirement to limit the interference between the gear and the surrounding structure as much as possible. Also the gear must be properly supported against side forces.

A retraction mechanism generally consists of a retraction actuator, a folding brace and a locking mechanism. The retraction of the gears positioned on the fuselage is most preferably done in the forward direction. This is to make sure that the gear can lock manually by gravity and air drag in the event of a hydraulic failure. The wing-mounted gears are mainly retracted inboard, because of the limited space available behind the wing spar to stow the gear. When retracting in the inboard direction the largest part of the gear, the bogie and wheels can be stowed in the fuselage. Doors for the main gear wheels may be left out of the design if the drag penalty is of less influence than the increased weight and retraction volume. This has for example been done on the Boeing 737 main landing gear.

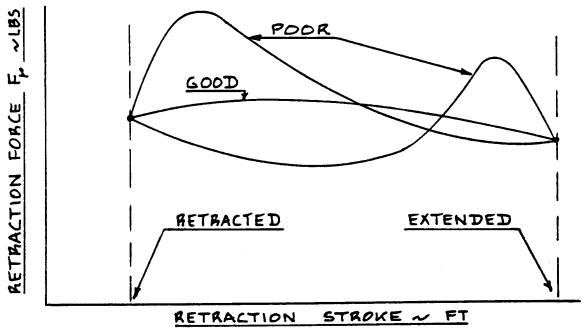

Figure 2.14: Example of a good and poor actuator travel versus actuator load diagram (Roskam, 1989a)

There are many different retraction schemes possible. To keep the retraction scheme as simple as possible each gear rotates about a single axis. To store the gear more efficiently it might also be necessary to rotate the gear bogie about the bogie pivot point (see figure 2.13 right). On most forward retracting gears the shock strut is shortened during retraction to minimise the stowed space. Also drag struts and side struts fold away during retraction with a more complicated scheme than for the main gear. The drag/side strut mechanism and the strut shortening mechanism are part of a more detailed analysis than the preliminary design. It is therefore only included in the multi-body dynamics computer simulation.

For the automatic design of the landing gear an algorithm needs to be developed that can determine the stowed position of the gear such that interferences with the wing/fuselage structure can be found. At the same time the pivot axis of the gear has to be aligned such that the extension or retraction of the gear can be done most effectively.

The actuator needs to be positioned such that the retracted actuator length is not smaller than one half of the extended length. The efficiency of the actuator needs to be checked as well. The forces acting on the gear during retraction are normally the aerodynamic drag and the gear weight. The aerodynamic drag can be determined from the gear drag estimation method from Roskam. The gear weight can be determined from a Class II weight estimation or a more sophisticated method.

Currey mentions that the geometric layout should be replaced with a mathematical analysis as soon as possible and that the moment arms should be checked to be satisfactory throughout the retraction motion.

To check the retraction efficiency, actuator travel should be plotted versus actuator load. The efficiency is then the area underneath the curve (which is the energy absorbed) divided by the product of the maximum actuator load and the total actuator travel. An efficiency of 70 per cent is considered high. The efficiency should be at least about 50 per cent (Torenbeek, 1982) and extreme variations in force should be avoided during retraction as shown in figure 2.14. Generally a low efficiency is used to obtain simplicity or stow the gear in a certain space. Only drawbacks of low efficiency are a longer retraction time or higher weight (Currey, 1988).

The time for extending the gear is limited to 15 seconds at temperatures higher than -29 $^{\circ}C$ and to 30 seconds at temperatures between -54 and -29 $^{\circ}C$. Retraction time of the gear is limited to 10 seconds at all temperatures.

All these checks could be performed by doing a handbook analysis as presented by Roskam, Currey and Chai and Mason. But a simulation with SimMechanics can produce a more accurate result. SimMechanics is therefore used to check the kinematics of the landing gear design.

2.1.8. Shock absorption

Shocks during landing and taxiing need to be absorbed by the landing gear and loads need to be reduced to an acceptable level. Both the tyres and the shock absorber(s) take up most of the loads.

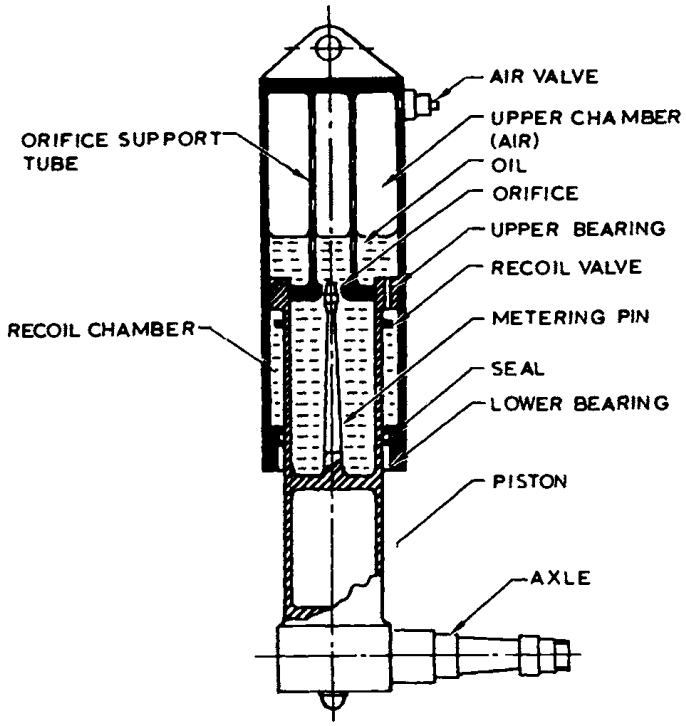

Figure 2.15: Working principle of an oleo-pneumatic shock absorber (Currey, 1988)

Shock absorbers can be constructed differently. They can be made as solid steel springs, rubber springs or a fluid spring with gas and/or oil. An oleo-pneumatic fluid spring is the only type of shock absorber that is considered. This is because of their widespread use on commercial transport aircraft and due to its relative low weight and high gear efficiency (Currey, 1988).

Oleo pneumatic shock absorbers absorb the loads by forcing oil through an orifice to a chamber with dry air or nitrogen. The area of the orifice is often controlled by a metering pin that has a varying radius as shown in figure 2.15. In this way the strut load is kept relatively constant at dynamic loading (Currey, 1988). When shock loads decrease the air pressure will press the oil back to the other chamber at a controlled rate.

The stroke of the absorber is an important design parameter. BothRoskam and Currey provide a method to size the shock stroke. The method of Currey is more detailed and is therefore used and explained here.

In this method first the landing load factor is selected from a range of 0.7 to 1.5. The value of 1.2 is however mostly used. Then using the required sink speed at landing (from FAA/EASA regulations) the energy absorbed during touchdown is approximated. In this approximation the tyres absorb a part of the energy and the other part is absorbed by the shock absorber. When the lift is assumed to be equal to the weight the shock stroke S is equal to (Currey, 1988, p.84):

$$S = \frac{\frac{V^2/2g}{N} - S_t \eta_t}{\eta_s} \tag{2.22}$$

Here V is the sink speed, N the landing load factor, S_t the tyre deflection due to load N. The influence of the tyre efficiency is not very high when the stroke is large and the shock efficiency is high. The tyre efficiency η_t can therefore be fixed at a value of 0.47. The shock absorber efficiency n_s is estimated between 80 and 90 per cent (Currey, 1988, p.35,77).

In the design of the shock absorber the stroke from static to fully compressed can be adjusted to the needs of the designer. For an initial design the ratio between the static and extended pressure is set to $P_1/P_2 = 4/1$. The ratio between static and compressed pressure is set to $P_1/P_3 = 1/3$. This is a typical value for transport

aircraft. The pressure from fully compressed to static varies within the shock absorber according to Boyle's law:

$$P_1 V_1 = P_3 V_3 = constant \tag{2.23}$$

The piston area is the static load divided by the static pressure (assumed 1500 psi). The change in volume is the piston area times the total stroke length. Using these all pressures and volumes can be found at the static, compressed and extended state. Pressures should be between 60 and 6000 psi (Currey, 1988, p.102).

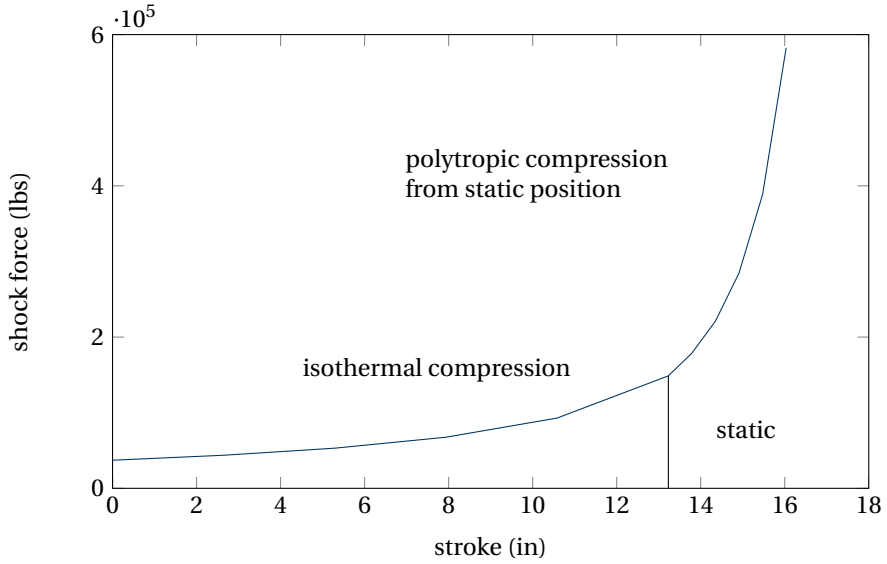

Figure 2.16: Load stroke curve for a Boeing 707-321 aircraft. From 0 to static is isothermal compression and from static to the right polytropic compression.

In figure 2.16 the shock absorber load is plotted as a function of the stroke. This is a combined plot of an isothermal part based on the equation

$$P_x = \frac{P_1 V_1}{V_x} \tag{2.24}$$

and an polytropic part using the equation

$$P_x = P_1 \frac{V_1^n}{V_x^n} \tag{2.25}$$

Assuming $n = 1.35$ for a shock with oil and gas separated during compression. Polytropic compression only has a significant effect on the shock force when the shock stroke is large. Therefore polytropic compression is used from the static stroke position onwards.

Figure 2.16 also shows the load at the fully compressed stroke position. The g-force is then 3.9 for this particular aircraft. For transport aircraft a g-force of 4 when it is fully compressed is suitable (Currey, 1988, p.102).

The minimum allowable overlap between the shock piston and cylinder should be 2.75 times the piston outer diameter. The minimum length of the cylinder should then be the stroke plus the minimum overlap.

The shock absorber orifice that restricts the flow of hydraulic fluid is sized with the following equation

$$A_{\text{orifice}} = \frac{0.3A}{r}\sqrt{\frac{AS}{W}} \tag{2.26}$$

Here A is the piston area, r the compressed load g-force and W the static load (Currey, 1988, p.119).

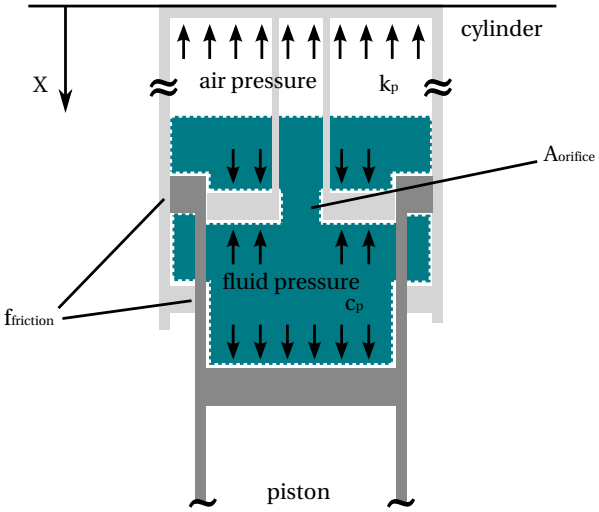

Figure 2.17: Model of the oleo-pneumatic shock absorber showing parameters used in equations.

A model of the oleo-pneumatic shock is a spring damper system. The pneumatic force of the shock can be modelled as a nonlinear spring which produces a force of (Milwitzky and Cook, 1953):

$$F_p = P_2 A \left(\frac{V_2}{V_2 - AX} \right)^n \tag{2.27}$$

Where P_2 and V_2 are the pneumatic pressure and volume at the fully extended state. This equation is derived using equation 2.25. The flow of oil through an orifice of the oleo-pneumatic shock produces a damping force that depends on the velocity squared and is given by (Milwitzky and Cook, 1953):

$$F_h = \frac{-\rho A_h^3}{2(C_d A_{\text{orifice}})^2} \dot{X} \left| \dot{X} \right| \tag{2.28}$$

ρ is the density of the hydraulic fluid, $A_h = A - A_{\text{orifice}}$ is the hydraulic area and C_d is the discharge coefficient.

The discharge coefficient can change during compression and is a function of fluid properties and the orifice shape. The discharge coefficient can range between 0.6 and 1.0. A different discharge coefficient can result in a difference of maximum displacements of 20 per cent (Milwitzky and Cook, 1953, p21). The orifice and fluid properties are part of a more detailed design of the shock absorber. Since there is only an initial design considered the discharge coefficient is set at a fixed value of 0.8.

The friction within the shock absorber will result in an additional force:

$$F_f = \mu(F_p + F_h) \tag{2.29}$$

A pessimistic value of the coefficient of friction, μ is 0.1 (Currey, 1988, p.99). Then the total shock absorber force is equal to

$$F = F_p + F_h + F_f \tag{2.30}$$

2.1.9. Economics of landing gear design

As mentioned in the previous sections, cost are an important factor in the landing gear design decisions that are made. Costs are to be considered for the design process, manufacturing, maintenance and disposal at the end of life.

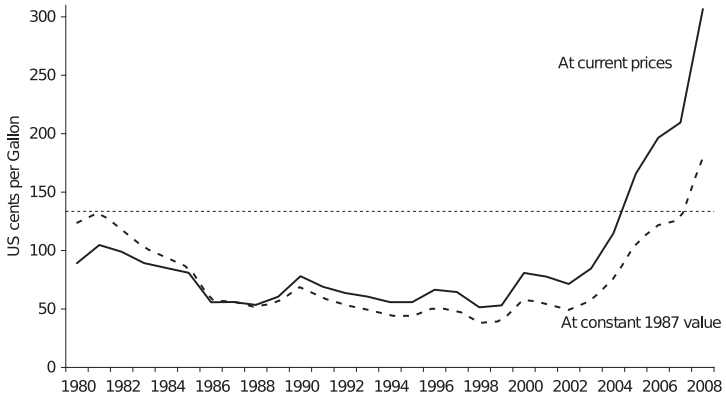

Figure 2.18: Average fuel price, from 1980 to 2008, paid by US airlines using current dollar cents and using 1987 dollar cents (Doganis, 2009)

The total cost of the gear as part of the aircraft when the aircraft will be delivered to the customer has to take into account many aspects. Some of these aspects include:

- development;
- materials;
- production processes;
- certification;
- marketing;
- overhaul;
- refurbishment;
- spares.

A study by Chai and Mason estimates the total gear program cost to be $10 to $12 million dollars. Relatively fixed costs are the cost of tyres, wheels and brakes. A bias ply main gear tyre for the Boeing 747 is priced at $2100, while a comparable radial tyre for a Boeing 777 main gear is $2900. The more expensive radial tyre is however still mainly chosen by airlines for new types of aircraft, because of a longer service life and lower weight. Wheels and tyres are replaced after 300 landings, making the cost for the wheel and tyre $5 per landing. Carbon brake replacement on the 747 is done after 1200 to 1500 landings (results in bake cost of $10 per landing).

Development of new larger tyres is costly, due to the cost of new manufacturing and testing equipment that will be necessary. The maximum size of tyres currently used is therefore limiting. For bias-ply tyres the maximum diameter is 56 inch and for radial tyres 58 inch (Chai and Mason, 1997).

Maintenance cost form an important part of the total operating cost: about 10% in the recent years (Doganis, 2009). The time between overhaul of the landing gear varies between 33000 and 42000 flight hours. Overhaul of the landing gear is preferably done on the complete gear to minimise downtime. Cost of this overhaul for a Boeing 747 type aircraft gear is estimated at $400000.

Weight is an important factor in cost calculations. When the aircraft airframe weight can be reduced with 1 per cent, the fuel consumption reduces with 0.25% for small aircraft (e.g. B737) to 0.50% for large aircraft (e.g. B747) (Greene, 1992).

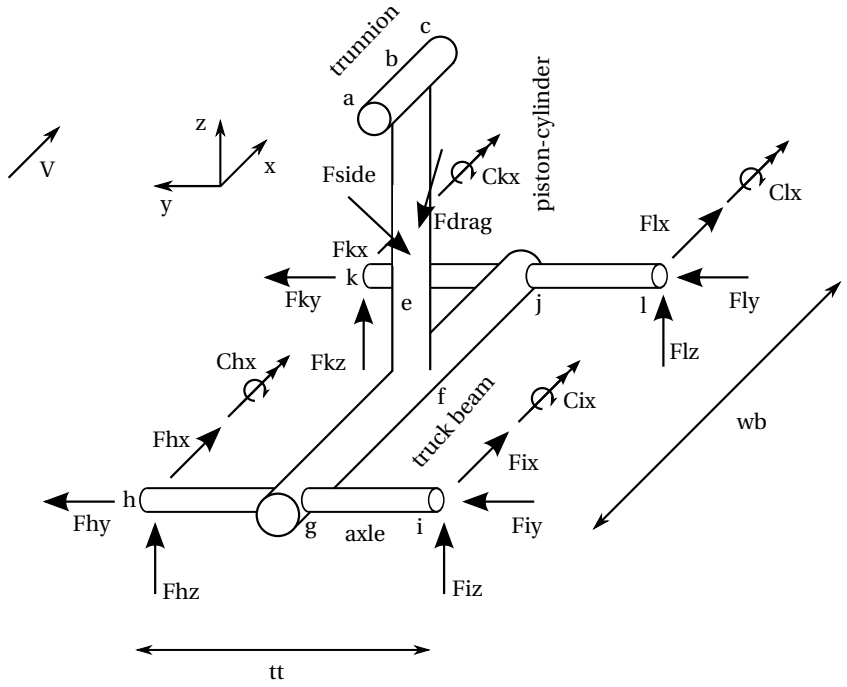

Figure 2.19: Structural model of a 4 wheel landing gear bogie used in the weight estimation. All externally applied loads are shown.

The part that fuel prices take up of the total operating cost has increased considerably the last 2 decades. In 1994 the fuel and oil cost were 11.4 per cent of the total operating cost, while this has increased to 25.4 per cent in 2007 (Doganis, 2009). Figure 2.18 shows the recent steep fuel price increase. Prices are not expected to decrease, due to factors as larger demand, lower reserves and the use of oil production quotas by oil producing countries. Further reductions in the weight of the landing gear is thus becoming increasingly important.

A further more detailed analysis of the impact of cost on the landing gear design is difficult to make. This is because there is very limited cost information available for aircraft systems, including the landing gear. Manufactures are not willing to present this information due to competitive concerns.

2.2. Landing gear assembly weight estimation

Estimating the landing gear total weight based on empirical relations cannot always produce accurate estimates. Also they do not respond to changes in landing gear design variables, making optimisation to minimum weight impossible (Chai and Mason, 1996, p. 72). A landing gear weight can be estimated analytically by modelling the landing gears as simple geometric shapes. Maximum stresses within the structure, due to dynamic and static loads, are calculated with simplified analytical equations and assuming an idealised structure. The dynamic and static loads, described in section 2.2.3, are the loads that are considered.

Figure 2.19 shows the three dimensional structural model used for the analytical weight estimation. In appendix A the complete landing gear structural model is shown, including applied and internal forces and moments for each component separately.

2.2.1. Tube stresses

The landing gear structure is constructed out of circular tubes. The structure is sized with fixed radii (scaled to the piston area) and by varying the thicknesses of the tubes. A beam can be accurately modelled as a thin walled structure if the maximum diameter divided by the thickness is larger than 20 (Hibbeler). The thicknesses required are expected to be larger than one tenth times the mean radius of the tubes. A thin-

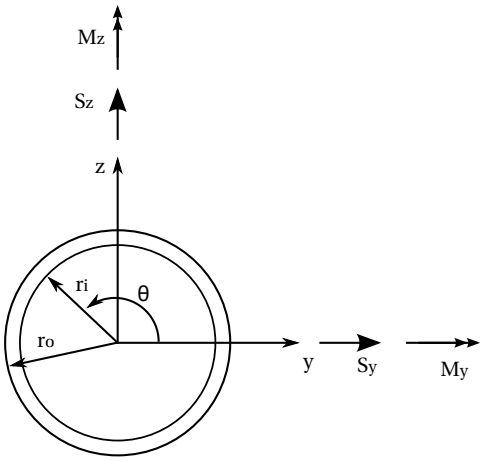

Figure 2.20: Tube cross-section showing the parameters used in the derivation of the stresses

walled approximation is therefore not valid and not used.

Figure 2.20 shows the used parameters in the following derivation graphically. The geometric properties of the tubes are:

$$A = \pi(r_o^2 - r_i^2)$$
$$J = \pi/2(r_o^4 - r_i^4)$$
$$I_{yy} = I_{zz} = J/2 = \pi/4(r_o^4 - r_i^4)$$

The normal stress in a tube due to the combination of an axial force and bending moments is

$$\sigma_{xx} = N/A + M_y/I_{yy} \cdot z - M_z/I_{zz} \cdot y \tag{2.31}$$

The maximum normal stress occurs at the outer edges

$$\sigma_{xx_{max}} = N/A + \frac{M_y \cdot r_o \sin(\theta) - M_z \cdot r_o \cos(\theta)}{\pi/4(r_o^4 - r_i^4)}$$

Differentiate with respect to θ and find the maximum at $d\sigma_{xx}/d\theta = 0$

$$\frac{\sigma_{xx_{max}}}{dx} = \frac{M_y \cdot r_o \cos(\theta) + M_z \cdot r_o \sin(\theta)}{\pi/4(r_o^4 - r_i^4)} = 0$$

solving for θ results in

$$\tan(\theta_{max}) = \frac{-My}{Mz} \tag{2.32}$$

which can be rewritten using $\sin(\theta)^2 = (1 - \cos(\theta)^2)$

$$\cos(\theta_{max}) = \frac{M_z}{\sqrt{(-M_y)^2 + M_z^2)}} \tag{2.33}$$

and using $\cos(\theta)^2 = (1 - \sin(\theta)^2)$

$$\sin(\theta_{max}) = \frac{-M_y}{\sqrt{M_z^2 + (-M_y)^2}} \tag{2.34}$$

Using these equations the maximum normal stress in the tube is at $\theta = 0$ and $\theta = \pi$

$$\sigma_{xx_{max}} = \frac{N}{\pi(r_o^2 - r_i^2)} \pm \frac{-r_o\sqrt{M_z^2 + (-M_y)^2}}{\pi/4(r_o^4 - r_i^4)} \tag{2.35}$$

Then the shear stress in the tube due to an axial torque

$$\tau_{xs_{max}} = \frac{Tr_o}{J} = \frac{Tr_o}{\pi/2(r_o^4 - r_i^4)} \tag{2.36}$$

The first moment of area which is needed to get the shear stresses due to shear forces is

$$Q_y = \int_A z \, \mathrm{d}A = \int_{r_i}^{r_o} \int_{-\pi/2+\theta}^{\pi/2-\theta} z \, r \mathrm{d}\theta \mathrm{d}r = \int_{r_i}^{r_o} \int_{-\pi/2+\theta}^{\pi/2-\theta} r \sin(\theta + \pi/2) \, r \mathrm{d}\theta \mathrm{d}r$$

$$= \frac{2}{3}\cos(\theta)(r_o^3 - r_i^3)$$

and the first moment of area needed for the bending about the y-axis is

$$Q_z = \int_A y \, \mathrm{d}A = \int_{r_i}^{r_o} \int_{-\theta}^{\theta} y \, r \mathrm{d}\theta \mathrm{d}r = \int_{r_i}^{r_o} \int_{-\theta}^{\theta} r\cos(\theta) \, r \mathrm{d}\theta \mathrm{d}r$$

$$= \frac{2}{3}\sin(\theta)(r_o^3 - r_i^3)$$

Shear stress due to shear forces in the y and z direction is

$$\tau_{xs} = \frac{-S_y Q_z}{I_{zz} t} - \frac{S_z Q_y}{I_{yy} t} \tag{2.37}$$

Filling in the equations for the first moment of area results in

$$\tau_{xs} = \frac{-2}{3I_{zz}t}(S_y(\sin(\theta)(r_o^3 - r_i^3)) + S_z(\cos(\theta)(r_o^3 - r_i^3)))$$

$$= \frac{2(r_o^3 - r_i^3)}{3\pi/4(r_o^4 - r_i^4)t}(-S_z\cos(\theta) - S_y\sin(\theta))$$

The maximum shear stress occurs when $\frac{\mathrm{d}\tau_{xs}}{\mathrm{d}\theta} = 0$

$$\frac{\mathrm{d}\tau_{xs}}{\mathrm{d}\theta} = \frac{2(r_o^3 - r_i^3)}{3\pi/4(r_o^4 - r_i^4)t}(S_z\sin(\theta) - S_y\cos(\theta)) = 0$$

which results in (similarly as for $\sigma_{xx_{max}}$)

$$\tan(\theta_{max}) = \frac{S_y}{S_z}$$

$$\sin(\theta_{max}) = \frac{S_y}{\sqrt{S_y^2 + S_z^2}}$$

$$\cos(\theta_{max}) = \frac{S_z}{\sqrt{S_y^2 + S_z^2}}$$

Using these equations in the equation for shear stress

$$\tau_{xs_{max}} = \pm\frac{8(r_o^3 - r_i^3)}{3\pi t(r_o^4 - r_i^4)}\sqrt{S_y^2 + S_z^2} \tag{2.38}$$

The total maximum shear stress due to torque and shear forces is then using equation 2.36 and 2.38

$$\tau_{xs_{max}} = \frac{2}{\pi(r_o^4 - r_i^4)}(Tr_o \pm \frac{4(r_o^3 - r_i^3)(\sqrt{S_y^2 + S_z^2})}{3t}) \tag{2.39}$$

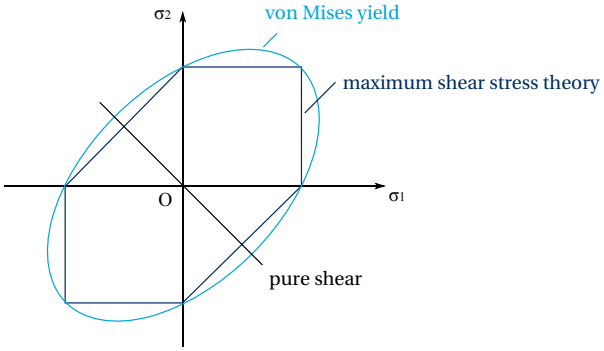

Figure 2.21: Comparison Von Mises yield criterion with the maximum shear stress theory. The difference is largest at pure shear.

The maximum shear stress theory predicts when yielding of the material begins. The maximum absolute shear stress to prevent yielding should be (Vable, 2012, p.486):

$$\tau_{max} = \frac{\sigma_Y}{2} \tag{2.40}$$

The maximum-distortion-energy theory sometimes also called the Von Mises yield criterion gives the maximum stress (Vable, 2012, p.487):

$$\sigma_1^2 - \sigma_1\sigma_2 + \sigma_2^2 = \sigma_Y^2 \tag{2.41}$$

Where $\sigma_1 = \frac{\sigma_{xx}}{2} + R$ and $\sigma_2 = \frac{\sigma_{xx}}{2} - R$ are the two principal stresses in Mohr's circle of radius R. Rewriting this equation and using $R = (\sqrt{\frac{\sigma_{xx}-\sigma_{yy}}{2})^2 + \tau_{xs}^2}$ and equation 2.41 results in

$$\sqrt{\sigma_{xx}^2 + 3\tau_{xs}^2} = \sigma_Y \tag{2.42}$$

The Von Mises yield criterion is used to determine limit loads, because it gives a more accurate prediction of the yield load than the maximum shear stress criterion. Actual load tests have shown that a maximum improvement in accuracy of 15 percent can be achieved by using the Von Mises yield criterion (Hibbeler, p.527). This happens when the structure is loaded in pure shear. This is also made visible in figure 2.21. The eliptical curve represents the Von Mises Yield criterian. If the stress is outside the boundary of the curve the material will fail.

Since the structure of the landing gear is based on the safe live principle an addition safety factor is applied. By adding a safety factor the structure is capable to deal with fatigue during the entire life of the aircraft structure.

2.2.2. Side struts sizing

Both the drag strut and the side strut can be simplified as a truss member. A truss is a two force member that is only loaded axially. When the truss is loaded axially in tension the required thickness to prevent yielding can be found from the yield criterion: $\sigma_Y = F/A$. The side struts cross-section can be modelled as a thin-walled I-beam with a constant thickness making the area, A equal to $t(2w+h)$ and moment of inertia $I = t(h/12 + w/2)h^2$.

When the truss is loaded in compression yielding is not longer the limit. The truss will buckle before yielding. The critical buckling load is equal to (Vable, 2012, p.503):

$$F_{cr} = \frac{\pi^2 EI}{l^2} \tag{2.43}$$

2.2.3. Landing gear dynamics analysis load cases

Several different limit load cases have been specified in the Certification Specifications Part 25. Loads are applied externally and the effect of the centre of gravity position has to be taken into account. The most critical position of the cg has to be considered. The maximum descent velocity to be considered is 10 feet per second. Then the analysis of the loads on the landing gear also has to take into account (European Aviation Safety Agency, 2012, p. 1-C-16):

- dynamic characteristics of the gear
- spring back and spin-up
- the rigid body response
- if significant: the airframe structural dynamic response

There are 7 different load cases that need to be considered. These are shown graphically in figure 2.22 to 2.26. In these figures T is the forward component of the inertia force and I is the pitch and roll moment of inertia that are needed for equilibrium. The subscript N and M stand for the nose gear and for the main gear.

1. The first load case is a landing at level attitude at the limit descent velocity of 10 fps at design landing weight. For a coefficient of friction between the ground and tyres a value of 0.8 is sufficient. This means that the horizontal force D_{M} on the main gear is 0.8 times the vertical force V_{M} and a similar horizontal load is applied on the nose gear.
2. The second load case is the tail down landing case, which is the same as the first only now the attitude of the aircraft is at the maximum possible angle of attack. The tail structure then hits the ground or the stall angle will be attained at this position.
3. Then the third load case is a landing on a single wheel. The ground forces on the gear are the same as for the first load case as shown in figure 2.23.
4. For the fourth load case, the lateral drift landing, only the main gear is in contact with the ground. A side load in the inward direction has a magnitude of 0.8 times the vertical reaction on one side (V_M) and on the other side a load of 0.6 times V_M acts outwards. These forces are assumed to be resisted by inertial forces and moments as is visible in figure 2.24.
5. A braked roll at design take-off weight (and at 1.2 times the design landing weight) is the fifth load case. A drag force is applied to each wheel of 0.8 times the vertical ground load on the wheel.
6. Then the sixth load case is a static loading condition: the ground turning load case. The side load on each wheel is 0.5 times the vertical ground load on each wheel. These forces are counteracted by a side load of 0.5 times the weight acting at the location of the cg (figure 2.25).
7. The final load case is a pivoting load case. On one side of the gear the brakes are applied with a coefficient of friction of 0.8. The aircraft is for this case at static loading conditions as can be seen in figure 2.26.

There are more load cases mentioned in CS 25 (European Aviation Safety Agency, 2012, p. 1-C-16), but the previously mentioned ones are the most significant. For example a rebound landing, a towing load case and a reversed braking load case are described.

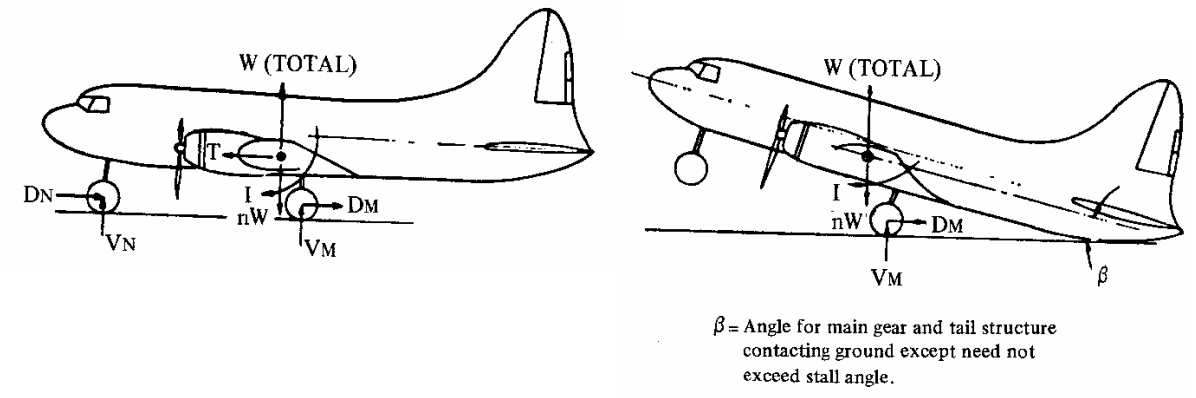

Figure 2.22: Level load case on the left and the tail down load case on the right (European Aviation Safety Agency, 2012, p. 1-App A-2)

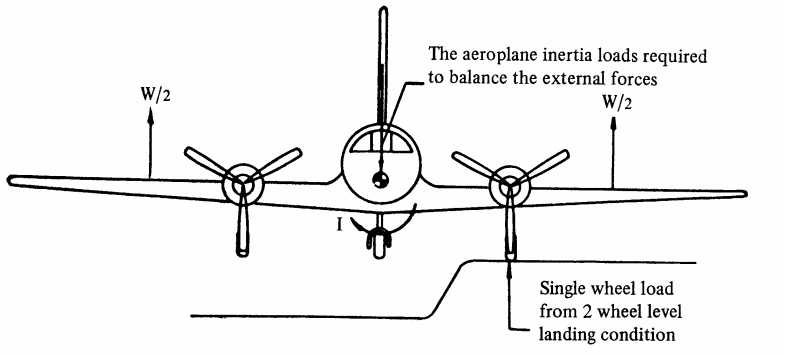

Figure 2.23: One wheel landing load case (European Aviation Safety Agency, 2012, p. 1-App A-3)

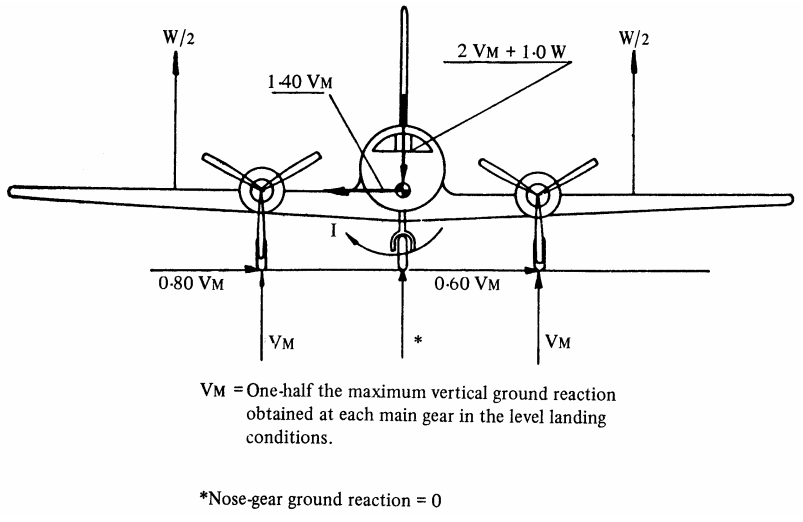

Figure 2.24: The lateral drift landing load case (European Aviation Safety Agency, 2012, p. 1-App A-3)

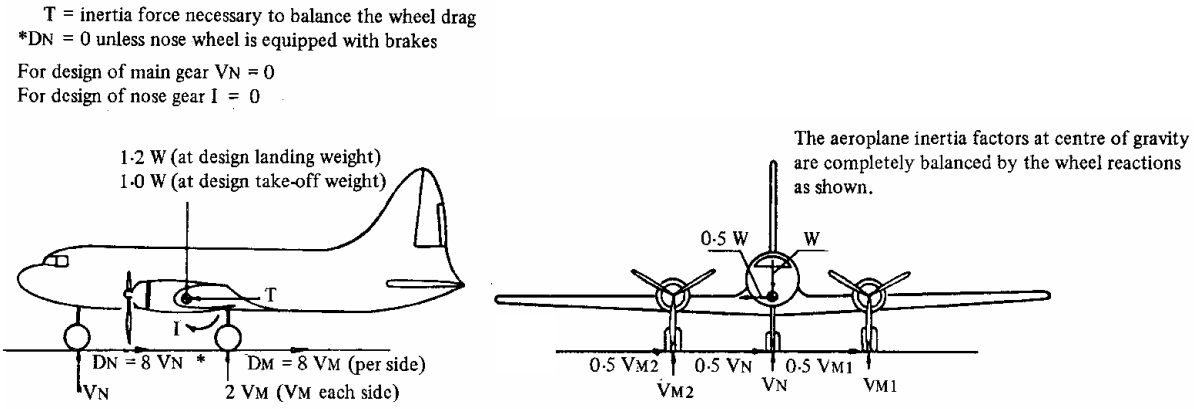

Figure 2.25: Braked roll load case on the left and the ground turning load case on the right (European Aviation Safety Agency, 2012, p. 1-App A-4)

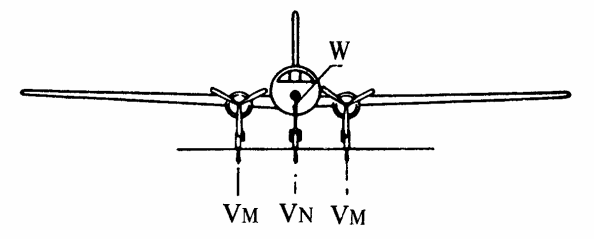

Figure 2.26: The pivoting load case (European Aviation Safety Agency, 2012, p. 1-App A-5)

2.3. Landing gear analysis

The landing gear can be seen as a system of interconnected rigid and deformable components, a multi-body system. The dynamics of this system is a complex problem, because it's highly nonlinear. In most cases the problem can only be solved with computer-based techniques (Shabana, 2005).

Matlab SimMechanics can model the multi-body dynamics of the landing gear model. The multi-body system is modelled with blocks that represent bodies, joints, constraints and force elements. Using provided input parameters SimMechanics then evaluates the equations of motion of the complete mechanical system and tests the landing gear for different load cases.

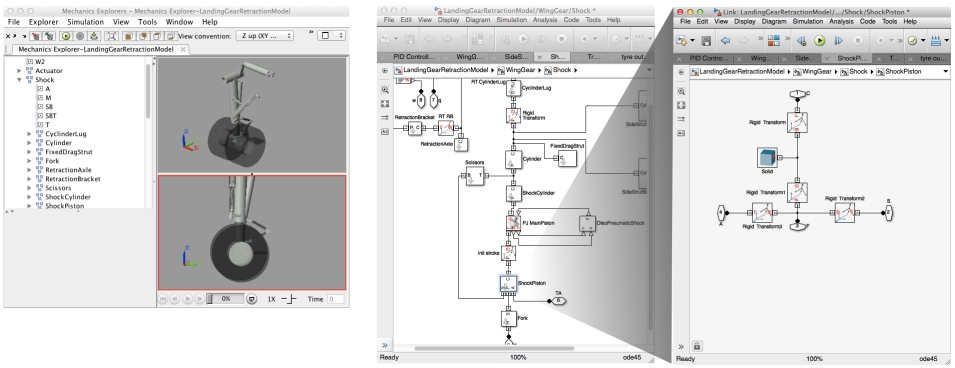

Figure 2.27: SimMechanics displaying a portion of the model of a landing gear (Mathworks, 2012)

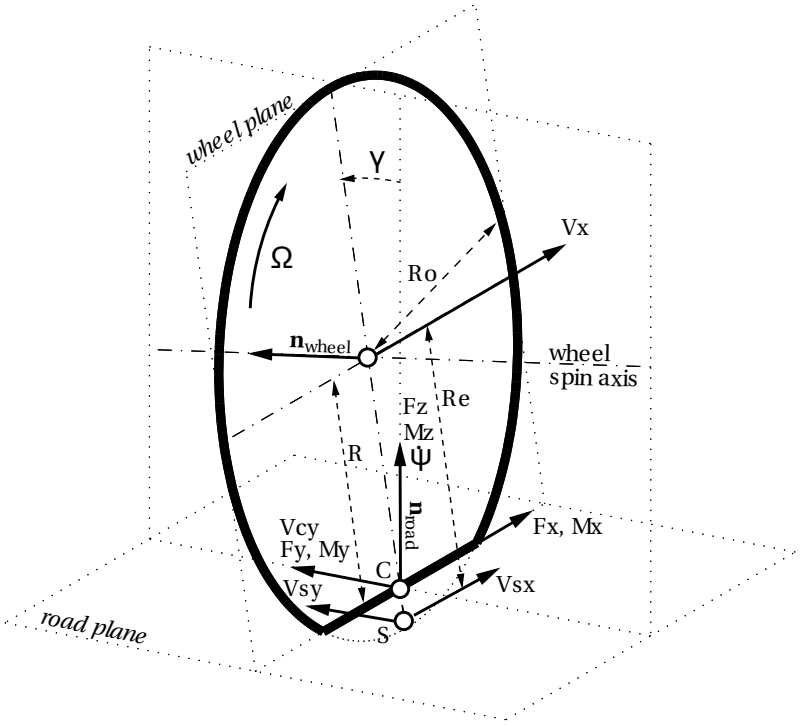

Figure 2.28: Tyre model description (Besselink, 2000)

2.3.1. Tyre model description

Simulating the dynamics of the landing gear can only be done accurately when using an accurate tyre model. The widely used tyre model of Pacejka, an empirical model called 'Magic Formula Tyre Model, can provide this accuracy.

MF-Tyre, made by TNO Automotive, is a software implementation of the tyre model of Pacejka. This tool is mainly focussed on automotive tyres, but new tyre data can be inserted such that aircraft tyres can also be modelled.

A description of the equations used in the MF-tyre implementation have been made available (Pacejka, 2006) (TNO Automotive, 2010), such that these can be used in the implementation. Output forces are forces in x, y direction F_x, F_y and moments M_x, M_y, M_z at the tyre contact point.

Input variables of the tyre model are the tyre slip angle α, the turn slip angle Φ_t, the forward velocity V_{cx}, the tyre inclination angle γ and the longitudinal slip κ. The tyre slip angle is equal to $\tan\alpha = -V_{cy}/V_x$. A turn slip angle occurs when the wheel is on a circular path with radius R_c and is equal to $\Phi_t = -\Psi/V_x = 1/R_c 2$ (as shown in figure 2.29). The tyre longitudinal slip is defined as $\kappa = -\frac{V_x - \Omega R_e}{V_x}$, where Ω is the radial velocity of the tyre.

In vertical direction the tyre vertical is modelled as a linear spring damper with stiffness K_{tyre} and damping coefficient C_{tyre} (see figure 2.31). The vertical force the tyre produces is then equal to:

$$F_z = -K_{\text{tyre}} X - C_{\text{tyre}} \dot{X} \tag{2.44}$$

TNO Automotive provides basic tyre model parameters for an aircraft tyre (H40x14), that is similar to an Airbus A320 tyre. The tyre data of this tyre is of the reduced format, because there is limited data available. Because the input data is of reduced format, estimation of the tyre response is less accurate. The unknown parameters are given the default value. The parameters included are the tyre dimension, nominal load, vertical stiffness, vertical damping, friction coefficients, slip stiffness coefficients and relaxation length coeffi-

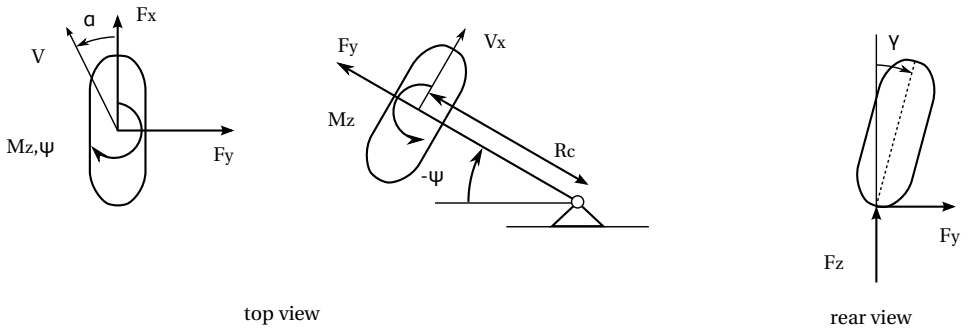

Figure 2.29: Tyre model coordinate system used

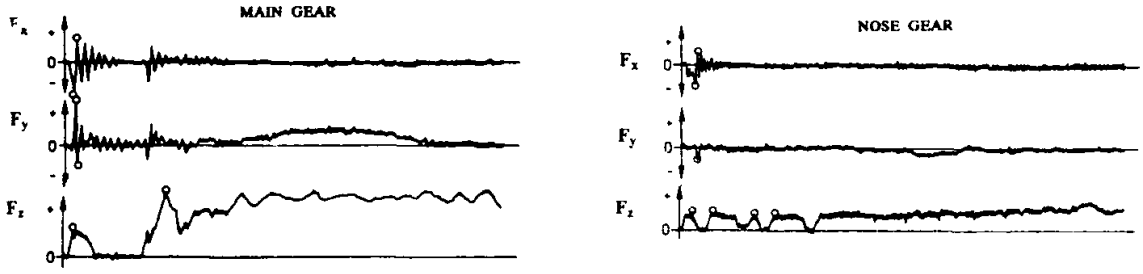

Figure 2.30: Measurement results showing the time histories of a typical loading during landing for an Airbus A300B2 main and nose landing gear (Ladda and Struck, 1991). The y-axis in the graphs represents the force in x-, y- and z-direction from top to bottom.

cients both longitudinal and lateral. Rolling resistance and aligning coefficients are also included. The highly recommended parameters (TNO Automotive, 2012) are thus available within the aircraft tyre data file and it can thus be used to model the combination of lateral and longitudinal slip, tyre relaxation length effects and response due to short wavelength obstacles.

2.3.2. Drop test load case

In figure 2.30 it can be seen that a typical landing impact load on the main gear is only about 40% of the static load (Christy, 2009), (Ladda and Struck, 1991). At a normal touchdown procedure only part of the aircraft weight is put on the ground. This is because the wings still provide a large lift force at touchdown. When speed is decreased during landing rollout, the lift is decreased gradually until all of the total aircraft weight presses on the landing gear.

The CS-25 certification specifications specify that during the landing the lift provided by the wings is equal to the landing weight. The dynamic landing load cases are at a descent velocity of 10 ft/s. For the dynamic touchdown the vertical ground load factor per shock strut N_v can be estimated with (Kraus, 1970):

$$N_v = \frac{F_v}{cW} = \frac{1}{\eta_s S \cos\theta}\left(\frac{V_s^2}{g} + S\cos\theta\right) \tag{2.45}$$

Here c is the load distribution factor, η_s the shock efficiency, S the shock stroke (in), V_s the descent velocity (ft/s), g the gravitational acceleration (32.17 ft/s^2), θ the pitch angle at touchdown. This vertical ground load factor is applicable locally at a single landing gear strut (see figure 2.31). At the aircraft centre of gravity a different load factor applies. Assuming the lift is equal to weight the load factor at the aircraft cg is equal to (Currey, 1988, p.34):

$$N_{cg} = \frac{\sum F_{ext}}{W} = \frac{F_v + L}{W} = N_v + 1 \tag{2.46}$$

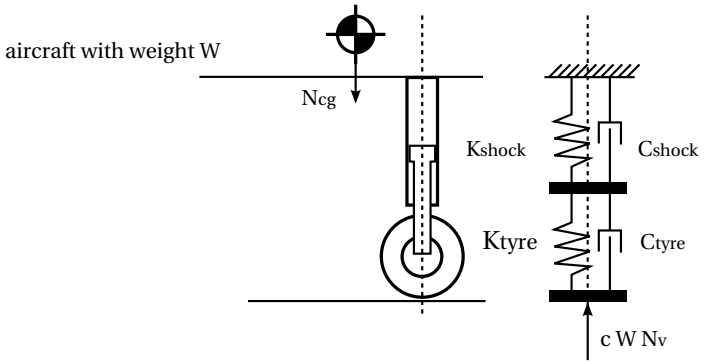

Figure 2.31: Tyre and shock absorber modelling. The tyre is modelled as a linear spring damper and the oleo-pneumatic shock as a nonlinear spring damper.

Tyre spin-up forces should also be taken into account for the drop test load case (European Aviation Safety Agency, 2012, p. 1-C-16). The maximum spin-up force that will occur is when the tyres are at rest before touchdown. The difference in speed between the ground and the tyre is the landing velocity. The tyre will spin-up from zero to landing velocity in a very short amount of time, putting a high load on the tyres.

3

Implementation and use cases

The implementation is split up in a landing gear design part and a landing gear analysis part. Implementation starts with designing the landing gear.

3.1. Implementing the landing gear design

The landing gear design is completely integrated into the TU Delft Aircraft Initiator, which is built using Matlab (Elmendorp, 2014). Using specified top level requirements, the Initiator can generate an aircraft parametric model. Which includes geometry and performance characteristics of a conventional or unconventional aircraft. The initiator is built-up out of several separate modules. In this way the user can generate an aircraft using only the required modules. Landing gear design is done in a new module called PositionLandingGear and in the class 2 weight estimation module (which is extended with basic landing gear design methods).

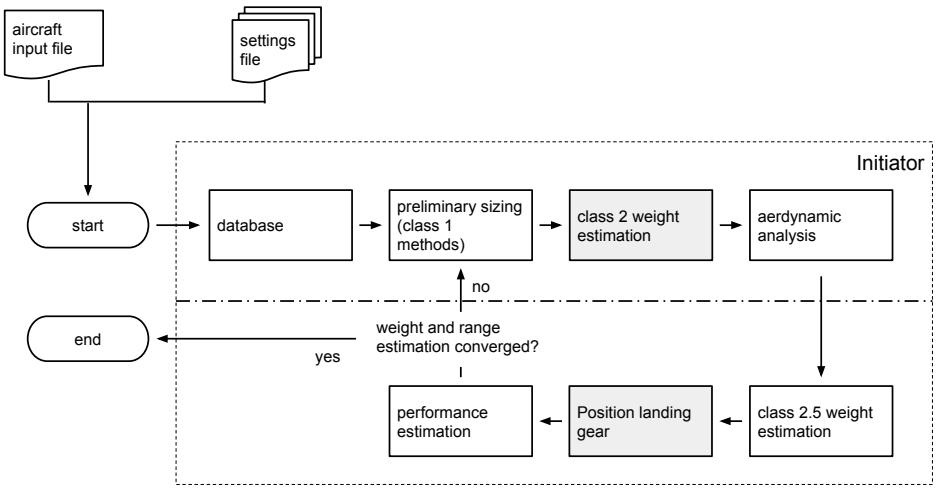

Figure 3.1: Overview of the workflow to make an aircraft class 2.5 weight estimation

The workflow needed to make a class 2.5 weight estimation of the aircraft is shown in figure 3.1. It starts with an aircraft input file and settings file that defines all requirements set by the user. Using these, similar reference aircraft are selected from a database. These are used to make a first estimate of the weight, performance and general geometry. Then a closer look is taken at the design of the cabin and a more detailed class

2 weight estimate of aircraft components can be made.

Now there is enough information available to make a class 2.5 component weight estimation which runs several modules iteratively. These modules include control allocation, aerodynamics estimation (AVLVLM), wing weight estimation (EMWETWeight), drag estimation, fuselage weight estimation (Schmidt, 2013) and finally landing gear weight estimation (position landing gear). The iteration stops when the estimation of the aircraft weight and range has converged.

3.1.1. Class 2 weight estimation

A class 2 weight estimation (CWE2) is a method that uses empirical relations to improve the class 1 weight estimation. The CWE 2 module implemented in the Initiator uses the empirical relations of Raymer to estimate aircraft component weights. One of these components is the landing gear weight.

The class 2 weight estimation methods require little computation time and are applicable to both conventional and unconventional aircraft. Raymer's empirical gear weight estimation relation only requires 10 different parameters for both the nose and main gear. Therefore simplified methods can be used to find the location of the gears. The results of the class 2 weight estimation is thus not a detailed analysis of the landing gear layout and position. For this purpose a separate module has been developed.

Class 2 landing gear weight estimation process

The flow of work performed by the CWE2 landing gear weight estimation is shown in figure 3.2. The gear component weight estimation is done last in the class 2 weight estimation. This is done because then the most accurate position of the aircraft centre of gravity is known by combining all aircraft component cg positions.

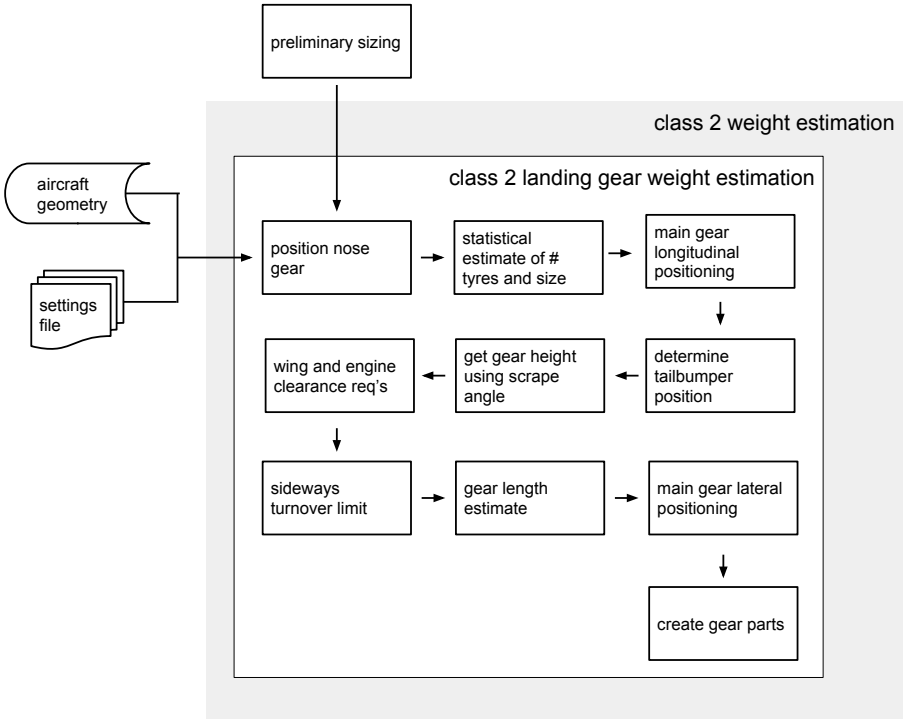

Figure 3.2: Class 2 landing gear weight estimation workflow

The nose gear is assumed to consist of 2 tyres and it is placed at a fixed position based on nose gear loading settings. It is also checked if nose gear loading will add limitations to aircraft operations. This will be explained in section 3.1.1.

The number of wheels required for the main landing gear are determined from a statistical relationship between the maximum take-off weight and the number of main gear wheels. All gear tyre dimensions are found using a relation from Raymer (Raymer, 1999, p.234). When the number of wheels is larger than 12, the number of main gear struts is set to 4. The track of the main gear bogie is fixed to 2.5 times the tyre width. This is based on reference data from reference aircraft shown listed in appendix D.

By checking the fuselage width to span ratio it can be determined if all main gears can be placed on the fuselage. For gears that can be placed on the fuselage, the longitudinal position of the main gears is only related to the aft centre of gravity position (independent of the wings). This also holds for aircraft that have a high wing and aircraft that have their main wing positioned far forward. Placement of the main landing gears under the nacelle of a turboprop is currently not taken into account.

If the wing is positioned far aft of the fuselage (canard), the gear can be placed on the wings. The longitudinal position of the main gear is set near the front spar position. This is done by setting the gear to a certain percentage of the mean aerodynamic chord depending on the forward or aft sweep of the wing. In this way the exact spar locations do not need to be calculated and complexity is reduced. For a conventional aircraft all these exceptions do not hold and the main gear can be positioned on the wing near the auxiliary spar. The MAC percentages used for the longitudinal position is 0.55 for an aft swept wing (Currey, 1988) or 0.88 for a forward swept wing. For the forward swept wing the MAC percentage is higher, because then a point inboard the MAC on the wing is further aft.

The point where the fuselage would hit the ground at take-off (a too large rotation) is called the tail bumper position (see figure 3.3). From the geometry of the fuselage xz-plane cross-section a third order polynomial is constructed. The location of the tail bumper is found when the derivative of the polynomial equation is equal to the fixed scrape angle of 12 degrees (to keep dependency on other modules and calculation time minimal). Only when the aft fuselage is not steep enough the tail bumper is positioned at the end of the fuselage.

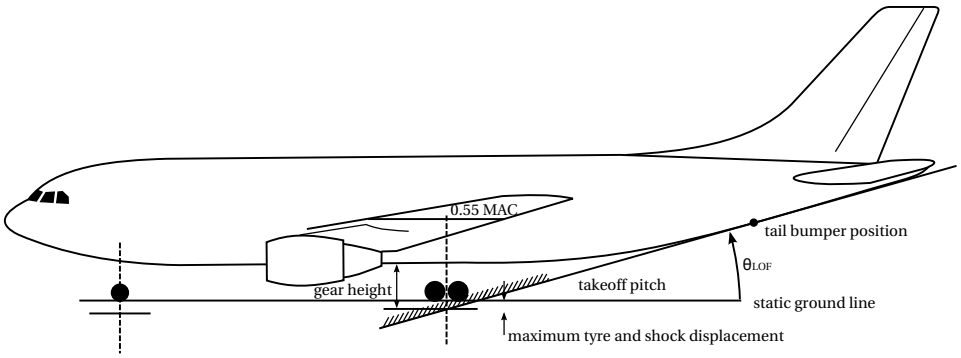

Figure 3.3: Side view showing take-off rotation limit and definition of main gear height.

The main gear height (as defined in figure 3.3) is the vertical distance of the line from the tail bumper forward towards the longitudinal position of the main gear. The clearance between the tyres and fuselage or other aircraft parts should be minimally 6 inch. Otherwise the main gear height is increased (Torenbeek, 1982).

The minimum lateral position of the main landing gear is found from engine clearance, wing clearance and the sideways turnover limit requirements. The engine clearance is found by drawing a line at 5 degrees (plus 6 inch clearance) from the lowest point of the engines to the main gear position. Similarly for wing clearance a line of 5 degrees plus clearance is drawn from the wing tip. Turnover of the aircraft can occur along the line from the most outboard wheel towards nose wheel, due to wind shear or a high speed turn during taxi. This turnover angle should not be larger than 63 degrees (Currey, 1988) as explained in section

2.1.2. The maximum of the engine, wing and turnover limits is the minimum lateral gear position.

Another check is done to see whether or not the gears collide when retracted. This will put an additional constraint on the lateral gear position. To do this, the complete length of the main gear needs to be known. In the case of a wing mounted main gear this is the length from the ground to the wing connection point. In the case of a fuselage mounted gear the gear length is the distance from the ground to the passenger floor. In case of a high wing with fuselage mounted main gears it is assumed these are placed in pods at the most outboard part of the fuselage. The gear length for this case is estimated as the length from the ground to the fuselage belly.

At this point the location of the main gear and the general dimensions are known. The resulting landing gear is then added to the aircraft model. A three dimensional plot can now be made where the gear position and dimensions are represented as tyres.

Finally the class 2 weight estimate equation for the nose gear and main gear is evaluated. This results in a mass for the main gear and the nose gear groups. The centre of gravity position is set at the centre of the gear at a height one third of the gear length from the ground.

Class 2 landing gear estimation assumptions

Some of the assumptions made in the CWE2 gear weight estimation have been mentioned in the previous section. The most important CWE2 landing gear sizing assumptions are listed below. When a specific value or percentage is used it is based on different conventional reference transport aircraft, listed in appendix D.

- Only the tricycle gear layout is supported;
- If the number of wheels is larger than 12 it is assumed that the number of main gear struts is 4 (3 main gears are not considered);
- The nose gear is assumed to consist of 2 wheels and placed at 25 percent of the prescribed nose gear stowage space (from settings or the input file);
- The aft cg position is estimated to be at the mean cg position plus 10 percent of the mean aerodynamic chord (MAC);
- Specific rear or forward spar locations are not taken into account;
- The maximum take-off scrape angle is assumed 12 degrees;
- In case of wing mounted gears the longitudinal position is set at 55 percent of the MAC for aft swept wings and at 85 percent for forward swept wings;
- In case of a wing mounted very far aft of the fuselage (aft of 60% of the fuselage length) the longitudinal position is assumed on 0% of the MAC for aft swept wings and 40% for forward swept wings;
- In case of a high wing or a wing far forward (forward of 30% of the fuselage) the main gears are assumed to be placed laterally on the fuselage most outboard position;
- If the main gears are positioned on the fuselage the longitudinal position is estimated as the aft cg position plus 4% of the fuselage length;
- Propeller clearances are not taken into account;
- Kneeling gears are not considered, because these are rarely applied to aircraft

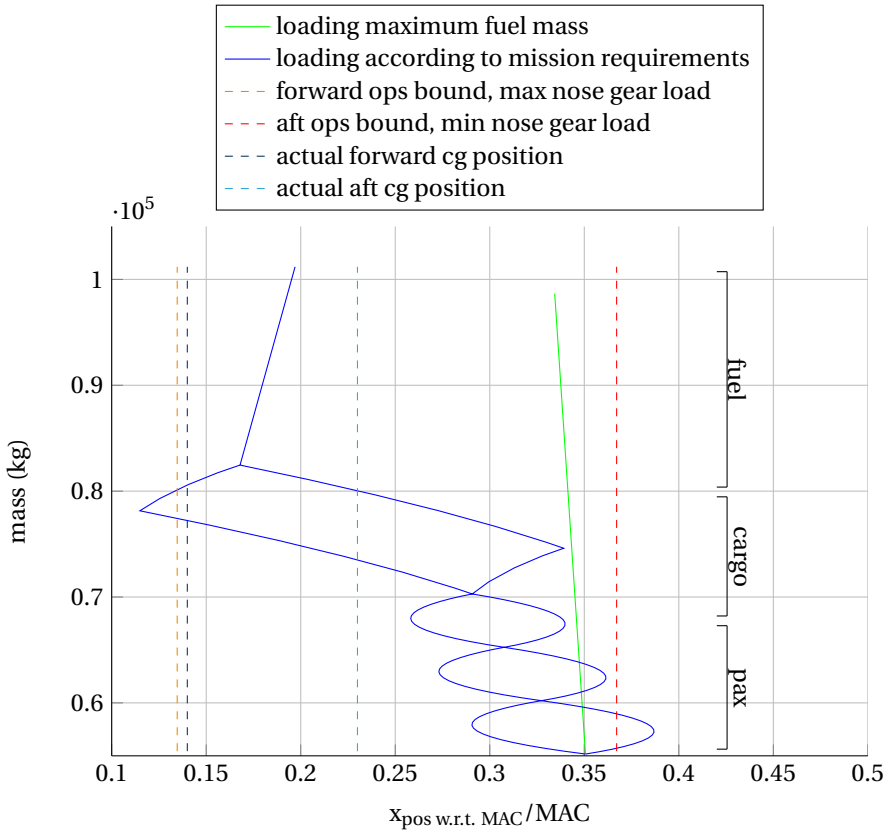

Figure 3.4: B707 loading diagram produced by the class 2 weight estimation module. Aft and forward operational cg bounds are shown as vertical lines.

Aircraft centre of gravity operational bounds

A class 2 weight estimation is usually done on an aircraft concept from which very little is known about the mass distribution of the aircraft. The CWE2 module calculates the range of centre of gravities that could occur during aircraft operations. A sample result for the Boeing 707-321 aircraft is displayed in figure 3.4.

The centre of gravity range that is produced by the class 2 weight estimation module seems too large. This is also visible by the operational bounds that need to be applied to the cg range. Operational bounds are calculated using the method described in section 2.1.2 of chapter 2. Operational bounds on the cg are not desirable, because they limit airplane operations. The forward operational bound prevents that the nose gear load will be too high. The aft operational bound will prevent that the nose gear load becomes too low to steer the aircraft adequately.

The Boeing 707 airport manual (Boe, 2011) provides the actual cg positions of the aircraft: the most forward cg is at 14% and the most aft cg at 23% of the mean aerodynamic chord (MAC). Clearly the centre of gravity distribution of the aircraft needs to be changed in order to improve the stability and control of the aircraft and to improve landing gear positioning.

This problem occurs on preliminary sizing of some aircraft. Adjustments on the centre of gravity range of the aircrafts will solve this, but is currently not done. Future work on the TU Delft Initiator will address this problem.

3.1.2. Landing gear design module

The landing gear design module called PositionLandingGear has the capability to position, size and estimate the weight of each landing gear. The module is composed of 3 parts: a gear positioning, a bogie design and

weight estimation part as is shown in figure 3.5. Each part of the module runs sequentially.

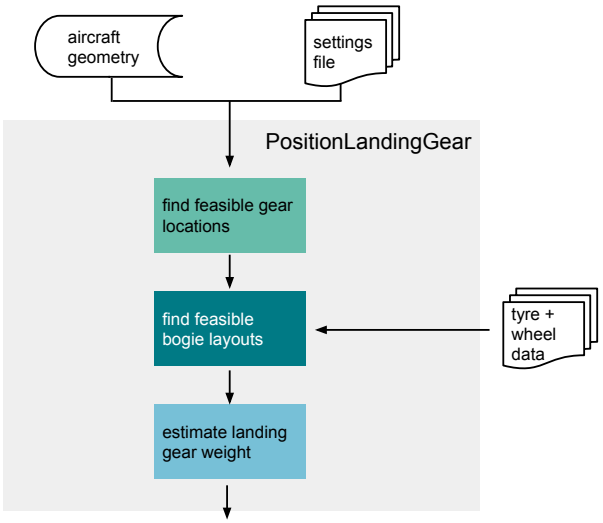

Figure 3.5: Components of the landing gear design module

Gear positioning

The gear positioning part of the PositionLandingGear module evaluates a design space of all possible landing gear heights versus take-off scrape angles. Figure 3.6 shows this design space bounded by positioning limits.

Positioning starts with the parameters that do not need to be evaluated for every design point. This includes the available stowage space and the main gear longitudinal position limits that are imposed by maximum and minimum nose gear loads.

The positioning steps in the PositionLandingGear module are displayed in figure 3.7. For each design point the take-off and landing angle is calculated. This also requires the calculation of the fuselage tail bumper location. The wing spar limits are estimated as well as main gear longitudinal limits from the maximum and minimum nose gear loads.

Currently the take-off angle is estimated empirically. If this angle can be calculated more accurately the module can be easily changed to use this more precise angle. When calculating gear positions, shock absorbers are at the extended position and tyres are at the undeformed state.

The nose gear lateral position is now also set from nose gear loading requirements (set in the input or settings file). The lateral position of the main landing gear is found from the wing and engine clearance, the sideways turnover limit, the stowage requirement and the limit preventing colliding gears when retracted. When the actual lateral gear position is known the position of the spars is also known.

The ability to turn on a runway and taxi requirements are also calculated. From all feasible landing gear design points the shortest possible is chosen. All methods used for the positioning of the landing gear are further explained in section 2.1.2 of chapter 2.

Bogie design

When the position of all landing gear bogies are known the static load is known for a forward and aft cg position. The aft cg position is most critical for the main gear and the forward for the nose gear. Tyres transfer the loads of the struts to the ground. There are many different bogie layouts with different number of tyres per bogie that can be made. But only the 8 different bogie types of figure 3.8 are considered.

For each of these bogie types the load per tyre is calculated. A database of 342 different tyres with accompanying wheels has been made using data from Goodyear (Goodyear, 2002). The tyre with a suitable rated

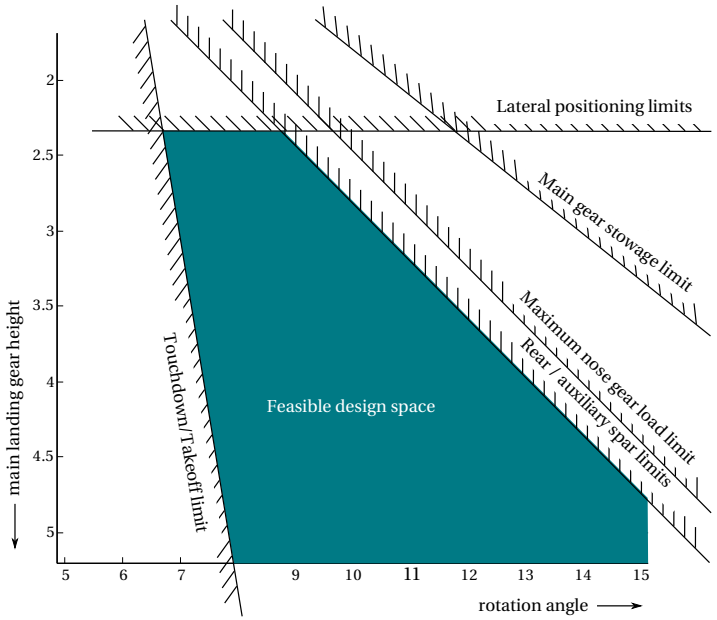

Figure 3.6: Graph showing the feasible design space of rotation angle versus height.

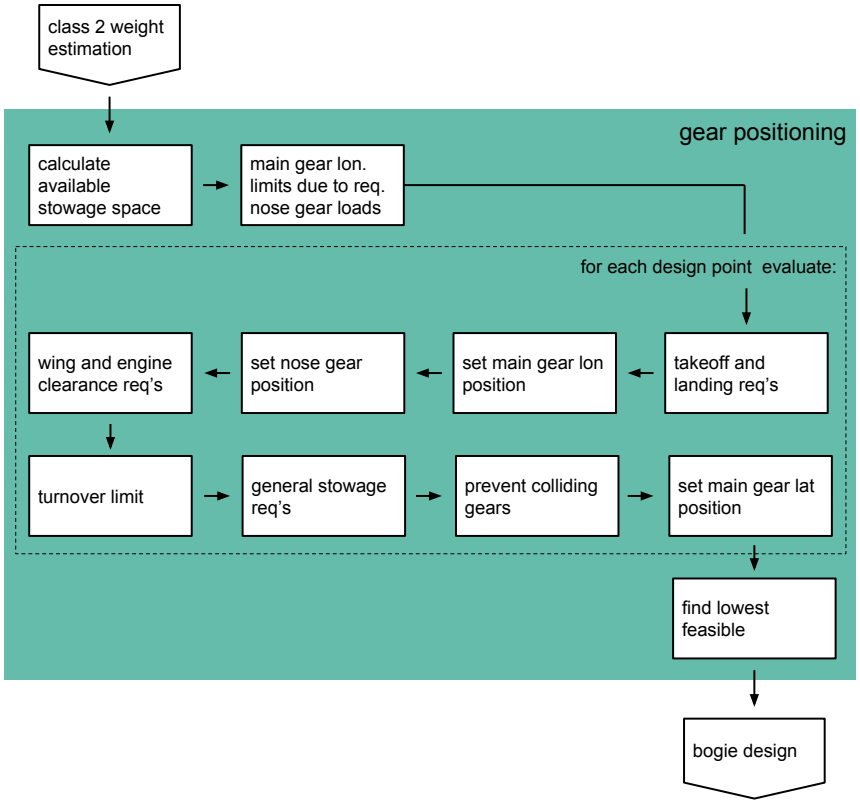

Figure 3.7: Workflow diagram of the gear positioning part of the PositionLandingGear module

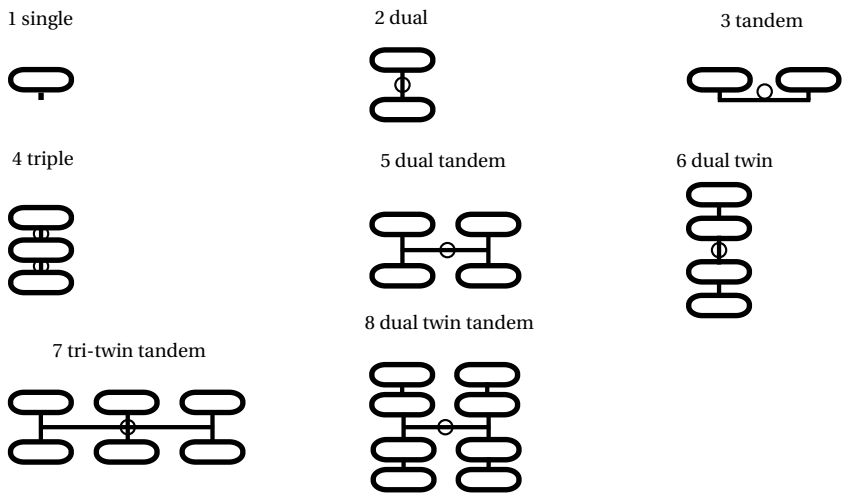

Figure 3.8: The bogie layouts that are being evaluated by the PostionLandingGear module

load is selected. This rated load includes a tyre safety factor (1.25 by default) such that for future growth of the aircraft design the tyres do not need to be changed (Currey, 1988). If the bogie type is capable of sustaining the static loads, the bogie design is refined by estimating tyre positions and tyre clearances. This is done using the dimensions and relations of Torenbeek (Torenbeek, 1982, p.382).

Pavement requirements for airports with flexible and rigid pavements are then evaluated by running an external module. This module is called FlotationAnalysis and is derived from the source code of the Federal Aviation Administration COMFAA 3.0 analysis tool (Federal Aviation Administration, 2011). The code has been rewritten from Fortran to Matlab to make sure that flotation analysis is completely integrated into the Initiator. Flotation analysis results in a so called Aircraft Classification Number (ACN) as explained in chapter 2, section 2.1.1. Calculation of the ACN requires many iterations and thus has a large impact on calculation time. The Matlab JIT-accelerator speeds up the code by converting it into a more efficient programming language. Therefore the flotation module has been optimised for the Matlab JIT-accelerator, such that the greatest performance benefit can be achieved (Mathworks, 2002).

Then the bogie bounding box that includes clearances is determined and the stowed position and retraction angle is calculated. It is then checked if the stowed bogie is still within the stowage boundaries predefined by the user.

The previous steps are done for every feasible bogie type as is shown graphically in figure 3.9. From these the least complex bogie type (the bogie with the least number of wheels) is selected. Reduced complexity keeps cost and weight minimal.

The nose gear type is of the dual bogie type, which is used on virtually all transport aircraft. Clearances, tyres and shock absorber sizing for the nose gear is done in a similar way as for the main gear. Finally the main gear brakes and the oleo pneumatic shock absorbers can be sized.

In the landing gear positioning and the bogie design part of the PositionLandingGear module the following most important assumptions are made:

- Only the tricycle gear layout is supported;
- Only conventional transport aircraft;
- The number of main gear struts is 2, 3 or 4. The third and fourth are assumed to be positioned on the fuselage;
- The nose gear has a fixed layout: 2 wheels placed symmetrically along a nose gear strut with a fixed track of 0.5m;

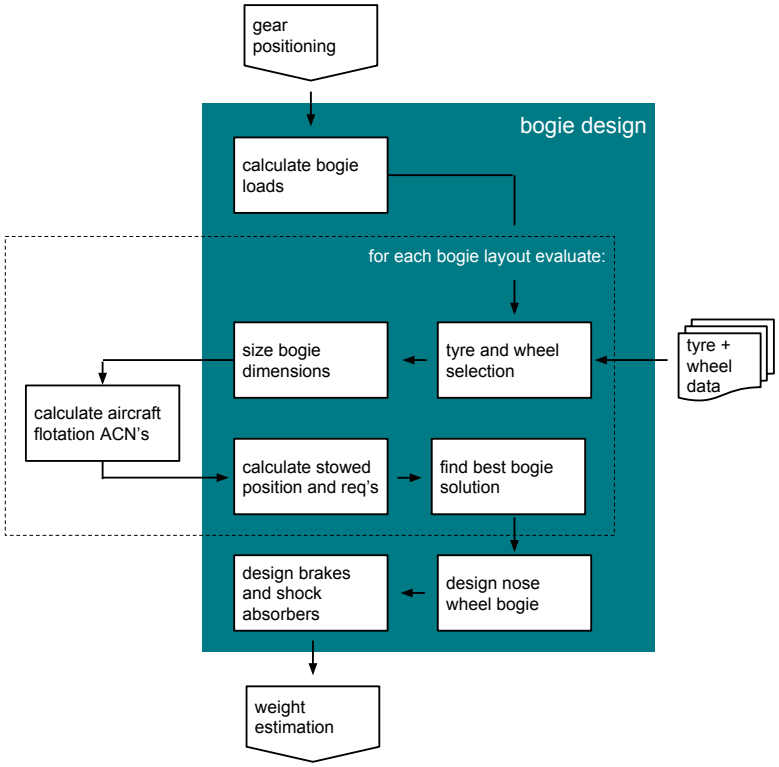

Figure 3.9: The bogie design part of the PositionLandingGear module

- The aircraft is symmetric in the xz-plane;
- The maximum touch down angle is assumed to be equal to the maximum take-off angle. And the maximum take-off angle is calculated empirically;
- In calculating the turnover angle, the nose gear track is not taken into account;
- Wing bogies are assumed to be connected to the wing between or on the rear and auxiliary spar. The gear-spar connection point is assumed located halfway along the spar height;
- A clearance angle of 5 degrees for nacelle with an additional 6 inch clearance is used. The wing tip has a set clearance angle and also an additional 6 inch clearance (Torenbeek, 1982);
- The maximum turnover angle allowed is 63 degrees;
- The aircraft will need to be able to turn on a runway and manoeuvre on a taxiway according to FAA advisory circular No. 150/5300-13A. Main gear steering is not taken into account;
- The drag strut on the wing main gear is set at a fixed angle of 10 degrees w.r.t the vertical and 0 degree w.r.t. the aircraft xz-plane. The side strut is assumed at a fixed angle of 45 degrees w.r.t. the yz-plane. The fuselage and nose gear bogies are assumed to have a side and drag strut at the same angle and are positioned symmetrically;
- The drag strut and side strut for each bogie is assumed to be attached at the same point on the main strut. This point is fixed halfway along the gear length;

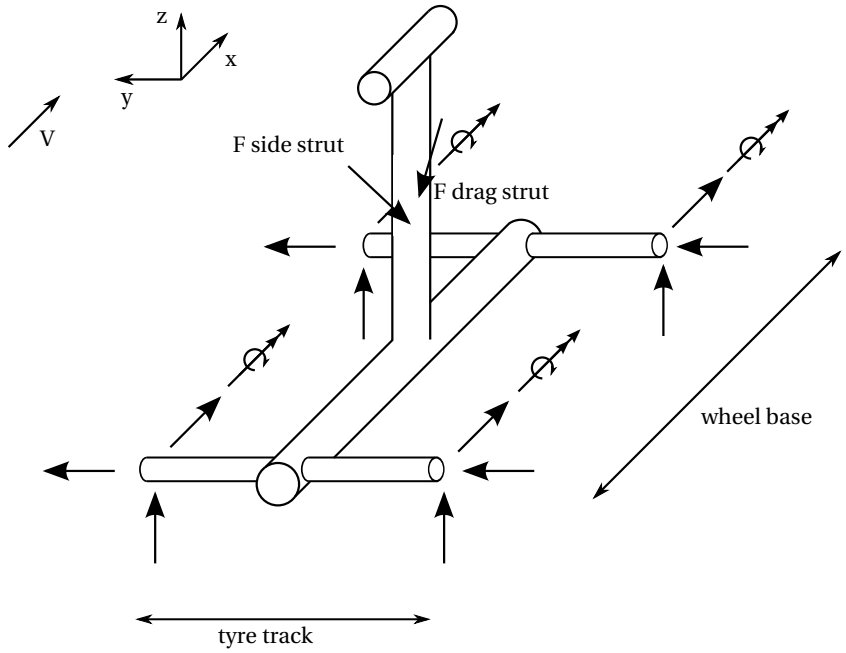

Figure 3.10: The structural components of a bogie with 4 tyres modeled with tubes

- All main gear tyres are assumed to be braked. The brake weight is derived from the requirement to perform 1 RTO, 5 stops at maximum landing mass with 10 ft/s deceleration and 250 stops at design landing mass with 10 ft/s deceleration (Currey, 1988);

- For the shock absorber the design methods explained in chapter 2, section 2.1.8, are used. The design parameters used are as follows. The maximum load factor is 1.2 (2.2 at the aircraft cg), the maximum sink speed is 10 ft/s, the tyre efficiency is 47% and the shock efficiency is 85%. The compression ratio is 4/1 static to extended, 3/1 compressed to static and the static pressure is 1500 psi (Currey, 1988). Polytropic compression is assumed where the oil and gas are separated. Only oleo pneumatic shock absorbers are considered.

3.1.3. PositionLandingGear class 2.5 weight estimation

The general dimensions of the landing gear components were calculated in the previous sections. To make a weight estimation it is convenient to model the trunnion, shock strut, truck and axles as tubes as is shown in figure 3.10.

At this point only the radii and thicknesses of the structural components need to be known to make a weight estimation. Only the required shock absorber inner radius is know from the piston area. The radii of the other structural components are set to a fixed value related to the piston area. Thicknesses of the structural members can be found by considering the maximum stresses within the structure that could occur due to the extreme load cases defined in chapter 2, section 2.2.3. The maximum stresses are found analytically using structural analysis theory (Megson, 1999). The complete analytical derivation of the maximum stresses can be found in section 2.2.1.

Figure 3.11 shows all steps of the class 2.5 weight estimation. First all dimensions of the structural members that are needed for the analysis are obtained. Then the maximum normal stress and axial force due to bending are calculated. The shear stress due to torsion and shear forces are also calculated. All stresses are combined to find the maximum stresses within the cross-section at different critical points within the structure. Stresses are then multiplied with a safety factor of 1.5. Thicknesses of all structural members are

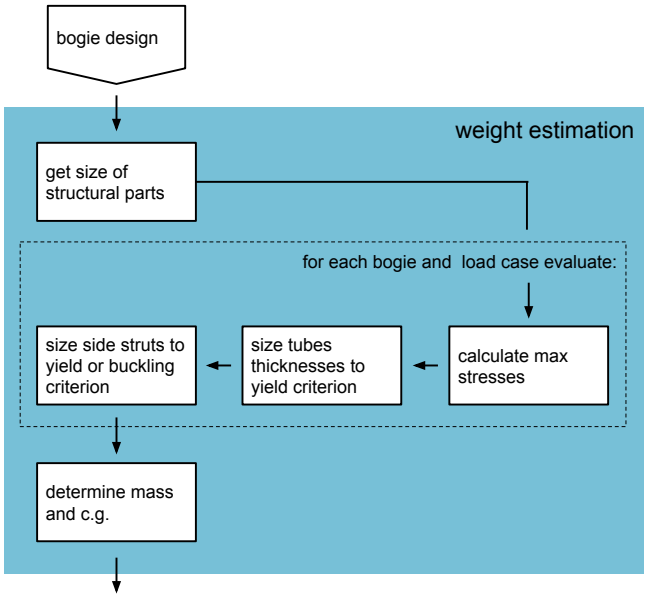

Figure 3.11: The weight estimation part of the PositionLandingGear module

calculated such that yield does not occur. If the side struts are loaded under compression the buckling criteria is applied.

Structural analysis is done for each main gear bogie separately, because lateral side loads put different loads on the side struts of the left and right main gear bogies. The nose gear is also evaluated separately. Finally when the thicknesses are known, masses and centre of gravity position are quantified. An example result for different load cases is presented in the next chapter (section 4.3.2).

The following assumptions have been made in the weight estimation part of the PositionLandingGear module.

- The landing gear structure is assumed to be made out of LESCALLOY 300M VAC ARC ultra high strength steel. This material is commonly used for landing gears (ASM International, 2013);
- A safety factor of 1.5 on maximum stresses;
- The structure is not allowed to yield at maximum load;
- All structural parts are assumed to be made out of tubes except for the side struts. The side struts are modelled as two force members with an I-beam cross-section. The side struts are thus only loaded axially;
- The tubes are analysed as thick-walled tubes. The side struts are considered thin-walled. The width and height of the strut cross-section are fixed at 0.15 m, only the thickness is varied;
- 8 different load cases determine the maximum loads. These include: static load, 3 point landing, one wheel landing and tail down landing at 10 fps, the lateral drift landing, braked roll turning and pivoting;
- Side loads on the wheels are assumed to only cause a moment about the x-axis. No other external moments are applied at the axle ends;
- The deflection of the side struts in z-direction is negligible;

- All radii of the tubular structural members are derived from the piston area;

All properties of the PositionLandingGear, Class2WeightEstimation module and LandingGear part are shown in a class diagram in figure 3.12.

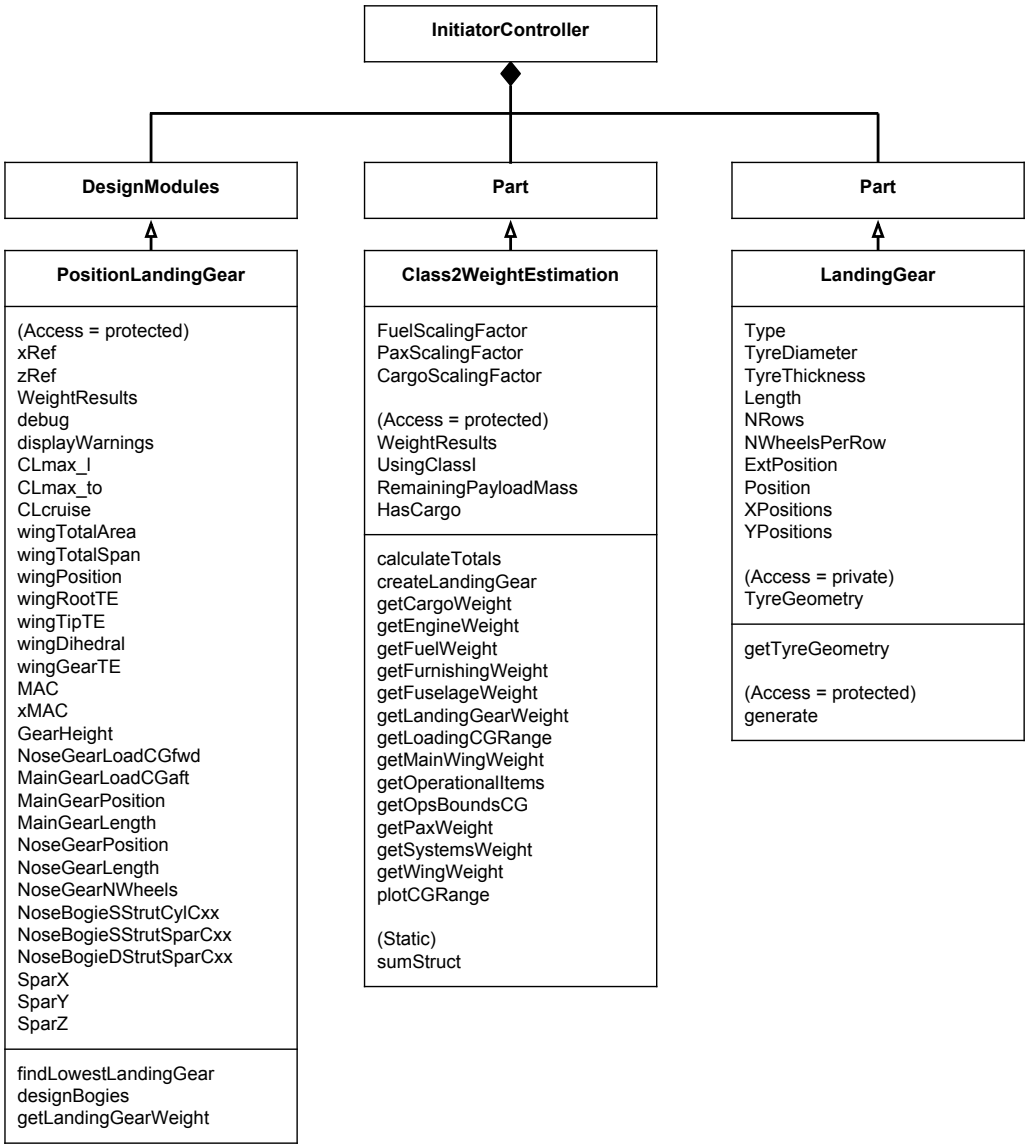

Figure 3.12: Class diagram of the PositionLandingGear, Class2WeightEstimation module and a LandingGear part.

3.2. Implementing the landing gear analysis

The landing gear analysis can verify loads within the structure for different European Aviation Safety Agency CS 25 load cases. The kinematics of the landing gear retraction mechanism of nose and main gear bogie is also verified.

Analysis of the landing gear has been made separate from the modules in the TU Delft Initiator. The analysis however does use the XML output of the Initiator as input. Dynamic analysis of the landing gear model is made as a SimMechanics application in Matlab. The multi-body system is modelled with blocks that represent rigid bodies, joints, constraints and force elements. The blocks of the implemented multi-body model can be seen in figure 3.16. Using provided input parameters, SimMechanics then evaluates the equations of motion of the complete system and tests the main landing gear for different load cases.

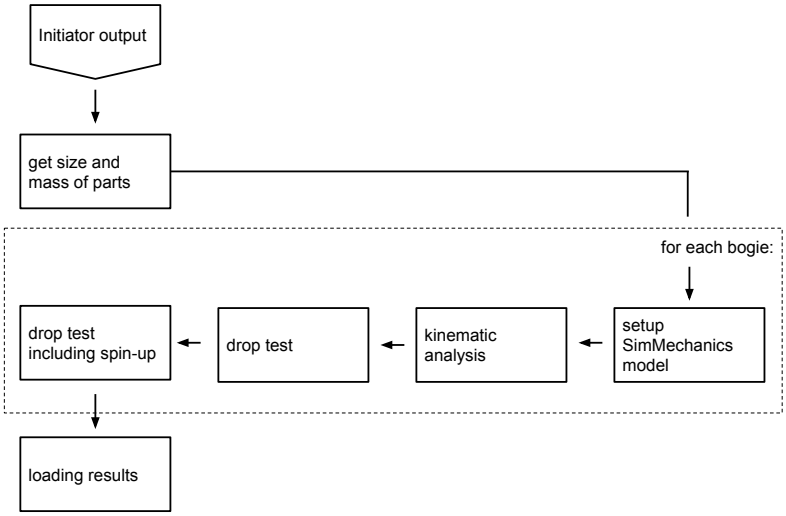

Figure 3.13: Landing gear analysis workflow

Steps taken in the landing gear analysis are displayed in figure 3.13. For each bogie the SimMechanics model is setup by automatically adding blocks from a library to the model. Added blocks include blocks for axles, wheels, tyres and a truck beam.

Then a kinematic analysis of the retraction mechanism is performed. The initial shock absorber stroke and the retraction angle is set to the extended position by default. The side strut locking mechanism is set initially to the locked position. The bogie rotates about a single axis as shown in figure 3.14. It is retracted and extended using actuators that control the retraction angle, the truck beam angle and the locking mechanism.

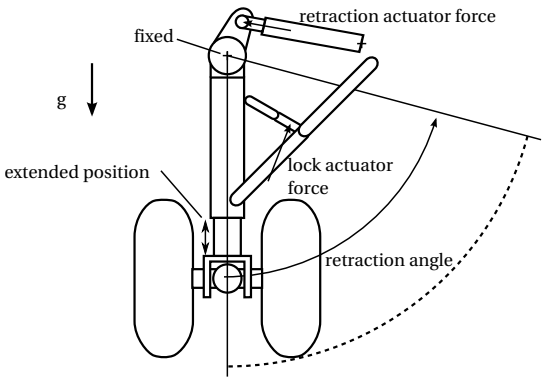

Figure 3.14: Landing gear analysis retraction model used for a retraction/extension simulation. The initial condition is shown.

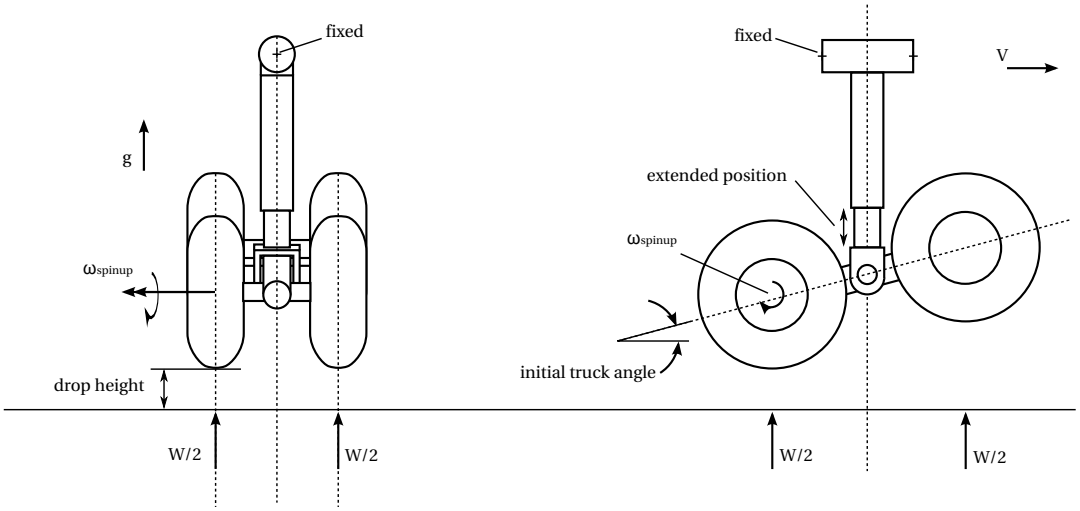

Figure 3.15: Landing gear analysis model used for performing a drop test simulation

The retraction analysis is followed by a drop test simulation, where the bogie is oriented in a landing state and dropped. The degree of freedom of the landing gear strut is limited only the vertical motion. The bogie initial height is set such that it will hit the ground at 10 feet per second due to gravity. This speed is prescribed by the three point landing, regular landing and one wheel landing load case in FAR 25 (European Aviation Safety Agency, 2012, p. 1-App A-2)). For the drop test simulation gravity is reversed in the upward direction, the ground will thus move upward. Tyre spin-up is not included for the first test case.

The drop test is then done a second time, but now a tyre spin-up initial condition is included in the touch-down analysis. Tyre spin-up is applied to all tyres with an equal angular velocity.

When the simulations complete, all results are combined and verified with results obtained from the class 2.5 weight estimation in the PositionLandingGear module.

The most important assumptions in the kinematic analysis are:

- The simplest form of gear retraction is assumed, which is a rotation only about the trunnion beam x-axis (figure 3.10);
- Only the number of wheels, tyres, axles, tube radii and thicknesses are varied;
- The shock absorber is oleo-pneumatic (non-linear);
- The empirical model of Pacejka is used to model the tyres. This model is called the magic formula tyre model;

The inputs and outputs of the tyre model are shown in figure 3.17. The actual tyre model is implemented as a Matlab function that is evaluated at each time step. The Matlab function implements the equations of the MF-tyre implementation (TNO Automotive, 2010) (Pacejka, 2006). In section 2.3.1 details of the tyre model coordinate system and input and output values are further explained.

The non-linear oleo-pneumatic shock absorber forces are modelled as a Matlab function block. The equations of chapter 2, section 2.1.8 are implemented in this function block.

3.3. User manual

Since the landing gear design and the landing gear analysis are separate modules, the user manual has also been split up in two parts. First the use of the landing gear design module is explained.

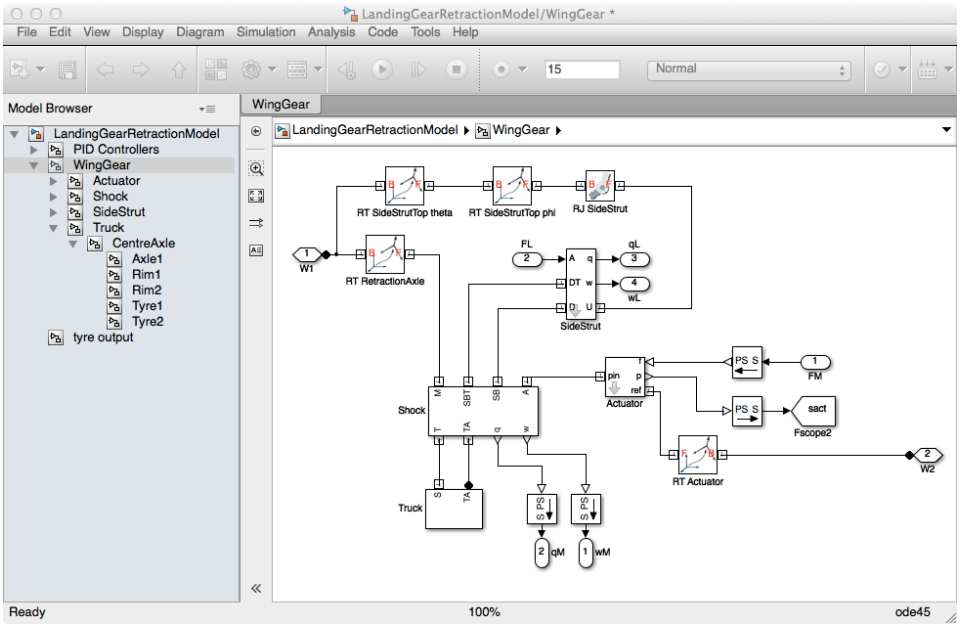

Figure 3.16: Landing gear SimMechanics model of a main landing gear. Components include a oleo-pneumatic shock absorber, side struts, axles, tyres and wheels.

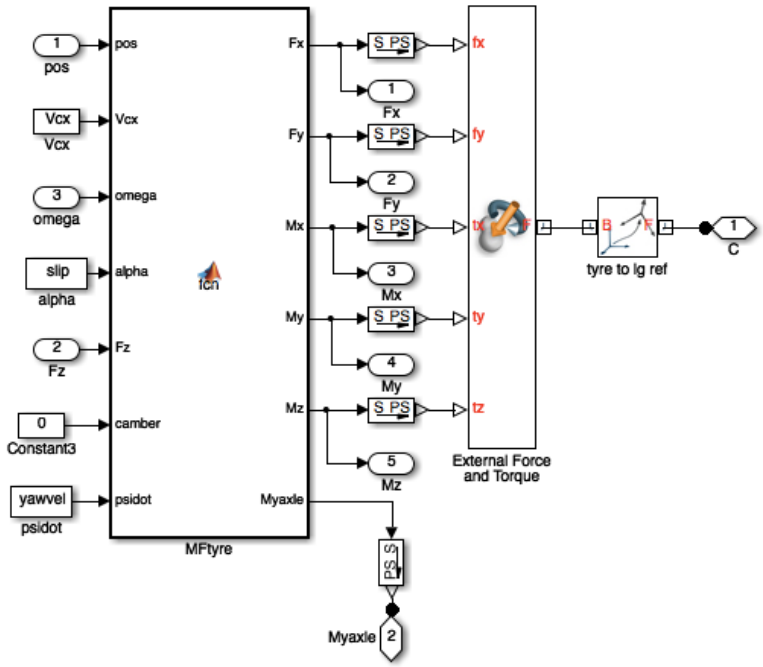

Figure 3.17: Tyre model block contents, which is part of the landing gear SimMechanics model.

Description	Input name	Default
number of struts	NumStruts	2
min selected airport flexible pavement	MinSelectedAirportFlex	Rotterdam Zestienhoven
min selected airport rigid pavement	MinSelectedAirportRigid	London Luton
heat sink material	HeatsinkMaterial	Carbon
forward and aft main gear stowage (fuselage length fraction)	MainGearStowage	0.35;0.45
main gear stowage width (fuselage width fraction)	MainGearStowageWidth	1.0
fuselage fairing height (meter)	FuselageFairingHeight	0
forward and aft nose gear stowage (fuselage length fraction)	NoseGearStowage	0.05;0.2
maximum nose gear load (maximum ramp mass fraction)	MaxNoseGearLoad	0.15
minimum nose gear load (maximum ramp mass fraction)	MinNoseGearLoad	0.6
tyre load safety factor	TyreLoadSF	1.25
aft centre of gravity x-position	xCGaft	-
forward centre of gravity x-position	xCGfwd	-

Table 3.1: List of possible inputs for the PositionLandingGear module

3.3.1. PositionLandingGear user manual

For the PositionLandingGear module the following is required to run the module.

- The take-off and approach speeds need to be defined in the input file;
- The aircraft needs to have a feasible aft and fwd centre of gravity position;
- The aft section of the fuselage needs to be properly shaped, such that the take-off scrape angle can be achieved;
- The wing needs to consist of either 1 or 2 parts;
- Results of the class 2 weight estimation module

One of the most important requirements is that the cg positions are feasible. This can be checked within the class2weight estimation. Results of the class 2 weight estimation are required, because at this stage the aircraft component geometries, weights and aircraft performance data is available.

When creating an input file one can add specific inputs listed in table 3.1. The inputs are all optional and if no input is given the default values are used.

The available stowage space within the aircraft is controlled by the NoseGearStowage, MainGearStowage, FuselageFairingHeight and MainStowageWidth inputs. The definition of these parameters is also made visible in figures 3.18 and 3.19.

The minimum selected airport for flexible and rigid pavements represent the airports where the aircraft should minimally be allowed to land. These parameters can be given as an airport name listed in appendix B. It can also be given as a PCN number, this has to be the PCN for subgrade category 4 (CBR 3).

When setting the aft and forward centre of gravity x-position in the input file, these values will be used in the analysis. This is usually done when results for a reference aircraft are needed. Centre of gravity positions are then already known. If xCGaft and xCGfwd are not entered in the input file, a centre of gravity position calculated by the class 2 weight estimation is used.

All default values can be set in the settings.xml file. These settings are currently set such that large number of aircraft by default can successfully run. If in future landing gear positions pose a problem (in a optimisation loop) settings can be set even less strict.

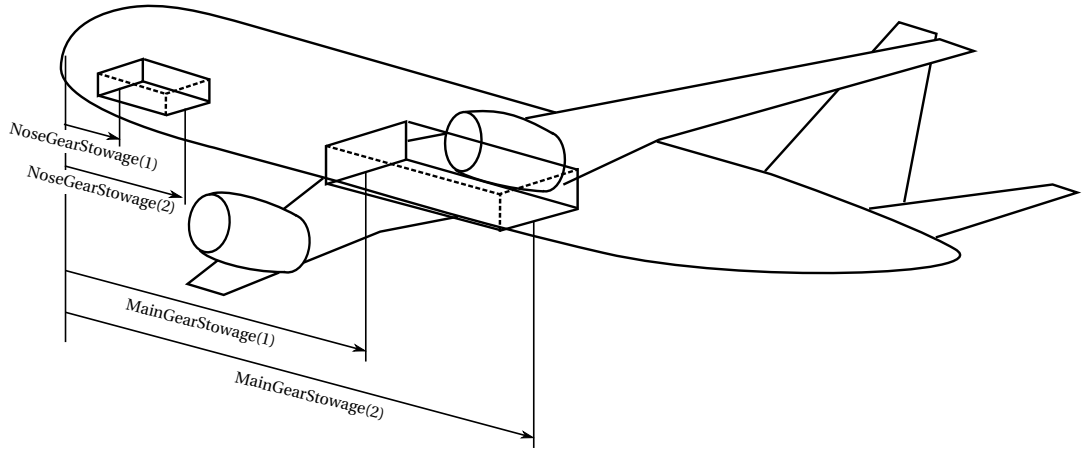

Figure 3.18: The input parameters that define the main gear and nose gear available stowage

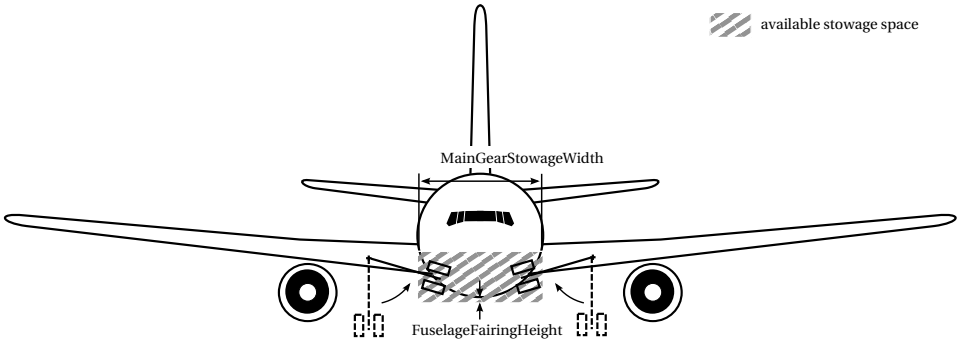

Figure 3.19: The input parameters that define the main gear and nose gear available stowage

There is also an addition setting called PlotRetractedGear which will put the right wing and right fuselage bogie in retracted position in the 3-dimensional plot.

Properties of the landing gear part are listed in table 3.2. A landing gear part is created by the class 2 weight estimation. When the PositionLandingGear module is run the class 2 gear parts are replaced by the results of this module.

All outputs of the landing gear sizing and selection tool are listed in table C.1 in appendix C. In this table some properties have the prefix WingBogie. The same properties names are applied to a fuselage bogie (if it exists) with a prefix FuseBogie or they are applied to a nose gear bogie without a prefix.

3.3.2. How to run the landing gear design module

The landing gear design module is run by first starting the Initiator:

```
C = InitiatorController(A380.xml);
```

Then the PositionLandingGear module can be run:

```
C.runModule('PositionLandingGear')
```

When the module finished results are written to the A380.xml file. Results are also available in the Matlab workspace as a C InitiatorController object. Another way to display the results is by making a report. The report will include positioning and bogie design details. If class 2.5 landing gear weights need to be included in the report the Class25WeightEstimation also needs to be run. This can be done by:

Description	Property
Position vector of the bogie centre on the ground (meter)	Position
Rotation about x, y and z axis (origin at the wing gear connection) (deg)	Orientation
Extended position vector of the bogie centre on the ground (meter)	ExtPosition
NoseGear or MainGear	Type
Maximum tyre diameter (meter)	TyreDiameter
Maximum tyre section width (meter)	TyreThickness
Gear length from ground to wing connection point (meter)	Length
Number of wheel rows	NRows
Number of wheels per row	NWheelPerRow
Option to override default position to predefined tyre x-positions (meter)	XPositions
Option to override default position to predefined tyre y-positions (meter)	YPositions

Table 3.2: List of properties of a LandingGear part

```
C.runModule(Class25WeightEstimation)
C.runModule(ReportWriter)
```

3.3.3. Module messages description

The Class2WeightEstimation and PositionLandingGear module can produces a number of messages. An description of each possible message is listed in the following sections.

The following warning messages could be displayed by the Class 2 weight and centre of gravity range estimation:

CG range limited by fwd ops bound due to nose gear load limits

The forward operational bound limits the centre of gravity range too much. The forward operational bound is imposed due to the maximum nose gear load (MaxNoseGearLoad in the settings or input file).

CG range limited by aft ops bound due to nose gear load limits

The aft operational bound limits the centre of gravity range too much. The aft operational bound is imposed due to the minimum nose gear load (MinNoseGearLoad in the settings or input file).

The warning messages of the positioning module are only shown if GearPositioningWarnings is set to true in the settings.xml file.

Unconventional aircraft types not supported

The aircraft that is being analysed is of unconventional type. Only the conventional aircraft type is supported by PositionLandingGear

Gear height needed seems large, check ac aftfinenessratio or nosegear loading setting

The lowest possible feasible landing gear layout is larger than 3 meters heigh from the belly of the fuselage.

Check wing position w.r.t. fuselage

The centre of gravity range is such that the nose gear cannot be placed properly. This is probably due to the lateral wing fuselage position.

wheelbase too large for taxiing

The landing gear wheelbase does not comply with the FAA Advisory Circular No. 150/5300-13A.

track too large for taxiing
The landing gear track does not comply with the FAA Advisory Circular No. 150/5300-13A.

turn radius too high
The landing gear turn radius does not comply with the FAA Advisory Circular No. 150/5300-13A. This problem can be solved by applying main gear steering.

Main gear cannot be positioned forward of auxiliary spar. Change the aft, fwd cg or aux spar position.
Nose gear loading limits and the current auxiliary spar position prevent the result of a feasible main gear position.

nacelle goes through ground
The lowest possible gear height selected places the nacelles through the ground. This is a validation check of the engine clearance calculations.

No feasible landing gear positions found, adjust cg range, aux spar, nosegearloading setting or stowage
This error message occurs when there can be no feasible landing gear position found in the design space. This only can be solved by adjusting the centre of gravity range, the nose gear loading setting and/or stowage settings. This error message stops further results of the PositionLandingGear module.

Number of struts higher than 4 not supported
The number of struts in the input file is set higher than 4. Only 2, 3 or 4 main gear struts are supported.

No feasible bogies found
Of the 8 different landing gear layouts none can be applied. This is usually due to improper stowage requirement settings or wing rear/auxiliary spar positions.

small wheels not supported for brake sizing
The given aircraft requires tyres that have a relatively small radius. Only conventional transport aircraft are supported by the PositionLandingGear module.

shock absorber pressure too low
The required shock absorber pressure is lower than 60 psi which will result in sticking due to friction. This is a validation check of the shock absorber design.

shock absorber pressure too high
The required shock absorber pressure is higher than 6000 psi, seal leakage could occur. This is a validation check of the shock absorber design.

trunnion radius increased
Loads on the bogie are high; a large tube wall thickness is required. To reduce the trunnion weight and manufacturability the trunnion radius is increased by 10 percent.

3.3.4. Landing gear analysis user manual

The landing gear analysis module performs several kinematic and multi-body simulations. The SimMechanics kinematic and multi-body analysis will give as output:

- a SimMechanics model of the nose gear, the wing landing gears and if they exist the fuselage landing gears;
- loads within the gear's structural members for several load cases;
- duration of retraction/extension and the retraction actuator efficiency;

- response behaviour to dynamic loading

Results of the landing gear design module in the Initiator are used as input of the analysis. The PositionLandingGear module gives several feasible landing gear layouts. Only one can be used in the multi-body analysis. By default the solution with the least number of wheels is used. If one would like to analyse a different combination, this can be set in the runsim.m Matlab run file.

There are a few extra settings that can be altered if the default kinematic solution is not sufficient. These include the position of the side strut bracket that forms the connection between the shock absorber and the side strut, shown in figure 3.20. Also the angle between of the locking mechanism needs to be set properly (figure 3.21).

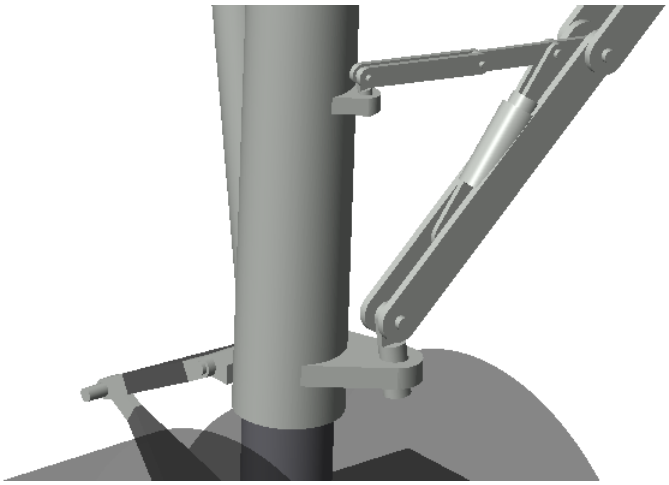

Figure 3.20: Connection between side strut and shock absorber

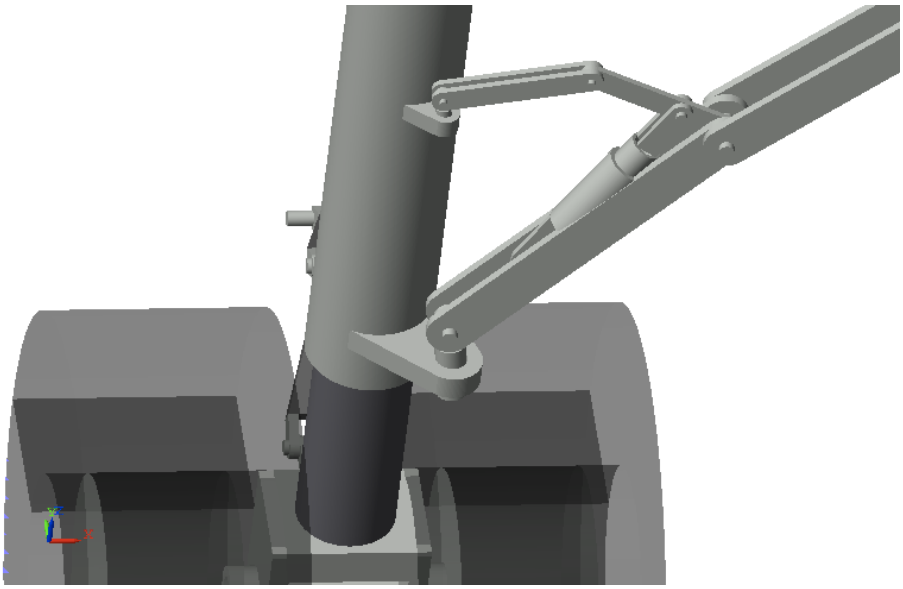

Figure 3.21: Locking mechanism between side strut and shock absorber

After finalising all simulations, results will be displayed in figures and as parameters in the Matlab workspace. The results are grouped together in a struct called Results.

The explanation of the messages that could be displayed during the simulation are listed below.

Gear needs to be connected above spar centre

The shock absorber stroke length required is longer than the piston cylinder length. Therefore the gear strut wing spar connection point is moved upwards.

Gear stroke too long to be placed on wing

The shock absorber stroke length required is longer than the piston cylinder length. The gear strut wing spar connection point required is even higher than the highest point on the wing spar. This is not feasible.

Structural thickness results incomplete

The structural thicknesses calculated by the weight estimation of the PositionLandingGear module contains a NaN value. This is a validation check of the weight estimation result.

Side strut top bracket goes through cylinder, position brackets differently

The bracket that connects the strut with the side struts needs to be moved.

3.3.5. How to run the landing gear analysis module

First the filename and path of the Initiator output xml file needs to be set in the runsim.m file. In this file also the initial conditions of the different analyses can be changed. The landing gear analysis module is then run by starting the simulation in Matlab with the following command.

```
runsim
```

3.4. Definition of use cases

The landing gear design modules in the Initiator can be used for many different use cases. Two different use cases will be explained in the following sections. The first example use case is a class 2 component weight analysis of 2 different aircraft concepts with comparable missions.

3.4.1. Class 2 weight estimation example use case

For this example use case the weight of the landing gear of a blended wing body aircraft can be compared with the gear weight of a conventional aircraft. It needs to be possible to do this rapidly, since the design is in a preliminary design phase.

This use case starts by defining an input file for a blended wing body. An input file called ovalbwb.xml for a blended wing body aircraft already exists in the CleanInputFiles folder. In this input file the mission requirements are set. Mission requirements include the required passenger and cargo payload, cruise speed, altitude and range. For a Class 2 weight estimation also other inputs are required, namely:

- performance parameters, such as lift coefficients at take off and landing;
- configuration parameters, as wing aspect ratio and location;
- fuselage shape definition, because of the nonconventional shape of a blended wing body this shape needs to be defined more precisely than would be necessary for a conventional aircraft. It is important to set the nose and aft shape to get the desired wide shape of the fuselage (Schmidt, 2013);
- a detailed right wing shape definition, which includes span, airfoils, thicknesses, taper, sweep, twist and dihedral at different wing sections. A similar separate left wing is also defined;
- engine positions;

This input file can then be analysed by the Initiator by running the following commands in Matlab

```
Initiator ovalbwb.xml --interactive
run Class2WeightEstimation
run PlotTool
plot geometry
```

A comparable aircraft to the oval blended wing body, in terms of mission requirements, is the Boeing 777-300ER aircraft. Class 2 weight estimation results are generated similarly as for the oval BWB aircraft. The B777-300ER.xml file in the CleanInputFiles folder is used here as input.

Figure 3.22 shows the graphical results of the oval BWB and figure 3.23 the results of the Boeing 777. Both aircraft have the same 6 wheel main gear bogies. For a blended wing body the fuselage is wide enough to place all main gear bogies on the fuselage. The 777 has the main gears placed on the main wing and therefore requires longer main gear struts. The weight of the 777 gear is therefore expected to be higher. Components weight results of both aircraft are compared in figure 3.24. The percentages of gear group weights are both comparable: 5.9 percent for the 777 and 5.5 percent for the BWB. When comparing the weights in kg, the total weight of the oval BWB aircraft is found 14 percent lower than the Boeing 777 gear weight.

3.4.2. Use case kinematic and multi-body analysis

Another use case is a kinematic and multi-body analysis on an existing conventional reference aircraft. The PositionLandingGear module and the kinematic module have been specifically designed for this use case.

First create an input file of the reference aircraft. Also define reference values for the weights and centre of gravity ranges in the input file. By defining these reference values, results of the preliminary sizing will not be used. Instead the more accurate reference values are used to create a more realistic model.

To perform the landing gear analysis the following steps need to be done:

- Run the PositionLandingGear module;
- Define the resulting output xml file in the input for the kinematic analysis;
- Select the bogie combination to be analysed;
- And select the load case to be analysed and change the initial conditions in the runsim.m file
- Analyse results

This is done by editing the runsim.m file and running the following commands in Matlab the Position-LandingGear module:

```
Initiator B777-300ER.xml --interactive
run PositionLandingGear
run ReportWriter
quit

runsim
```

Additionally by running the report writer module a pdf report is generated with landing gear characteristics. In this report also figures are included that show the wing, engine clearance angles, the take off scrape angles and the landing gear footprint.

The kinematic feasibility of the kinematic model and loads due the different load cases are the result of the analysis. These can be evaluated by inspecting the results displayed in figures and in the Results struct in the Matlab workspace.

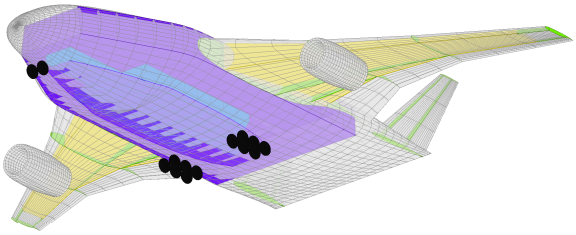

Figure 3.22: Oval blended wing body CWE2 result

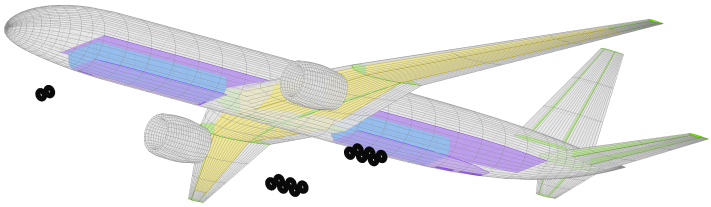

Figure 3.23: Boeing 777ER CWE2 result

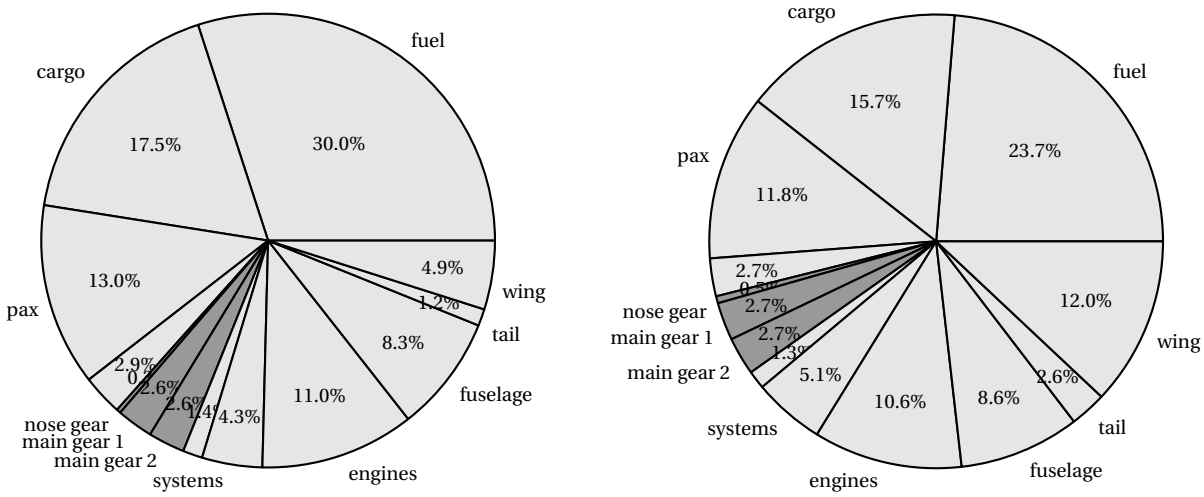

Figure 3.24: Comparison of class 2 weight estimation results of an oval BWB right and a Boeing 777 aircraft left. Both aircraft have the same mission requirements.

4

Results and verification

4.1. Positioning results

To check whether the output of the positioning module makes sense the result is compared against real aircraft data found in airport planning manuals published by aircraft manufacturers. This is done graphically in figure 4.1 and tyres are compared in table 4.1. Reference aft cg, forward cg, reference stowage positions and reference aircraft weights have been used here. Estimations of the class 2 weight estimation have been left out to make a better comparison.

Description	Nose gear tyre	Rated load (kg)	Main gear tyre	Rated load (kg)
A320-200	39x13	6.80e3	H46x18.0-20	23.2e3
A320-200 actual	30 x 8.8 R15	6.50e3	46 x 17 R20	20.9e3
A340-500	B46x16.0-23.5	24.4e3	1400x530R23	34.0e3
A340-500 actual	45x18.0R17 36PR	22.8e3	1400x530R23	34.0e3
A380-800	54x21.0-23	31.1e3	54x21.0-23	32.7e3
A380-800 actual	1270 x 455R22 32PR	24.9e3	1400 x 530R23 40PR	34.0e3
B787-800	40x14	12.6e3	1400x530R23	23.7e3
B787-800 actual	40 x 16.0 R16 26PR	13.2e3	50 x 20.0 R22 34 PR	25.9e3
B777-300ER	H42x16.0-19	17.1e3	1400x530R23	34.0e3
B777-300ER actual	43X17.5R17, 32PR	20.6e3	52X21R22, 36PR	30.2e3
B707-321	15.50-20	9.30e3	49x17	18.0e3
B707-321 actual	39x13, 16PR	8.80e3	46x16, 30PR	20.3e3

Table 4.1: Calculated tyre results compared with actual aircraft tyres used (Goodyear, 2002), (Michelin Aircraft Tire, 2001)

For the 6 different aircraft in figure 4.1, the lateral tyre positions differ with 0.49 m and longitudinal positions with 0.28 m. Deviation with reference data is thus small. Also the number of wheels and clearances between the wheels match, indicating that the flotation analysis and Torenbeek clearance equations produce good results for these type of aircraft.

The calculated A380 landing gear differs from the actual aircraft. The fuselage and wing bogies have been interchanged. Also the calculated fuselage gear has been placed further aft, since only forward retracting fuselage gears have been taken into account. This resulted in a nose gear tyre that has a significant higher rated load (see table 4.1). The calculated gear position is however a good result. Airbus also considered this

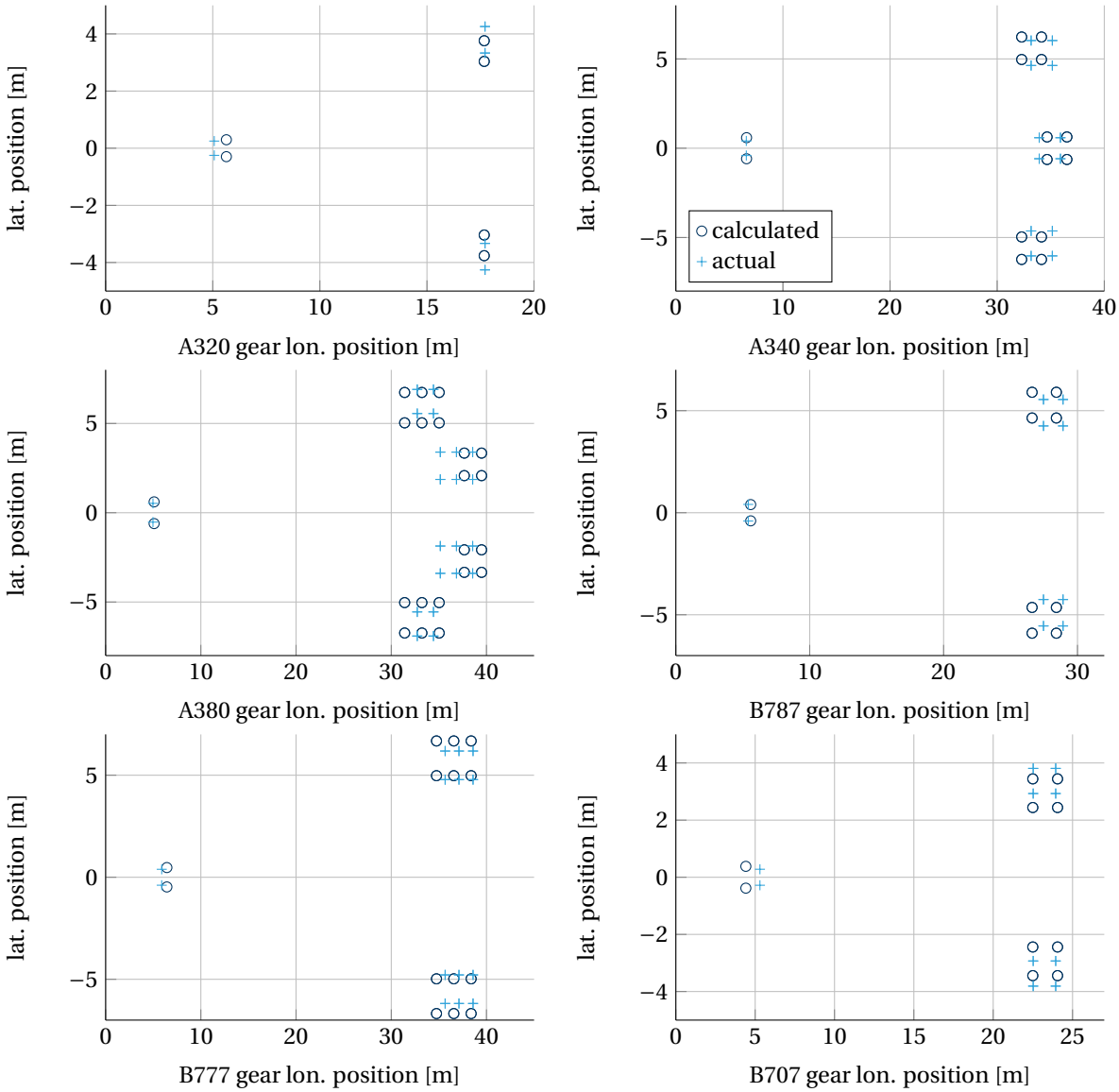

Figure 4.1: Comparison between calculated landing gear positions and actual positions as published by aircraft manufacturers

option in the design of the A380 (Hebborn, 2008). Airbus discarded the 4 wheel fuselage bogie concept in a trade-off further in the design process. At this design stage Airbus had more details available (more than in the current analysis) to make a better trade-off.

4.2. Runway flotation analysis

The FAA COMFAA program has an extensive database of commercial and military aircraft (Federal Aviation Administration, 2011). As a check of the flotation results the calculated ACN values of a number of aircraft are compared with results of the original FAA COMFAA program. This is done using the same COMFAA input values. It has to be notes that the results of the COMFAA program might differ from actual ACN values as published by aircraft manufacturers.

Results are shown in table 4.2 and as can be seen calculated results have a small error. Only for the Airbus A380-800 aircraft the results deviate more. Maximum deviation found here is 15 percent. A cause for this deviation has not been found. The deviation is however small enough to not influence the final landing gear result.

Aircraft	**CBR 3**	**CBR 6**	**CBR 10**	**CBR 15**
COMFAA: ACN flex A380-800 fuselage bogie	105.2	74.7	61.7	55.9
calculated: ACN flex fuselage bogie A380-800	105.2	74.4	61.3	55.9
COMFAA: ACN rigid A380-800 fuselage bogie	109.6	88.1	67.6	54.8
calculated: ACN rigid fuselage bogie A380-800	109.7	88.1	68.5	63.1
COMFAA: ACN flex wing bogie A380-800	102.1	75.1	63.6	58.2
calculated: ACN flex wing bogie A380-800	110.8	82.2	67.7	62.7
COMFAA: ACN flex rigid wing bogie A380-800	90.2	78.1	65.8	56.3
calculated: ACN flex rigid wing bogie A380-800	90.2	78.1	65.9	57.5
COMFAA: ACN flex B777-300ER	120.3	89.3	71.3	63.8
calculated: ACN flex B777-300ER	120.3	89.3	70.3	63.5
COMFAA: ACN rigid B777-300ER	131.9	109.8	85.7	66.1
calculated: ACN rigid B777-300ER	131.9	109.8	85.8	68.3
COMFAA: ACN flex A320-200	50.2	44.4	40.0	38.5
calculated: ACN flex A320-200	50.2	44.3	39.4	38.4
COMFAA: ACN rigid A320-200	50.4	48.4	46.0	43.5
calculated: ACN rigid A320-200	50.4	48.4	46.0	43.5
COMFAA: ACN flex B737-200	39.3	35.2	31.1	30.0
calculated: ACN flex B737-200	39.3	35.2	30.6	29.7
COMFAA: ACN rigid B737-200	39.3	37.8	35.9	34.0
calculated: ACN rigid B737-200	39.3	37.8	35.9	34.0

Table 4.2: Comparison of flotation calculations of several reference aircraft for rigid and flexible pavements.

4.3. Gear weight estimation accuracy

4.3.1. Class 2 weight estimation results

Table 4.3 lists the actual total landing gear group weights for 4 different aircraft (Roskam, 1989b). The aircraft size of these aircraft can be categorised from small to large. The actual weights are compared with landing gear weight results from the class 2 weight estimation module. Class 2 results are of the same order of magnitude and the average error is 17 percent.

Aircraft	Estimate (kg)	Actual (kg)	Est/Act
Boeing 737-200	2528	1975	1.28
Boeing 727-200	3770	3271	1.15
Boeing 707-321	4643	5799	0.80
DC 10-10	9855	9576	1.03

Table 4.3: Comparison of class 2 wing and nose bogie assembly weight with actual weights as given by Roskam

The class 2 weight estimation gives all Boeing aircraft 2 main gear struts with 4 tyres, but with different tyre sizes. The McDonnell Douglas DC10 is given 2 main gear struts with 6 tyres. In reality this is different: the B737 has 2, the B727 2, the B707 4 and the DC10 has 4 tyres per main gear strut. Considering the assumptions that have been made at this design stage, positioning and weight estimation results are better than expected.

4.3.2. Structural parts weights

The weights of the structural parts are determined from maximum stresses that could occur for 8 different load cases. The thickness of each part is adjusted such that the maximum stress in the structure does not exceed the yield stress multiplied by a safety factor of 1.5. The maximum stress is here determined from the Mises yield criterion as explained in section 2.2.1.

Deflections and internal moments as calculated by the class 2.5 weight estimation part of the landing gear design module can be plotted for each load case. The reference load case is the static load case when the maximum ramp weight is put on the main gear. The results of this load case for a Boeing 707-321 is shown in figure 4.2. The displacement u, v and w is the displacement in x-, y- and z-direction. The coordinate system of figure 3.10 is used here.

There are only a few load cases that are most critical. For the Boeing 707 aircraft analysed here, the most critical load cases are the tail down landing (figure 4.3) and the lateral drift landing (figure 4.4). The axles are sized based on the tail down landing and the other parts are sized on the lateral drift landing load case. Specifically the lateral drift load case for the left landing gear, since the aircraft gear is loaded asymmetrically. The loads are significantly higher than the right gear, because of the side struts that will be loaded differently. The load on the side struts are also highest for the left gear for this load case.

Structural thicknesses and weights as calculated for the Boeing 707 are listed in table 4.4. The longest and the most heavily loaded parts are given the highest thicknesses as expected. As a result these parts also have the highest weights.

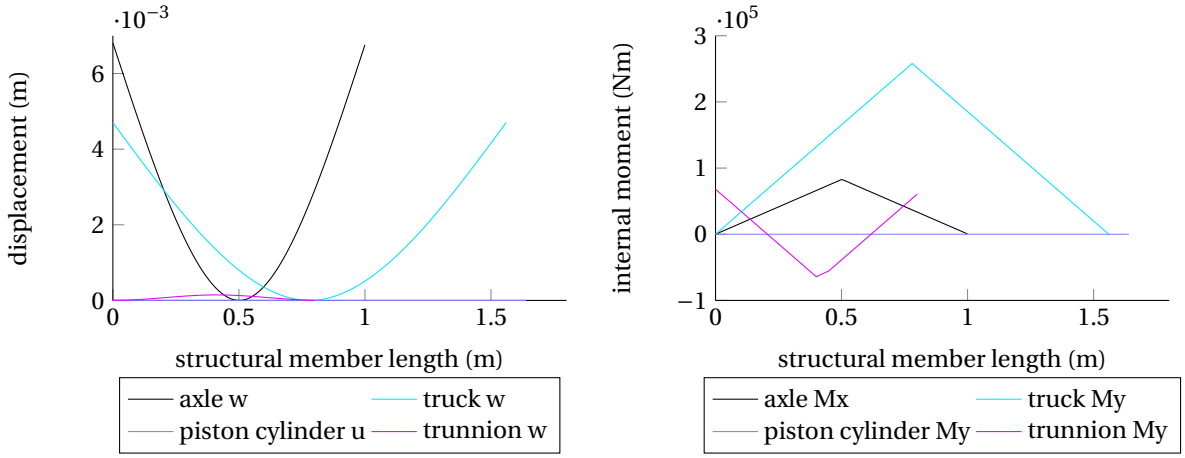

Figure 4.2: Structural deflections and internal moments for the static load case. These results are for the right main gear of a Boeing 707.

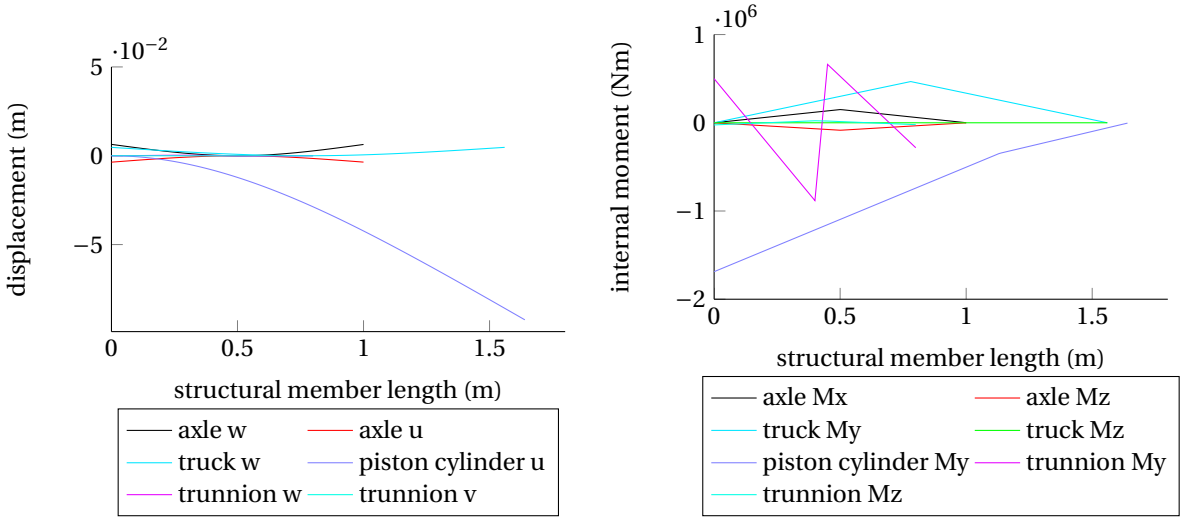

Figure 4.3: Structural deflections and internal moments for the tail down landing load case. These results are for the right main gear of a Boeing 707.

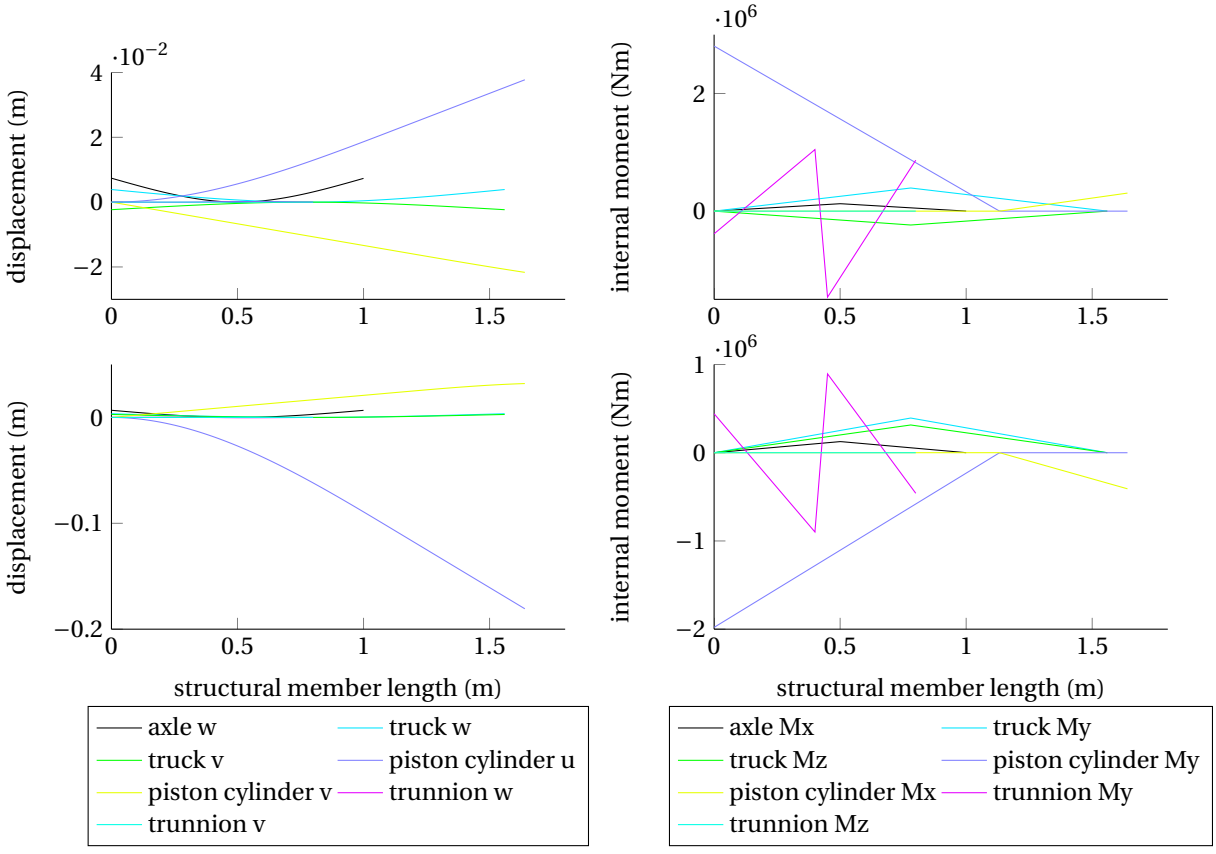

Figure 4.4: Structural deflections and internal moments for the lateral drift landing load case. The top 2 graphs are for the left main gear and the bottom 2 for the right main gear of a Boeing 707.

Part	Beam radius (m)	Wall thickness (m)	Weight (kg)
axle	57.1e-3	16.2e-3	106
truck beam	111e-3	12.2e-3	127
piston cylinder	143e-3	22.7e-3	281
trunnion	117e-3	30.5e-3	183
side strut	-	1.29e-3	8.3
drag strut	-	2.05e-3	8.3

Table 4.4: Boeing 707 main landing gear structural component weight

Aircraft	Estimate (kg)	Actual (kg)	Est/Act
Boeing 737-200 main gear	300.1	348	0.86
Boeing 737-200 nose gear	75.2	65.7	1.14
Boeing 727-200 main gear	708	751	0.94
Boeing 727-200 nose gear	121	148	0.82
Boeing 707-321 main gear	712	1150	0.62
Boeing 707-321 nose gear	119	101	1.18

Table 4.5: Comparison of wing and nose bogie structural weight with actual weights as given by Currey and Chai and Mason

4.3.3. Comparison weight estimation

To validate that the class 2.5 weight estimation method produces satisfying results, the calculated structural weight are compared to a landing gear structural weight estimation of Roskam. In this weight estimation the landing gear structure is modelled similarly. The structural weight here do not include all structural parts of the gear. Items such as torsion links, fittings and internal components of the shock absorber are not included. These, including controls, represent about 23 percent of the total main gear and 44 percent of the total nose gear structural weight (Currey, 1988, p.264). Results are presented in table 4.5 and do not include these items.

Structural weight data of the landing gear cannot be found easily. The weight data of Chai and Mason and Currey are the only data sources found usable for a comparison. These data sources contain data for only a few different transport aircraft. For the total landing gear group weight more information is available. Torenbeek gives landing gear group weights for several commercial aircraft as well as Roskam, Currey and Chai and Mason.

Results for the main gear structural weights deviate with an average of approximately 19 percent from the actual value. Nose gear weight deviate with an average of approximately 17 percent. These structural weight errors match with results obtained by Chai and Mason and Kraus. Kraus found an average error of 13 percent and Chai and Mason found an error of 10 percent.

Tyres, wheels and brake weights have all been determined before and can now be added. All remaining parts can also be added. These include fittings, controls and miscellaneous parts. The total assembly weights of all main and nose gears combined are compared with actual total assembly weights of Roskam in table 4.6. The average deviation from actual weights for these 4 aircraft is 15 percent.

4.3.4. Estimating weights for different aircraft types

The overall weight estimation capability of both the class 2 weight estimation module and the class 2.5 weight estimation is compared by generating results for many different aircraft. Figure 4.5 shows the results for all analysed aircraft. The aircraft size ranges from the Boeing 737 to the largest Airbus A380.

The class 2 module overestimates the gear weight for the smaller aircraft types. This is mainly due to the number of wheels required per bogie is calculated higher than actual as mentioned before. For the most

Aircraft	Estimate (kg)	Actual (kg)	Est/Act
Boeing 737-200	1741	1975	0.88
Boeing 727-200	3200	3271	0.98
Boeing 707-321	4143	5799	0.71
DC 10-10	11337	9576	1.18

Table 4.6: Comparison of wing and nose bogie assembly weight with actual weights as given by Roskam

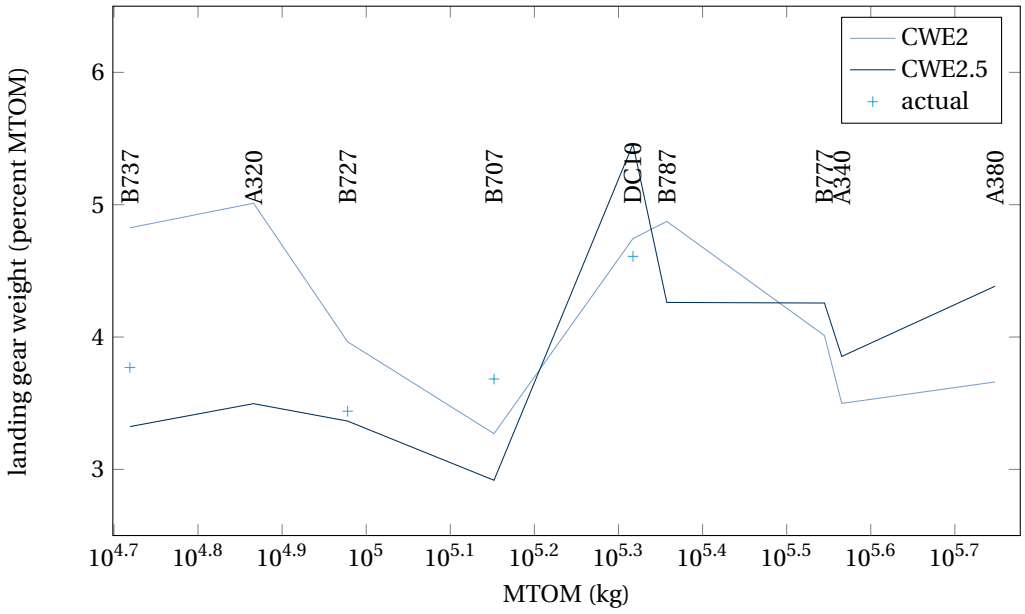

Figure 4.5: Comparison between weight estimation results of the class 2 weight estimation module, the class 2.5 weight estimation module and actual weight percentages as published by Roskam. The x-axis is the maximum take-off mass and has a logarithmic scale.

heavy aircraft analysed actual gear weights are not available. But for the Boeing 747 the gear weight is gear weight is 4.2 percent of the MTOM of 3.2e5 kg (Chai and Mason, 1997). Both the class 2 and the class 2.5 lines in figure 4.5 are close to the B747 values. A further comparison for the heaviest aircraft cannot be made due to the absence of reference data.

Overall the class 2.5 weight estimation is more close to the actual weight results of Roskam than the class 2 module. The class 2.5 weight estimation is based on a lot more information than the class 2 estimate. It is therefore anticipated that the class 2.5 results are better.

There are many factors that can be changed in the design of the landing gear. Each of these factors influence the overall weight of the landing gear. If for example safety factors are changed, calculated weights will change significantly. This is the most important reason why weight estimates shown in figure 4.5 are deviating quite a bit.

4.4. Tyre model verification

The tyre model equations listed in Pacejka (2006) and TNO Automotive (2010) are implemented in a Matlab script. The model will give the resulting forces F_x, F_y, F_z and moments M_x, M_y, M_z produced by the tyre due to a given velocity vector, slip angle α, slip ratio κ, path curvature $a\phi_t = -a/R$ and camber angle γ.

To verify that the magic formula equations produce correct results reference tyre parameters of Pacejka are used. Several plots are made as can be seen in figure 4.6 and these are compared with the results as shown in Pacejka (2006, p. 189)

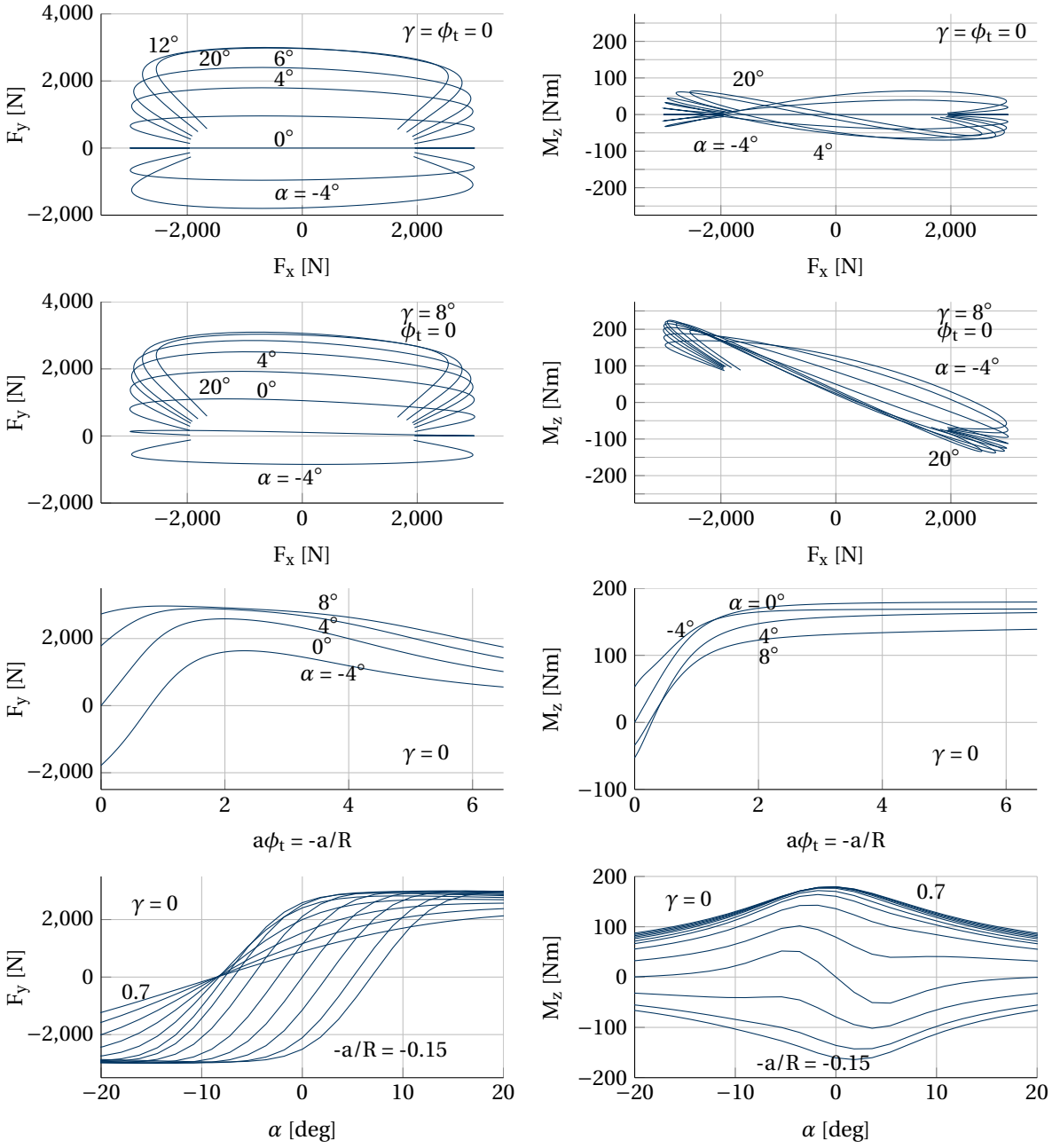

Figure 4.6: Tyre model verification outputs using the hypothetical model parameters of Pacejka. Tyre forces F_x, F_y and self aligning moment M_z are plotted against slip angle α, slip ratio κ and path curvature $a\phi_t = -a/R$. The camber angle is γ.

The results given here exactly match with the results of Pacejka. The equations of the tyre model thus produce correct results for the given reference tyre parameters. The results of the tyre model are more detailed than required for the aircraft tyre model that will be used. This is because the number of parameters available for an aircraft tyre from TNO Automotive is less than the reference tyre presented here (TNO Automotive, 2012). When more detailed aircraft tyre data is available tyre model results will be more accurate.

4.5. Landing gear analysis results

4.5.1. Drop test results for an Airbus A320

A landing gear analysis has been performed on an Airbus A320-200 main landing gear. This is the simplest bogie type and does not introduce loads due to rotation of the bogie truck. A schematic representation of the simulation, including degrees of freedom, is available in section 3.2. The default ode45 solver can efficiently solve the equations of motion and is therefore used in the drop test simulations. The order of accuracy of this solver medium (Mathworks, 2012). When more accuracy is required a ode113 solver can be used, but this requires a lot more time steps to run the complete simulation.

Figure 4.8 and 4.9 displays the results for which it has been assumed that lift is equal to weight. The landing is performed at maximum landing weight with a touchdown vertical velocity of 10 ft/s (3 m/s). A maximum load of 4.32e5 N is found on the main gear strut. This is 1.27 times the static maximum ramp weight strut load (which equal to a load of 3.62e5 N per strut). An estimate of the dynamic load factor of 1.33 for a 10 ft/s landing has been found before using equation 2.45. Estimated dynamic loads were used in the analytical weight estimation and are thus only slightly over-dimension the landing gear structural parts.

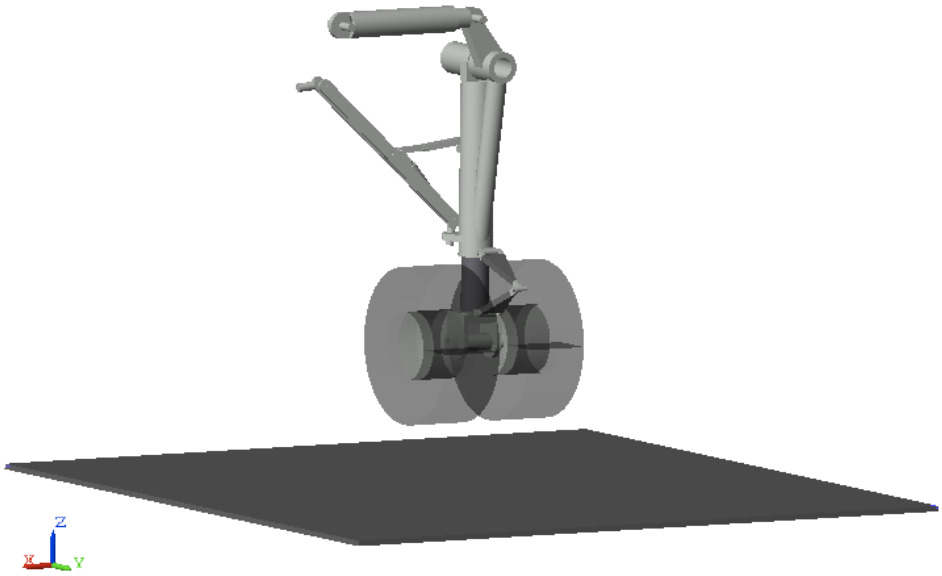

Figure 4.7: Drop test simulation of the multi-body model of an Airbus A320 main landing gear

The drop test performed here is not a regular landing, but an extremely hard landing. This should almost never occur during the life of the aircraft. The landing gear has been designed for a load factor of 1.2. During a normal landing the impact load will be much lower: about 40 percent of the static load (as mentioned before in section 2.3 of chapter 2).

The tyre deflection when a static load is applied is for the A320 tyre 0.21 m. In figure 4.9 the maximum tyre deflection is only 0.13 m. The vertical force of a hard landing is thus not the critical vertical force on the

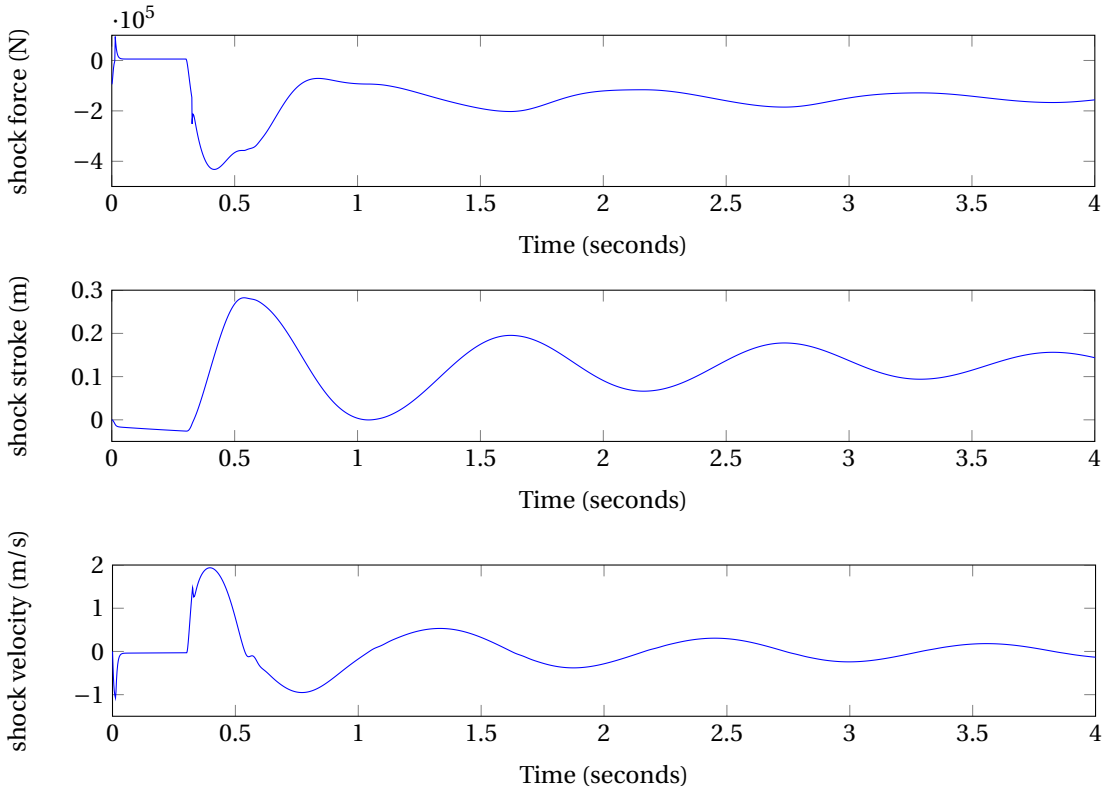

Figure 4.8: Shock absorber force, stroke and velocity for a two wheel A320-200 main landing gear landing at 10 ft/s

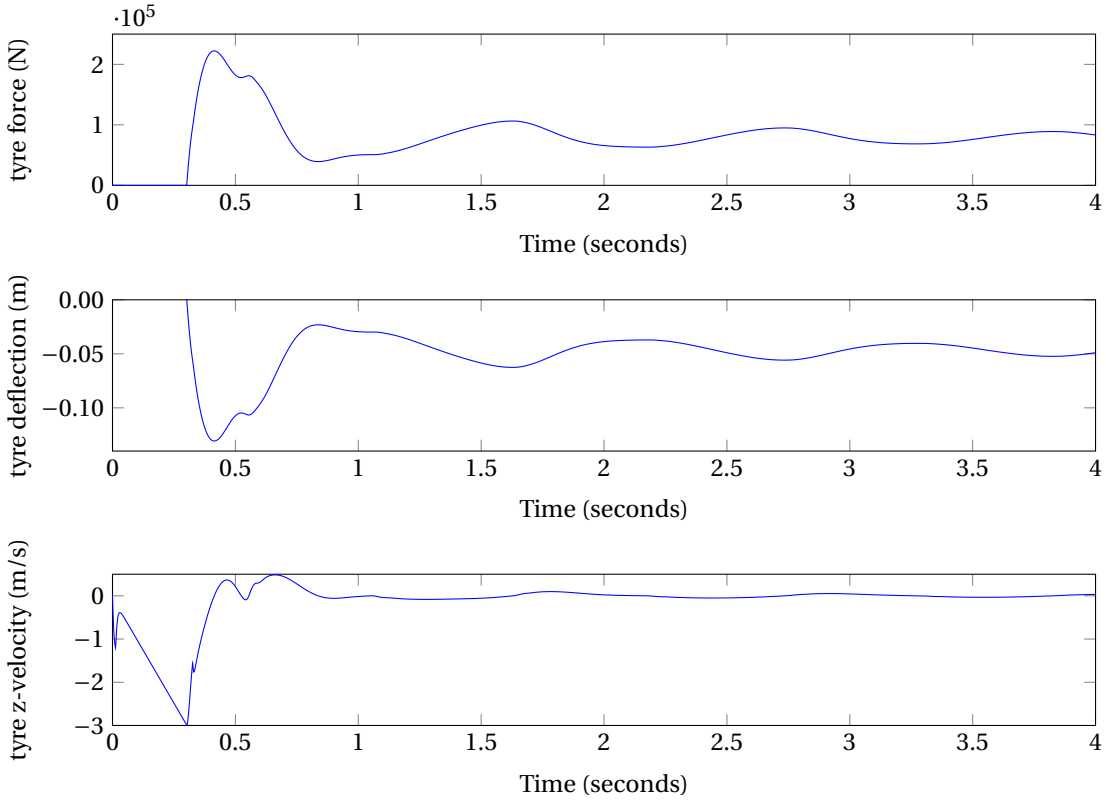

Figure 4.9: Tyre vertical force, deflection and velocity for a two wheel A320-200 main landing gear landing at 10 ft/s

tyre, when tyre spin-up before touchdown and a horizontal friction force is not taken into account.

When comparing the results with actual measurement results of Ladda and Struck the shock force response in z-direction is initially similar. When looking on a longer time span the result of the model does not increase as the measurement results. This is mainly due to the change in lift force, which is not taken into account. Therefore an evaluation for a longer time period is not represented accurately by this model. In reality the lift on the wings reduces rapidly when lift dumpers are deployed during the landing rollout.

The behaviour of the oleo-pneumatic shock absorber and the tyre to the applied load is good. The vibrations in the shock and tyre damp out rapidly during a short time. There are no high frequency loads seen in the results. This is desirable when considering fatigue in the landing gear material.

4.5.2. Drop test results for a Boeing 777

The Boeing 777-300ER has a large 2 strut main landing gear with 6 wheels per strut. For this simulation of a drop test the same initial conditions apply as for the A320 landing gear. The gear lands at 10 fps and lift is assumed equal to weight. Only now there is a bogie truck placed at an initial angle of 15 degrees with respect to the horizontal. The results for the shock absorber and the rear axle tyre are shown in figures 4.11 and 4.12. The rear axle tyre will hit the ground first at touchdown.

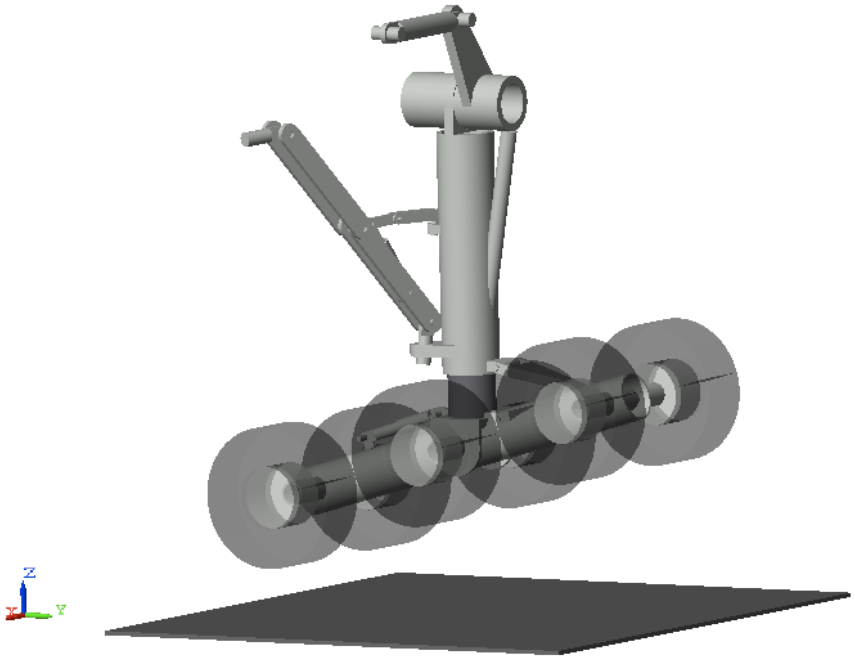

Figure 4.10: Drop test simulation of the multi-body model a Boeing 777-300Er main landing gear

The interaction with the front axle and the rear axle tyres is important here. The result of this interaction is that the landing gear bounces several times after the first impact. Also there are high frequency loads on the gear. At the point when both the front and rear axle tyres simultaneously hit the ground the load on the shock strut is 2.6 times the strut static load. Because of the high rotational velocity of the truck beam the shock and tyre is highly loaded briefly. When the truck beam velocity reduces, maximum loads are considerably lower. The maximum load factor after the first simultaneous impact is 0.7.

After 2.5 seconds the bouncing of the gear stops and the landing loads can be damped more effectively. The shock force however still fluctuates at high frequency. This is because the truck beam motion is undamped. The peak loads can be reduced by adding a damping force to the truck beam actuator as well as adjusting the shock absorber design.

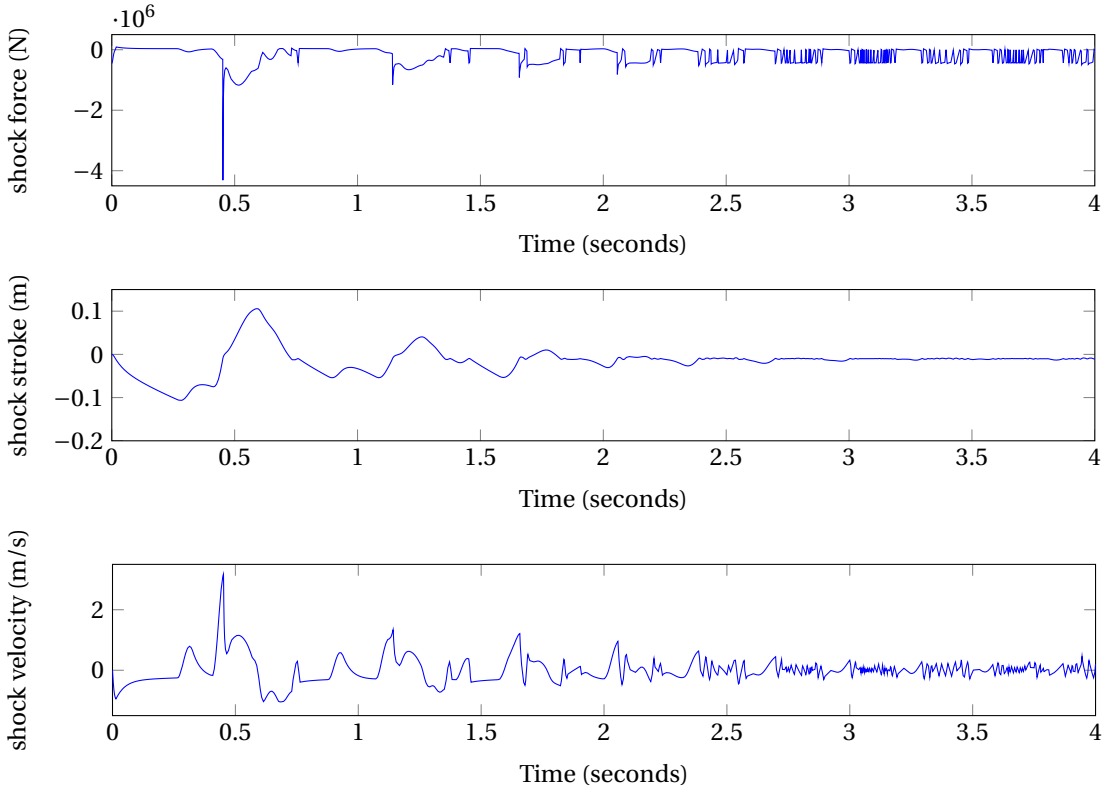

Figure 4.11: Shock absorber force, stroke and velocity for a six wheel B777-300ER main landing gear landing at 10 ft/s

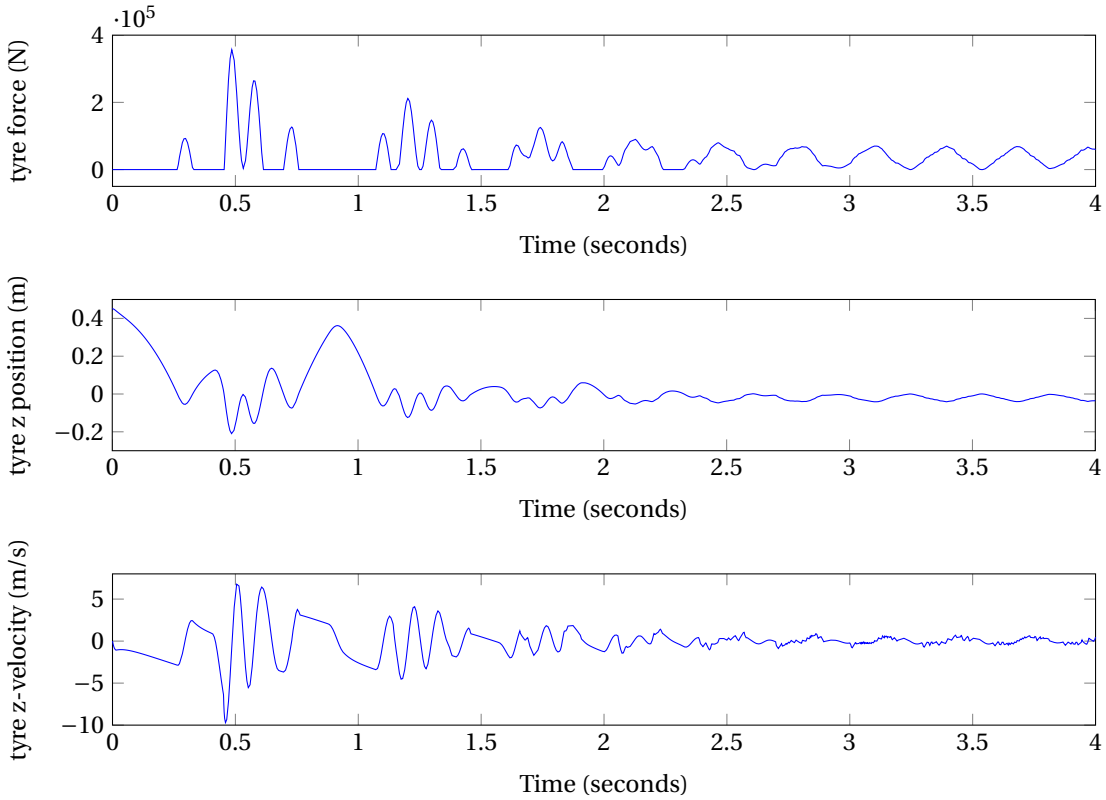

Figure 4.12: Rear axle tyre vertical force, position and velocity for a six wheel B777-300ER main landing gear landing at 10 ft/s

4.5.3. Tyre spin-up influence

If the landing gear tyres are not spin-up before touchdown, the difference in speed of the tyres with the ground is the approach velocity. To simulate such a landing the tyres are given an initial radial velocity of $\Omega = V/R$, which is for an Airbus A320 68.9 m/s / 0.58 m = 118 rad/s or 19 rotations per second. The simulation is performed using the same initial conditions as in 4.5.1. Results are shown in figure 4.13.

The tyre stops spinning after the first impact. There is a high force required to stop it from spinning: the maximum tangential force is 3160 kg. This high force is a consequence of the fast change in rotational velocity. The tyre and shock dynamics after the first impact are the same as for the impact without spin. The influence of the tyre spin is only that the maximum force on the shock is increased to 4.38e5 N. This is only 1 percent higher than a landing without spin-up. The influence of the tyre spin on the landing gear model response is thus minimal.

4.5.4. Landing gear retraction simulation

To make sure that the landing gear design can actually be stowed in the fuselage a retraction and extension simulation is performed. There is an actuator installed on the trunnion beam, on the lock links and if applicable on the truck beam. Retraction is performed by applying a predetermined sequence. The gear initial condition is the completely extended position. A schematic representation of the simulation is available in section 3.2. The default ode45 solver is used to solve the equations of motion in the simulation. This solver is efficient and has a medium accuracy that is sufficient for the retraction simulation.

First the truck beam is positioned in retracted position (horizontally). Then the lock actuator is enabled, which then pushes the lock links upward. Finally the largest actuator rotates the complete assembly inboards. Rotation stops when the maximum rotation angle (calculated in the stowage analysis) is reached.

The actuator forces are controlled by PID controllers. PID controller are widely used for many industrial control problems, because the controller structure is simple and performance is satisfactory in many applications (Toscano, 2005).

By adjusting the deploy/retract sequence and the PID parameters the retraction system is given the desired properties. The PID parameters are tuned to achieve a low steady state error percentage (fully reaching the retraction angle) and are tuned to get no overshoot in the response. The stroke-force curve for the main retraction actuator is shown in figure 4.15. The retraction angle is almost completely achieved and the steady state error is 5 percent. There is no overshoot and retraction happens without sudden movements. A drawback of the chosen retraction tuning is that the force changes are large during the stroke of the actuator (see the stroke force curve). Efficiency of the actuator is thus not high and can be improved if actuator efficiency proves too low later in the design.

Figure 4.14 and 4.16 displays the retraction and extension motion of an Airbus A320 main landing gear. The retraction signal is given at 2.5 seconds. Then it takes about 3 seconds to fully retract the gear. Extension starts at 6 seconds and complete extension and locking finishes about 4 seconds later. At the final stage of extension it takes some time for the lock actuator to fully lock the landing gear. Retraction is faster than the required 10 seconds and extension is faster than 15 seconds.

The design of the actuation systems is not completed at this stage. Further optimisations and a more detailed analysis should be done later in the design process. The results presented here show that the landing gear design is kinematically feasible and the required retraction and extension motion can be achieved by the system. Also it is shown that the required stowage space is kept minimal.

4.6. Calculation run time

The calculation time required to run the PositionLandingGear module is in the order of 5 seconds for a 2 strut main gear and 9 seconds for a 4 strut main gear. Timing tests have been performed on a computer with a

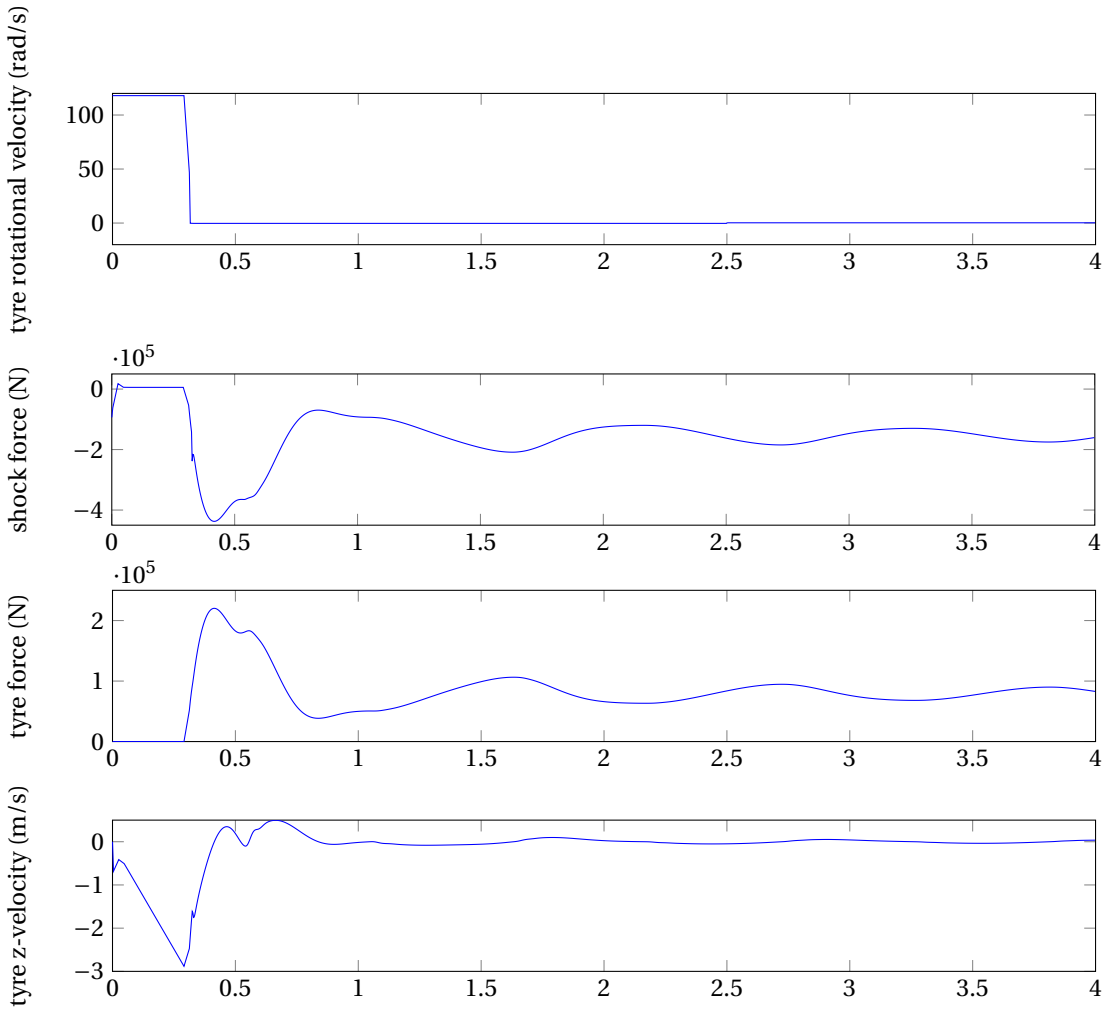

Figure 4.13: Landing simulation with tyre spin-up. Tyre spin velocity, shock absorber force, stroke and velocity for a two wheel A320-200 main landing gear landing at 10 ft/s

Figure 4.14: Retraction motion of the multi-body model an Airbus A320 main landing gear

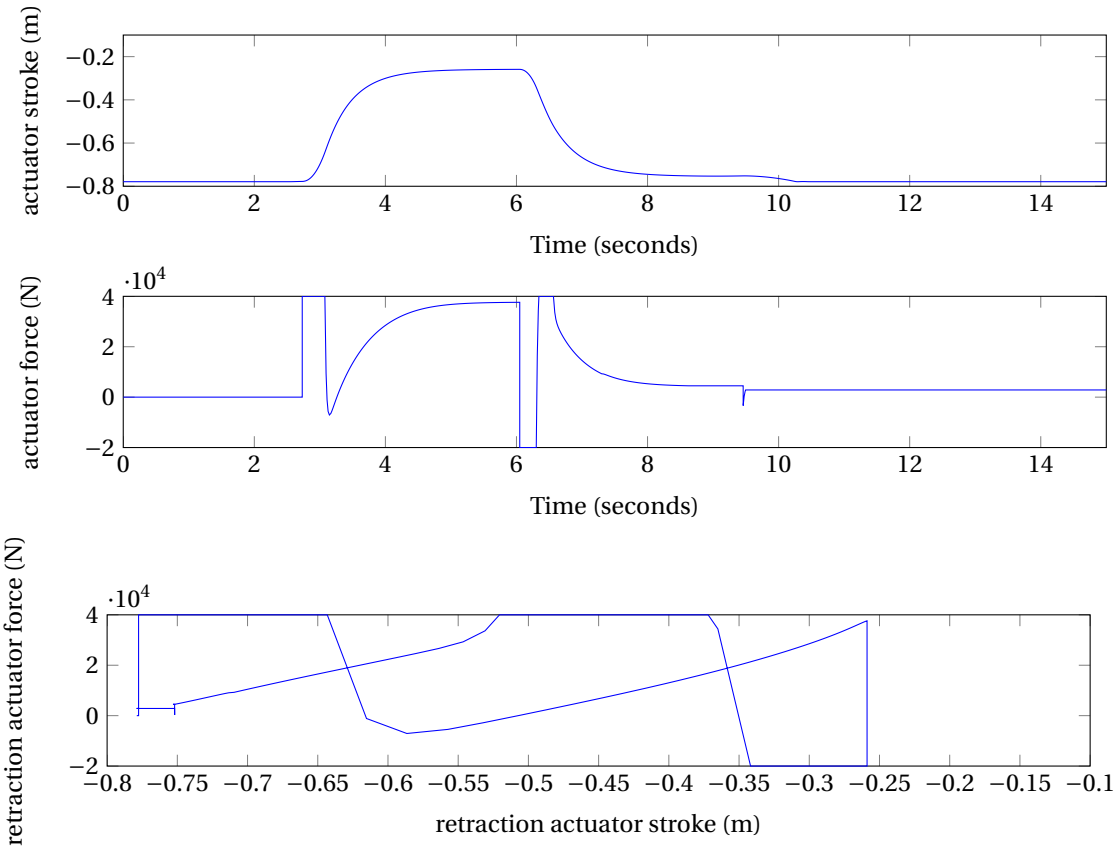

Figure 4.15: Retraction actuation stroke versus force of an Airbus A320 main landing gear.

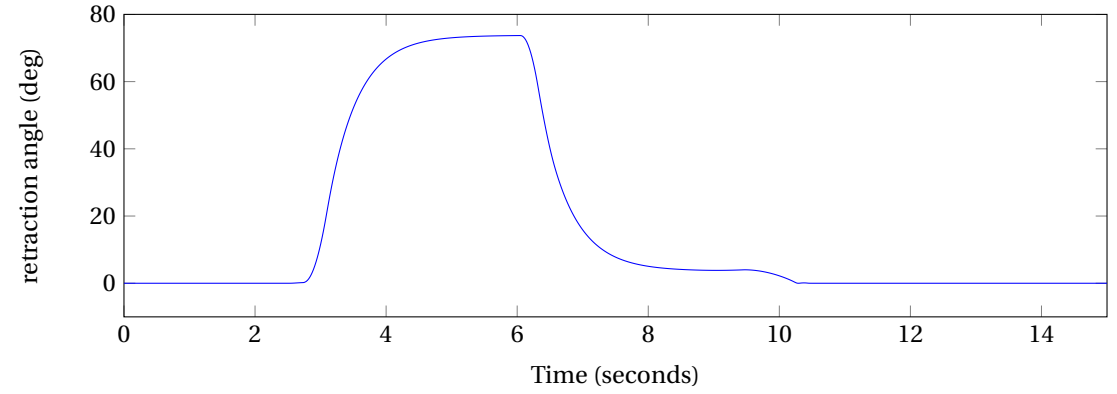

Figure 4.16: Retraction/extension angle of an Airbus A320 main landing gear. The gear is initially in a extended position.

2GHz Intel Core 2 Duo processor. These run times are comparable to other weight estimation modules that are available within the Initiator. The time required is low enough to be able to use the module within an optimisation loop.

Profiling of the code shows that most time is spent on the flotation analysis: 55 percent on the rigid ACN calculation and 9 percent is spent on the flexible ACN calculation. This is due to the large number of iterations required to get an ACN result. An increase in the number of main gear struts will increase the number of bogie combinations that need to be analysed for the flotation requirement. This explains the relatively large increase in calculation time for aircraft with more than 2 struts.

The flotation analysis calculation time has been reduced as much as possible by optimising for the Matlab JIT accelerator as described in section 3.1.2. A further reduction in calculation time is difficult to achieve.

5

Conclusions

The objective of the master thesis was to expand the knowledge base of the existing automated design environment by creating and integrating an automated landing gear design tool. The automated landing gear design includes analysis of structures, kinematics, runway flotation and weight.

When finding a feasible position of the nose and main landing gear there are several limiting factors. First there is the take-off stability requirement that makes sure that the aircraft can safely pitch up or down. During landing the aircraft should have a pitch down tendency in order to make a safe landing. A crosswind landing should also be possible without touching the ground and taxi turns need to be possible without the tendency to tip on its side. Additional ground clearance should be kept between the engines or wing tips for a possible sideways landing. Loads on the nose gear should be high enough to keep the ability of proper steering. The main gear also should keep a high enough load to make sure that the brakes can provide enough braking power. Ground operational requirements dictate that the aircraft should be able to make a 180-degree turn on a runway. Also airport taxiway turns need to be made by keeping the nose gear on the turn centre line without going outside the pavement boundary. The combination of all these limits results in a main and nose landing gear lateral position, a longitudinal position and a landing gear height.

Based on the landing gear position maximum loads on the landing gear struts can be calculated and tyres can be selected from a catalogue. Accompanying wheels are then also selected. The size of the brakes is found from the required stopping power to make a rejected take-off stop, several landing stops at design landing mass and several stops at maximum landing mass. Both steel and carbon brakes are considered.

The design and analysis of the retraction and extension of the gear (kinematics) results in joint and actuator positions. When considering different kinematic schemes, the least complex scheme is preferred, considering safety and maintenance and costs. Retraction of each landing gear is done by rotation about a single axis while side braces and a locking mechanism are folded in. The geometric kinematic analysis is replaced by a mathematical analysis or numerical simulation as the landing gear design gets more detailed.

When shocks occur caused by hard landings and by taxiing over rough surfaces they are absorbed efficiently by oleo-pneumatic shock absorbers and tyres. The shock absorbers need to be able to cope with different load cases provided by certification specifications. To show compliance with these specifications the piston stroke, the internal pressures and volumes are designed. The oleo-pneumatic shock absorber forces can then be modelled accordingly and landing load cases can be evaluated. For maintenance, keeping complexity low is important as maintenance forms an important part of the costs. Reduced complexity will also keep landing gear weight minimal. And as fuel prices increase, reductions in weight are given higher priorities.

Empirical relations mainly estimate the landing gear weights. But empirical relations are limitedly dependent on aircraft and landing gear design variables. An analytical weight estimation does not have this drawback and is therefore better suitable for use in an optimisation loop. Analytically estimating the weight of the landing gear can be done by generating a structural model and finding maximum stresses when the structure is under extreme loads. The extreme load cases are prescribed in certification specifications. Yield stresses should not occur during the entire life of the structure, also buckling should not happen when the side struts are put under compression. From the maximum stresses, required component thicknesses are found by including an additional factor of safety.

Based on the information of the previous analyses a multi-body dynamical model can be automatically made. In this model structural parts are modelled as rigid bodies. The oleo-pneumatic shock absorber forces and motion are modelled using an analytical relation. And tyre motion and forces at the contact point are modelled using the empirical relations of the MF-tyre model.

A detailed model of both the shock absorbers and tyres allows the evaluation of extreme landing load cases and verification of the estimated dynamic landing loads used in the weight estimation. In addition to the landing simulation a simulation of the landing gear retraction mechanism is done. The simulation forms a check on kinematic feasibility and a check of compliance to certification requirements.

Implementation of the above-mentioned procedures is done by integrating the landing gear positioning, bogie design and weight estimation into the TU Delft Initiator. This is done in the form of a landing gear design module. Additionally a separate empirical module is made that is also applicable to nonconventional aircraft concepts. And a separate multi-body dynamics simulation program is also implemented that validates the kinematics and performance of the shock absorber and tyres during an extreme landing.

To verify the results produced by the implemented landing gear design modules, landing gear designs for a number of different aircraft are generated. Calculated landing gear positions closely match with actual landing gear positions given by aircraft manufactures. The analytical weight estimation of the landing gear assembly estimates the total gear weight with an error of 15 per cent compared to an empirical weight estimation error of 17 per cent. This result shows that an empirical weight estimation method cannot be fully replaced by an analytical method. Both methods complement each other, but when using a weight estimation in an optimisation loop the analytical method is preferred due to its highly dependency on landing gear and aircraft design parameters.

Multi-body simulation results show that dynamic loads during an extreme landing are about 5 per cent lower than the estimated dynamic loads. A hard landing with a landing gear with multiple rows of tyres creates high frequency peaks in the shock loads. These peaks originate from the interaction between front and rear axle tyres hitting the ground at different times. Loading peaks of twice the maximum load for a single axle gear could occur. Therefore measures need to be taken in the design of multi-axle landing gears to damp out these high peaks. When adding the effect of tyre spin-up forces, these are found to have a low impact on overall landing loads.

The kinematic simulation produces bogie retraction/extension time and retraction actuator efficiency, which can be used to further optimise the landing gear design. The simulation also shows that the retraction and locking mechanisms work and can be stowed within the available space.

Finally it can be concluded that the implemented landing gear design tools add essential extra information to the overall aircraft design. By not leaving out the landing gear design in the aircraft design, unfeasible aircraft configurations can be identified early in the design process.

6

Recommendation

There are a number of recommendations for improvement and additional research that can be made. An improvement would be to increase the level of detail of the landing gear analysis model by adding systems such as a steering system, a hydraulic actuation system and structural component interfaces.

When more detail is added to the landing gear model, structural component weight estimates can be further improved. Also adding a finite element analysis of the structure improves confidence in the produced landing gear result. This also allows for the optimisation of the shape of landing gear components and can reduce overall weight.

Aerodynamic drag and interference with the flow over the wing is a subject that also is valuable to be analysed. It can then also be checked if the landing gear is able to withstand aerodynamic loads and can be extended by gravity in an emergency during the landing.

When the landing gear multi-body model is added to a complete aircraft model further simulations and verification can be done. A simulation of ground handling or a crosswind landing simulation is a valuable addition.

For the TU Delft Initiator it can be recommended that the centre of gravity range optimisation needs to be improved. It can often occur that this range is outside operational bounds, leading to an operational limited aircraft. Centre of gravity range optimisation is not only important for landing gear positioning, stability and control of the aircraft during flight is also highly dependent on the cg range.

The analytical weight estimation is currently applicable only to conventional aircraft. Support for non-conventional aircraft can be added by adding additional limitations and checks in the analysis. Added support for evaluation of nonconventional aircraft concepts will then add the capability to perform the design process within a multidisciplinary optimisation loop.

A

Landing gear structure free body diagrams

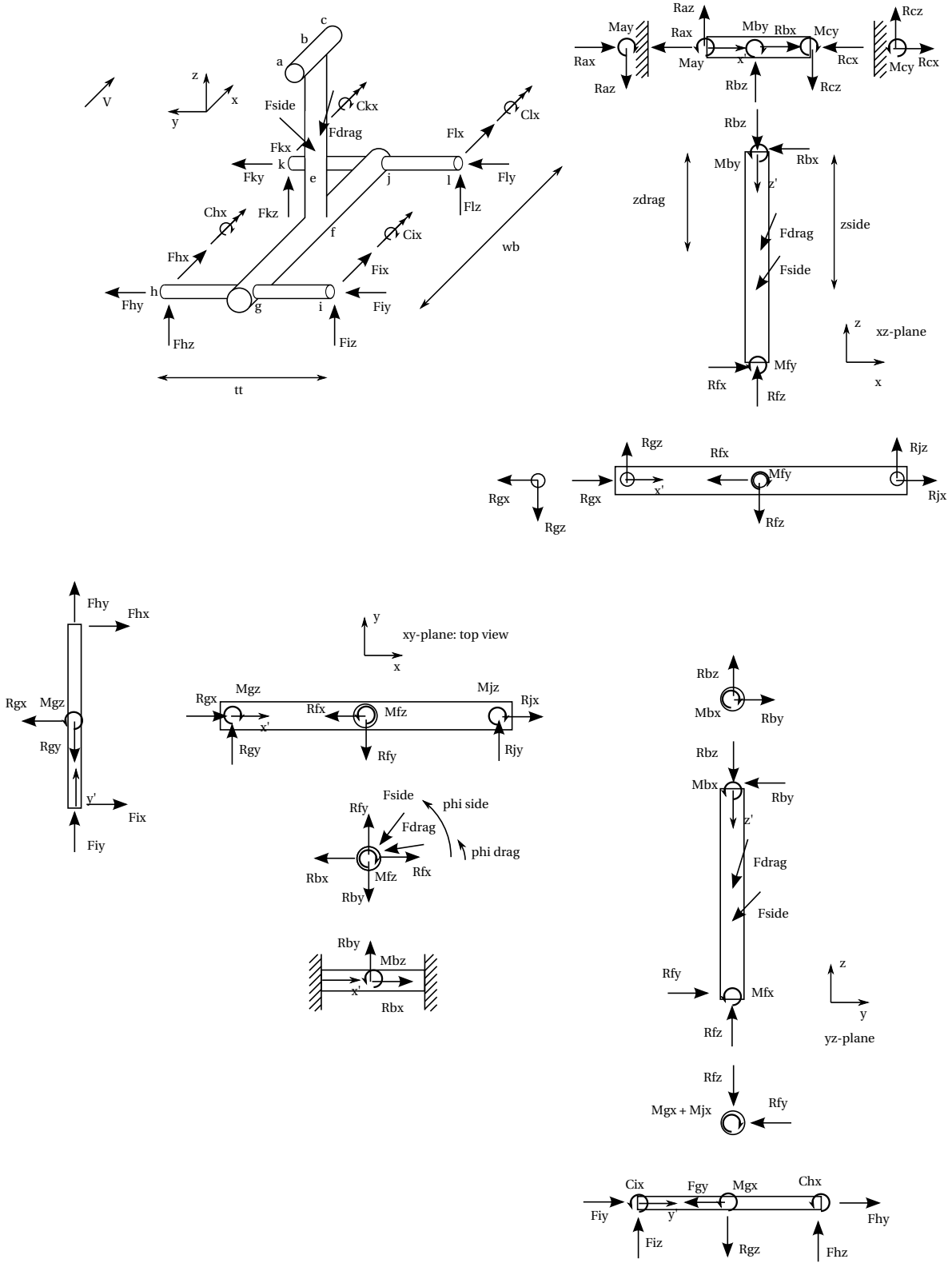

Figure A.1: Free body diagram of a general 4 wheel main landing gear bogie

B

Reference airport pavement classification numbers

Airport	PCN	Subgrade category	Min runway length	Min runway width
London Heathrow	83	1	3660	50
Amsterdam Schiphol	90	3	3300	45
New York John F Kennedy Intl	90	2	3048	45
San Diego Intl	78	2	2865	61
Rotterdam Zestienhoven	74	4	2200	45
Trondheim Norway	50	1	2999	45
Svalbard Norway	58	2	2483	45
Maastricht Aachen	71	3	2500	45
Eindhoven	60	1	3000	45
Groningen Eelde	55	1	1500	45
Lelystad	19	4	1250	30

Table B.1: List of airports with flexible pavements and their accompanying Pavement Classification Number (PCN) and associated subgrade category

Airport	PCN	Subgrade category	Min runway length	Min runway width
Atlanta Intl	62	1	2743	45
Chicago O'Hare Intl	108	3	2461	45
Los Angeles Intl	70	1	3134	45
Kuala Lumpur Intl	90	3	4000	60
Washington Dulles Intl	81	3	2865	45
Washington Andrews AFB	54	3	2973	45
Los Angeles Edwards AFB	64	2	3658	60
Las Vegas Nellis AFB	43	3	3085	60
Manchester	79	3	3050	45
London Stansted	86	3	3049	46
London Luton	75	4	2160	46
Prague	62	2	3250	45
Auckland Intl	120	4	3535	45
Buffalo Niagara Intl	38	2	2996	45

Table B.2: List of airports with rigid pavements and their accompanying Pavement Classification Number (PCN) and associated subgrade category

C

PositionLandingGear output variables

Description	Property
Aircraft Design Group	ADG
auxiliary spar x-position at main gear y-position	AuxSparX
rear spar x-position at main gear y-position	RearSparX
aircraft ACN's flexible pavements	ACNsFlex
aircraft ACN's rigid pavements	ACNsRigid
single brake volume (m3)	BrakeVolume
single brake weight (kg)	BrakeWeight
feasible main gear bogie types	FeasibleBogies
landing gear height w.r.t fuselage belly	Height
landing load factor	LandingLoadFactor
load fraction of MRM at aft cg position	LoadCGaft
load fraction of MRM at forward cg position	LoadCGfwd
wing maximum z-position at main gear y-position	MaxGearSparCxxZ
bogie type with the least number of wheels	MinNWheelsSolution
minimum shock piston length (m)	MinPistonLength
shock piston orifice area (m2)	PistonOrificeA
rim diameter (m)	RimDiameter
rim flange height (m)	RimFlangeHeight
rim weight (kg)	RimWeight
rim width (m)	RimWidth
shock stroke length at static loading (m)	ShockStaticStroke
maximum shock stroke length (m)	ShockStroke
g force when fully compressed	StrutCompressedG
shock absorber p1 pressure	StrutP1
shock absorber p2 pressure	StrutP2
shock piston area (m2)	StrutPistonArea
strut static load (kg)	StrutStaticLoad
shock absorber v1 volume	StrutV1
shock absorber v2 volume	StrutV2
shock absorber v3 volume	StrutV3
total number of wheels on all main gears	TotalNWheelsFeasible
tyre name	Tyre
tyre diameter (m)	TyreDiameter
tyre database row number	TyreId
tyre pressure (kPa)	TyrePressure
tyre rated load (kg)	TyreRatedLoad
tyre diameter at rated load (m)	TyreStaticDiameter
tyre weight (kg)	TyreWeight
tyre width (m)	TyreWidth
wing bogie cg z-position (m)	WingBogieCGz
wing bogie drag strut connection point on wing (m)	WingBogieDStrutSparCxx
structural tubes inner radii (m)	WingBogieInnerR
wing bogie length (m)	WingBogieLength
wing bogie mass (kg)	WingBogieMass

Description	Property
wing bogie number of wheel rows	WingBogieNRows
wing bogie number of wheels	WingBogieNWheels
wing bogie number of wheels per row	WingBogieNWheelsPerRow
wing bogie loading MRM fraction	WingBogiePcntLoad
right wing bogie position (m)	WingBogiePositionRight
wing bogie retraction angle (deg)	WingBogieRetractionAngle
wing bogie side strut cylinder connection point (m)	WingBogieSStrutCylCxx
wing bogie side strut wing spar connection point (m)	WingBogieSStrutSparCxx
wing bogie structural tube thicknesses (m)	WingBogieThicknesses
wing bogie weight per structural tube (kg)	WingBogieTotalWeights
wing bogie layout number	WingBogieType
wing bogie tyre track (m)	WingBogieTyreTrack
wing bogie wheelbase (m)	WingBogieWheelBase
shock absorber polytropic N number	polyN
total landing gear mass of least number of wheel solution (kg)	Mass
nacelle height from ground (m)	NacelleHeight
nacelle clearance angle (deg)	Phi_nacelle
wing clearance angle (deg)	Phi_wing
sideways turnover angle (deg)	SidewaysTurnoverAngle4
total tube structure weight per bogie (kg)	TotalStrucWeight
total landing gear mass (kg)	TotalWeight
scrape angle when fuselage hits the ground (deg)	theta
maximum take off scrape angle (deg)	thetaLOF

Table C.1: List of all output variables

D

List of tested reference aircraft

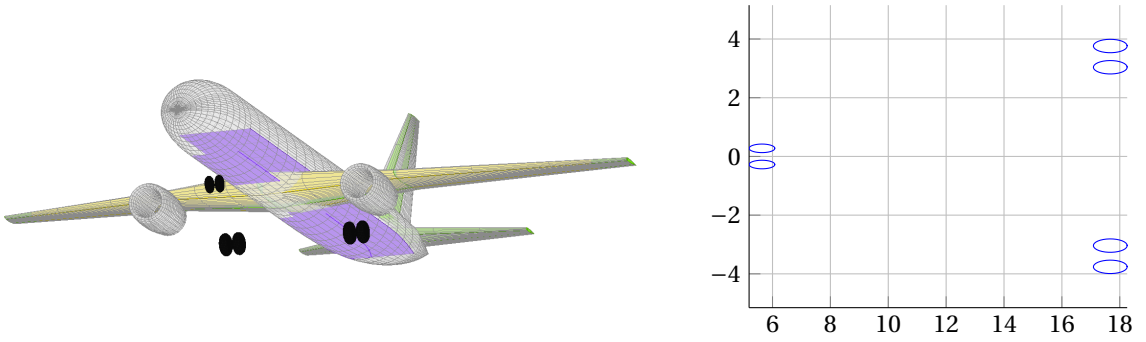

Figure D.1: Airbus A320-200

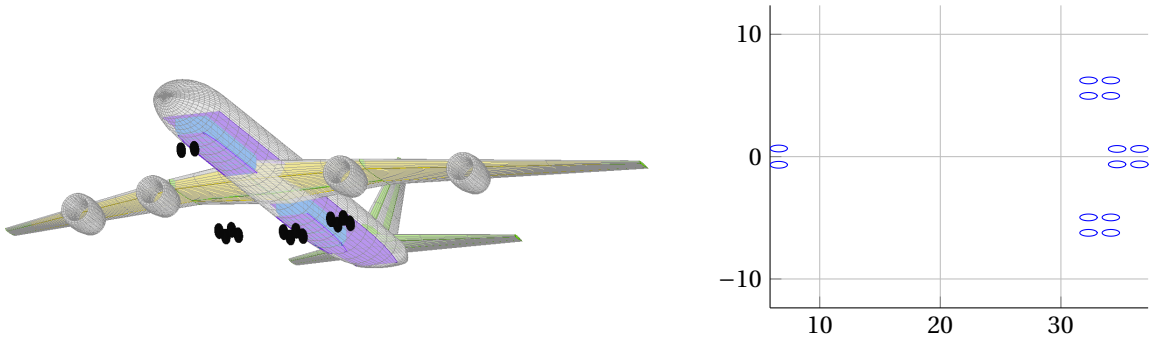

Figure D.2: Airbus A340-500

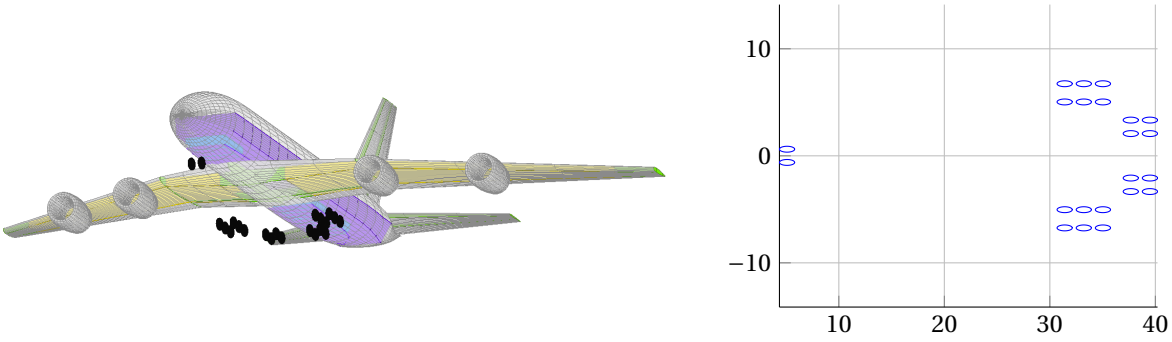

Figure D.3: Airbus A380-800

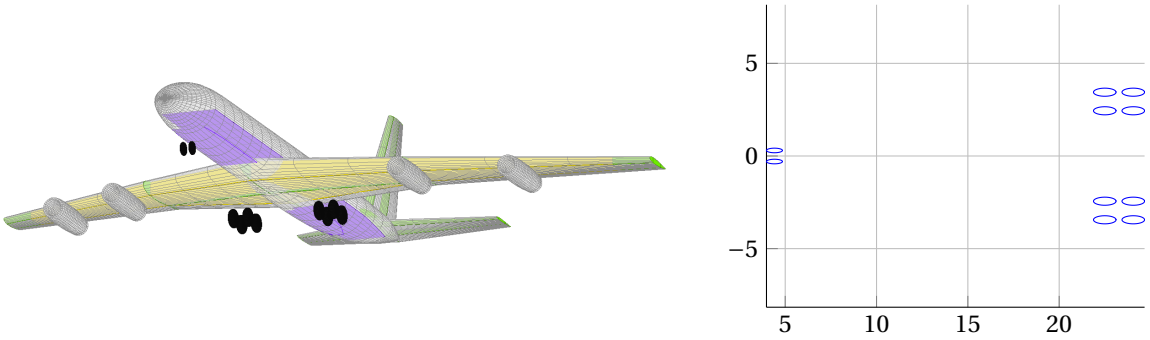

Figure D.4: Boeing 707-321

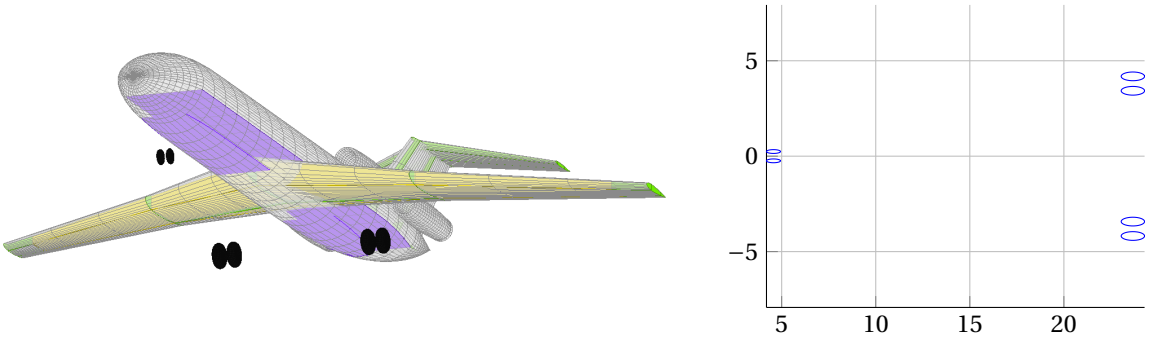

Figure D.5: Boeing 727-200

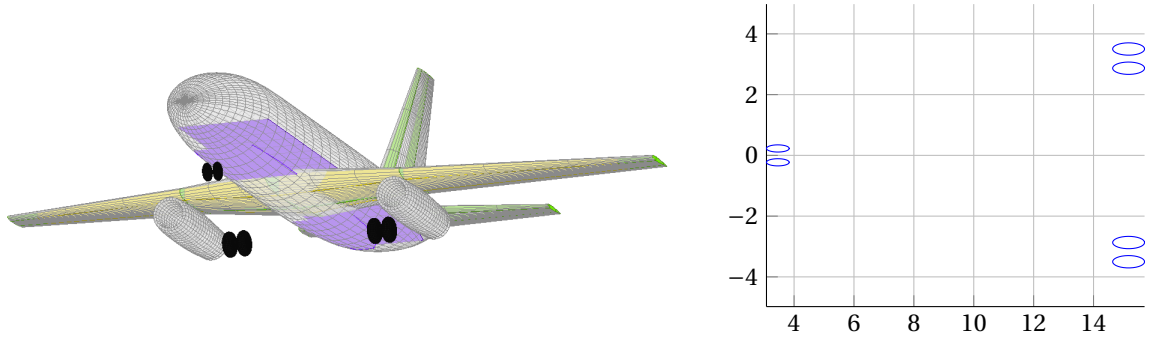

Figure D.6: Boeing 737-200

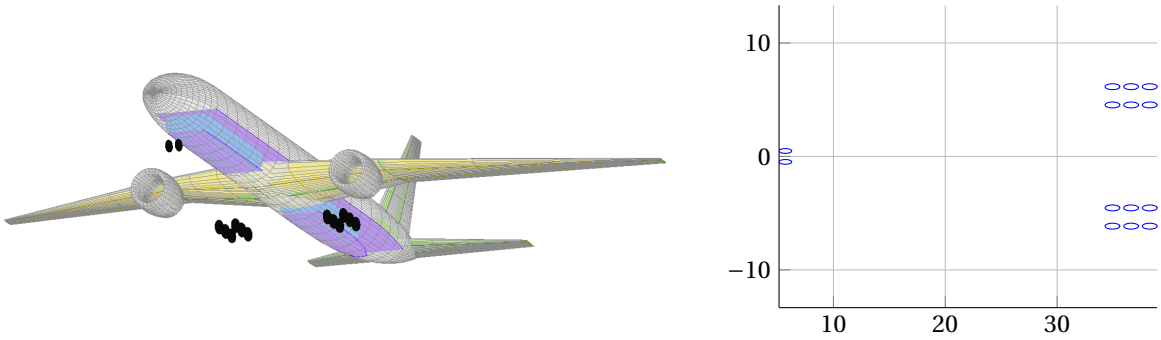

Figure D.7: Boeing 777-300ER

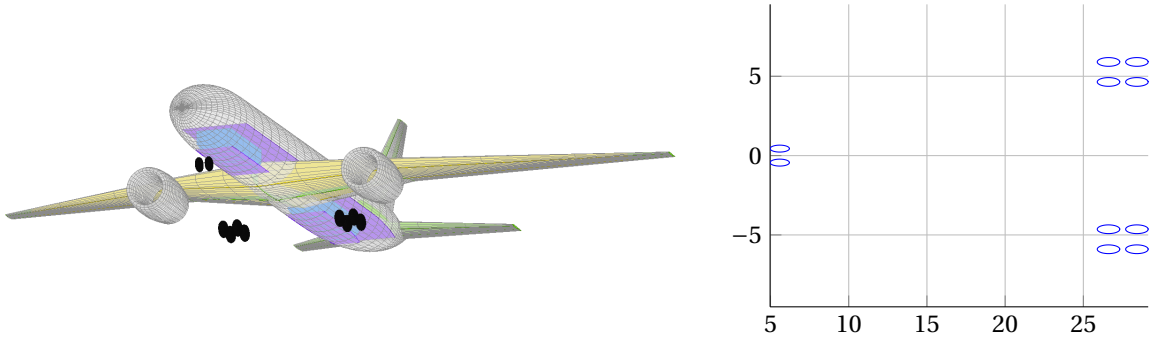

Figure D.8: Boeing 787-800

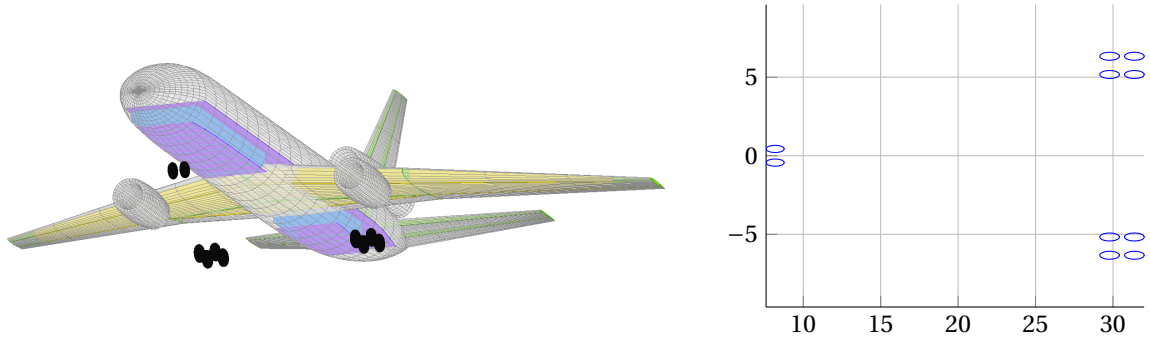

Figure D.9: McDonnell Douglas DC10-10

Bibliography

The Materials Information Society ASM International. Asm materials information, 2013. URL http://products.asminternational.org/matinfo/index.jsp.

I.J.M. Besselink. Shimmy of aircraft main landing gears. Master's thesis, Delft University of Technology, Mekelweg 2, Delft, The Netherlands, September 2000.

Boeing 707 Airplane Characteristics, Airport Planning. Boeing, Seattle, WA, revision 3 edition, May 2011.

M. Boschetto, R. Bianco Mengotti, GL Ghiringhelli, and S. Gualdi. Analysis of landing gear behaviour for trainer aircraft. In *Proceedings of the 15th European ADAMS Users' Conference, Rome*, pages 15–16, 2000.

Sonny T. Chai and William H. Mason. Landing gear integration in aircraft conceptual design. Technical report, Virginia Polytechnic Institute and State University, Blacksburg, Virginia, 24061-0203, March 1997. URL http://www.dept.aoe.vt.edu/~mason/Mason_f/M96SC.html.

S.T. Chai and W.H. Mason. Landing gear integration in aircraft conceptual design. Technical report, Virginia Polytechnic Institute and State University, 1996.

John Christy. Flight operations engineering: runway loadings. Technical report, Boeing Commercial Airplanes, 2009.

EB Coetzee, B. Krauskopf, and MH Lowenberg. Nonlinear aircraft ground dynamics. 2006.

H.G. Conway. *Landing gear design*, volume 3. Chapman & Hall, 1958.

S. Cumnuantip, M. Spieck, and WR Krueger. An approach for sizing and topology optimization integrating multibody simulation. In *46 th AIAA/ASME/ASCE/AHS/ASC Structures, Structural Dynamics, and Materials Conference*, pages 1–10, 2005.

N.S. Currey. *Aircraft landing gear design: principles and practices*. American Institute of Aeronautics and Astronautics, 370 L'Enfant Promenade, S.W., Washington, D.C. 20024, 4th edition, 1988.

R. Doganis. *Flying Off Course IV: Airline Economics and Marketing*. Taylor & Francis, 2009.

R.J.M. Elmendorp. Synthesis of novel aircraft concepts for future air travel. Master's thesis, Delft University of Technology Faculty of Aerospace Engineering, January 2014.

European Aviation Safety Agency. Certification specifications and acceptable means of compliance for large aeroplanes cs-25, July 2012.

Federal Aviation Administration. Comfaa 3.0. software, August 2011. URL http://www.airporttech.tc.faa.gov/naptf/download/index1.asp.

Federal Aviation Administration. Federal aviation regulations part 25—airworthiness standards: Transport category airplanes, September 2012a. URL http://www.faa.gov/regulations_policies/faa_regulations/.

Federal Aviation Administration. Advisory circular: Airport design ac 150/5300-13a, September 2012b. URL http://www.faa.gov/airports/resources/advisory_circulars/index.cfm/go/document.current/documentNumber/150_5300-13/.

Goodrich. 787 electro-mechanical brake system, 2012. URL http://www.goodrich.com/Goodrich/Businesses/Aircraft-Wheels-and-Brakes/Products/Literature-Listing.

Goodyear. Aircraft tire data book. Technical report, The Goodyear Tire and Rubber Co., 2002.

D.L. Greene. Energy-efficiency improvement potential of commercial aircraft. *Annual Review of Energy and the Environment*, 17(1):537–573, 1992.

Andy Hebborn. A380 landing gear and systems – the feet of the plane. Lecture for RAeS, DGLR, VDI and HAW Hamburg, June 2008.

RD Hibbeler. Mechanics of materials. 1997.

Honeywell. *Boeing 737 NG Wheel and CERAMETALIX Brake*. Honeywell, 1944 E, Sky Harbor Circle Phoenix, AZ, April 2008.

F. Hürlimann, R. Kelm, M. Dugas, K. Oltmann, and G. Kress. Mass estimation of transport aircraft wingbox structures with a cad/cae-based multidisciplinary process. *Aerospace Science and Technology*, 15(4):323–333, 2011.

P.R. Kraus. *An Analytical Approach to Landing Gear Weight Estimation*. SAWE, Incorporated, 1970.

G. La Rocca, T.H.M. Langen, and Y.H.A. Brouwers. The design and engineering engine. towards a modular system for collaborative aircraft design. Technical report, Delft University of Technology, 2012.

V Ladda and H Struck. Operational loads on landing gear. *AD-A239 914*, 1991.

LMS International. Cessna uses lms virtual.lab motion for the making of the citation columbus, 2008. URL http://www.lmsintl.com/cessna-citation-columbus-uses-lms-virtual-lab-motion-to-design-biggest-business-jet.

Mathworks. Accelerating matlab: The matlab jit-accelerator. Technical report, The Mathworks Inc., 2002.

Mathworks. Key features - simmechanics for matlab and simulink, 2012. URL http://mathworks.nl/products/simmechanics/description1.html.

T.H.G. Megson. *Aircraft Structures for Engineering Students*. Referex Engineering. Edward Arnold, 1999. ISBN 9780340705889. URL http://books.google.nl/books?id=5qTPMgEACAAJ.

Michelin Aircraft Tire. Aircraft tire: engineering data, 2001.

Benjamin Milwitzky and Francis E Cook. Analysis of landing-gear behavior, 1953.

M.C.Y. Niu. *Airframe structural design: practical design information and data on aircraft structures*, volume 67. Conmilit Press, 1999.

H.B. Pacejka. *Tire and vehicle dynamics*, volume 372. 2006.

J.J.W. Pinsker. The dynamics of aircraft rotation and lift-off and its implication for tail clearance requirements, especially with large aircraft. Technical report, Ministry of Technology. Aeronautical Research Council, 1969.

D.P. Raymer. *Aircraft design: a conceptual approach*. American Institute of Aeronautics and Astronautics, 1999.

J. Roskam. *Airplane design Part 4: Layout design of landing gear and systems*. 1989a.

J. Roskam. *Airplane design Part 5: Component weight estimation*. 1989b.

R.K. Schmidt. A semi-analytical weight estimation method for oval fuselages in novel aircraft configurations. Master's thesis, Delft University of Technology Faculty of Aerospace Engineering, November 2013.

A.A. Shabana. *Dynamics of multibody systems*. Cambridge Univ Pr, 2005.

M. Spieck. *Ground dynamics of flexible aircraft in consideration of aerodynamic effects*. PhD thesis, Technische Universität München, Universitätsbibliothek, 2004.

TNO Automotive. Mf-tyre/mf-swift 6.1.2 equation manual. Technical report, TNO Delft-Tyre, 2010.

TNO Automotive. *MF-Tyre/MF-Swift 6.1.2 Help Manual*. TNO, March 2012.

E. Torenbeek. *Synthesis of subsonic airplane design: an introduction to the preliminary design, of subsonic general aviation and transport aircraft, with emphasis on layout, aerodynamic design, propulsion, and performance*. Springer, 1982.

R Toscano. A simple robust pi/pid controller design via numerical optimization approach. *Journal of process control*, 15(1):81–88, 2005.

M. Vable. *Mechanics of Materials*. Oxford University Press, August 2012. ISBN 9780195133370.

H. Zhang, J. Ning, O. Schmelzer, and M.D. Incorporation. Integrated landing gear system retraction/extension analysis using adams. In *North American ADAMS User Conference, June*, pages 19–21, 2000.